



HAL
open science

Precision calculations in supersymmetric extensions of the Standard Model

Pietro Slavich

► **To cite this version:**

Pietro Slavich. Precision calculations in supersymmetric extensions of the Standard Model. High Energy Physics - Phenomenology [hep-ph]. Université Pierre et Marie Curie - Paris VI, 2013. tel-00824019

HAL Id: tel-00824019

<https://theses.hal.science/tel-00824019>

Submitted on 20 May 2013

HAL is a multi-disciplinary open access archive for the deposit and dissemination of scientific research documents, whether they are published or not. The documents may come from teaching and research institutions in France or abroad, or from public or private research centers.

L'archive ouverte pluridisciplinaire **HAL**, est destinée au dépôt et à la diffusion de documents scientifiques de niveau recherche, publiés ou non, émanant des établissements d'enseignement et de recherche français ou étrangers, des laboratoires publics ou privés.

Precision calculations in supersymmetric extensions of the Standard Model

Pietro Slavich

*LPTHE, CNRS, Université Paris 6 (UPMC)
4, Place Jussieu, F-75252 Paris, France*

In partial fulfillment of the requirements for the *Habilitation à Diriger des Recherches*
at Pierre et Marie Curie University in Paris

17/05/2013

Contents

Preface	iii
1 Introduction	1
2 SUSY extensions of the SM	7
2.1 The Minimal Supersymmetric Standard Model	7
2.2 The Next-to-Minimal Supersymmetric Standard Model	11
2.3 Patterns of supersymmetry breaking	14
2.4 Input parameters and renormalization schemes	20
3 Higgs-boson production in gluon fusion	27
3.1 Higgs production via gluon fusion in the MSSM	28
3.2 Computation of the quark-squark-gluino contributions	35
3.3 Stop contributions: comparing different expansions	43
3.4 Sbottom contributions: dealing with large corrections	50
3.5 Implementation in public codes	57
4 Higgs-boson masses in the NMSSM	63
4.1 One-loop corrections to the Higgs mass matrices	64
4.2 Two-loop corrections in the effective-potential approach	65
4.3 Numerical examples	69
4.4 Further developments	74
5 BR[$B \rightarrow X_s \gamma$] in the MSSM with MFV	77
5.1 NLO determination of BR[$B \rightarrow X_s \gamma$]	78
5.2 Two-loop gluino contributions to the Wilson coefficients	82
5.3 Treatment of the $\tan \beta$ -enhanced contributions	87
5.4 Further developments	89
6 Outlook	91

Preface

This dissertation is written in partial fulfillment of the requirements for the *Habilitation à Diriger des Recherches* (HDR) at Pierre and Marie Curie University (UPMC) in Paris. According to the guidelines by the UPMC thesis committee, the dissertation should review the candidate’s recent work, situating it in the context of the international literature and outlining the prospects for future developments. Here I broadly interpret “recent” as referring to work published after my appointment as CNRS researcher [1]–[14]. However, for the sake of conciseness and in view of the experimental developments at the LHC, the dissertation will focus mostly on my recent work on the production of MSSM Higgs bosons at hadron colliders [6, 10, 12, 13, 14]. My work on the Higgs sector of the NMSSM [3, 8] and on precision calculations of flavor observables in extensions of the SM [1, 4, 7, 9], will be summarized more briefly, and I will not dwell on my work on split supersymmetry [15, 2] nor on my work aimed at streamlining the interface between public codes for precision calculations in BSM theories [16, 5, 11].

Being necessarily focused on my own scientific production, this dissertation cannot aim at a comprehensive review of the different topics treated. Consequently, I will not even try to provide complete lists of references, and I will cite only papers that are strictly relevant to the discussion. The readers interested in the broader context are pointed once and for all to the many reviews already available in the literature, such as, e.g., the one by S.P. Martin on supersymmetry [17], the ones by A. Djouadi on the phenomenology of the Higgs boson(s) in the SM [18] and in the MSSM [19], and the one by U. Ellwanger, C. Hugonie and A.M. Teixeira on the NMSSM [20].

Many of the results presented in this dissertation were obtained in collaboration with G. De-grassi. Among the colleagues with whom I co-authored refs. [1]–[14], I should also mention B.C. Allanach, E. Bagnaschi, N. Bernal, A. Delgado, S. Di Vita, A. Djouadi, P. Gambino, G.F. Giudice, G. Hiller, D.R.T. Jones and A. Vicini. It is also my pleasure to acknowledge a collaboration with K.H. Phan, as well as many fruitful discussions over the recent years with K. Benakli, M. Cacciari, U. Ellwanger, K. Ender, A. Falkowski, M. Goodsell, T. Hahn, R. Harlander, S. Heinemeyer, H. Mantler, M. Mühlleitner, S. Liebler, W. Porod, F. Riva, H. Rzehak, P. Skands, M. Spira, F. Staub and A. Strumia – and probably quite a few others who I hope will forgive me for momentarily forgetting about them.

Chapter 1

Introduction

The discovery of a Higgs boson with mass around 125 GeV by the ATLAS and CMS experiments at the Large Hadron Collider (LHC) [21, 22] marks the beginning of a new era in particle physics. The Higgs mechanism, as realized in the Standard Model (SM) of the electroweak and strong interactions, now stands on a firm ground as the correct description of electroweak symmetry breaking (EWSB). More precise measurements at the LHC (and at a future e^+e^- collider) will tell us whether the properties of the just-discovered particle follow the accurate predictions of the SM or deviate from them, turning the Higgs boson into a portal through which new physics beyond the SM (BSM) can be accessed.

However, even if the Higgs boson proved to be fully SM-like, all of the issues that motivated the physics community to consider possible extensions of the SM over the past four decades would still stand. On the observational side, the SM does not account for neutrino masses and oscillations, it does not include a suitable Dark Matter candidate, and it cannot justify the matter-antimatter asymmetry in the Universe. On a more theoretical side, the SM suffers from the well-known *hierarchy problem*: quantum corrections destabilize the Higgs-boson mass, inducing a quadratic dependence on the cut-off scale used to regularize the loop integrals. If the SM was valid as an effective description of particle physics up to the Planck scale $M_P \approx 10^{19}$ GeV at which quantum-gravity effects become relevant, the natural value for the Higgs boson mass (and for all the other masses resulting from EWSB) would also be of the order of M_P . A fantastically accurate cancellation between the Higgs-mass parameter in the bare SM Lagrangian and the quantum corrections, occurring at all orders in perturbation theory, would be required to ensure that the EWSB scale stays at its observed value of $\mathcal{O}(100 \text{ GeV})$. Barring such an extreme fine tuning of the fundamental parameters of the theory, some new physics must intervene at an energy scale not much larger than the EWSB scale, and stabilize the hierarchy between the latter and the Planck scale.

Among the possible extensions of the SM, supersymmetry (SUSY) has long been considered the most attractive candidate. At the price of doubling the particle content of the SM, by introducing a bosonic (fermionic) *superpartner* for each known fermionic (bosonic) particle, SUSY provides a solution to the hierarchy problem, because the quadratically divergent contribution of each SM particle to the

quantum correction to the Higgs-mass parameter cancels against the contribution of its superpartner, leaving behind a quadratic dependence on the SUSY-breaking mass of the latter (indeed, SUSY must be broken, otherwise all of the *superparticles* would have the same mass as their ordinary SM partners). Moreover, supersymmetric extensions of the SM can feature a suitable candidate for Dark Matter, a natural mechanism to generate EWSB through quantum corrections, and an improved high-energy convergence of the gauge couplings. On the minus side, direct searches at the LEP, at the Tevatron and now at the LHC – after the first two-year run with reduced center-of-mass energy – have so far failed to provide evidence for the existence of superparticles. The resulting lower bounds on the superparticle masses bring back a certain degree of fine tuning in the EWSB process, unless rather special patterns of SUSY-breaking parameters are considered.

A remarkable feature of SUSY extensions of the SM is the requirement of an extended Higgs sector, with additional neutral and charged bosons. In such models the couplings of the Higgs bosons to matter fermions and to gauge bosons can differ significantly from those of the SM Higgs. Moreover, in contrast to the case of the SM, the Higgs-boson masses are not free parameters, as SUSY requires them to be related to the gauge-boson masses. For example, in the minimal supersymmetric extension of the SM, the MSSM, the tree-level mass of the lightest Higgs scalar is bounded from above by the Z -boson mass. However, radiative corrections involving loops of SM particles and their superpartners alter the tree-level predictions for the Higgs-boson masses, introducing a dependence on several superparticle masses and couplings and allowing for a SM-like Higgs scalar with mass around 125 GeV. Similarly, radiative corrections induced by superparticle loops can significantly alter the SM predictions for the Higgs production and decay processes. Consequently, a measurement of the properties of the just-discovered Higgs boson will allow us to constrain the parameter space of SUSY extensions of the SM, independently of the actual observation of superparticles or additional Higgs bosons.

In order to use the information on the Higgs sector to discriminate between different SUSY extensions of the SM, precise calculations of their predictions for masses, production and decays of the Higgs bosons are necessary. In many cases the inclusion of potentially large radiative corrections from diagrams involving gluons or their superpartners, the *gluinos*, requires a two-loop calculation, with all the related technical difficulties. Indeed, over the past two decades an impressive theoretical effort has been devoted by several groups to a precise characterization of the Higgs sector of the MSSM.

For what concerns the predictions for the MSSM Higgs masses, full one-loop calculations have been available since the mid-1990s, while the dominant two-loop corrections controlled by the strong gauge coupling and the top and bottom Yukawa couplings, evaluated under the approximation of vanishing external momentum in the Higgs-boson self-energies, had been computed by the early 2000s. Indeed, in the early stages of my research activity I contributed to the computation of these two-loop corrections [23, 24, 25, 26, 27], which were then implemented [28, 29] in existing codes for the calculation of the MSSM mass spectrum [30, 31, 32, 33]. More recently, a nearly complete two-loop calculation of the MSSM Higgs masses, including electroweak effects and part of the external-momentum dependence, has become available, as have the leading three-loop effects.

For what concerns the production of Higgs bosons [34, 35, 36], one of the most important mechanisms at the LHC is the loop-induced gluon fusion, where the coupling of the gluons to the Higgs boson is mediated by loops of heavy colored particles. In the SM the dominant contributions to the gluon-fusion amplitude arise from top-quark loops and, to a much lesser extent, bottom-quark loops. The SM prediction for the Higgs-production cross section in gluon fusion is by now extremely advanced, including the full next-to-leading order (NLO) QCD corrections; the next-to-next-to-leading order (NNLO) QCD corrections due to top-quark loops; soft-gluon resummation effects; the first-order electroweak (EW) corrections; estimates of the next-to-next-to-next-to-leading order (NNNLO) QCD corrections and of the mixed QCD-EW correction.

In the MSSM the effect of the bottom-quark loops can be considerably enhanced, and loops involving the superpartners of the heavy quarks, the *stop* and *sbottom* squarks, can also give sizable contributions, resulting in measurable deviations from the SM prediction for the cross section. However, in the MSSM the cross section is currently known only at the NLO (although approximate calculations of some NNLO effects exist). The contributions of two-loop diagrams with quarks and gluons can be obtained from the corresponding SM results with an appropriate rescaling of the Higgs-quark couplings, and the contributions of two-loop diagrams with squarks and gluons had been fully computed by the late 2000s. On the other hand, due to the number of different masses involved, a full computation of the two-loop diagrams with quarks, squarks and gluinos has proved a much more daunting task. Results based on a combination of analytic and numerical methods were presented in refs. [37, 38], but neither explicit analytic formulae nor public computer codes have been made available so far (indeed, the codes turn out to be extremely slow and suffer from numerical instabilities, which makes them unpractical for phenomenological applications).

However, the early results from SUSY searches at the LHC set preliminary lower bounds on the squark and gluino masses of the order of the TeV, although for third-generation squarks the bounds are somewhat weaker. This suggests that – if the MSSM is actually realized in nature – there might be wide regions of its parameter space in which all of the Higgs bosons are lighter than the squarks and the gluino. In the presence of such a hierarchy between the Higgs-boson mass and the superparticle masses, approximate analytic results for the quark-squark-gluino contributions can be derived. This is indeed one of the main subjects of my recent research. In particular, in refs. [6, 10, 12, 14] we provided both the results of a Taylor expansion in the Higgs boson mass, which are valid in the top-stop-gluino case for a Higgs boson lighter than the top quark, and the results of an asymptotic expansion in the heavy superparticle masses that does not assume any hierarchy between the Higgs-boson mass and the quark mass, thus covering both the top-stop-gluino and bottom-sbottom-gluino cases. The former results confirmed and extended earlier calculations valid in the limit of vanishing Higgs-boson mass [39, 40], whereas the latter were not previously available. As a byproduct of our calculations, we also obtained new results for the two-loop SUSY-QCD contributions to the decays of Higgs bosons into photons and into gluons.

Unlike the exact two-loop results for the gluon-fusion amplitude, the approximate analytic results of refs. [6, 10, 12, 14] can be easily implemented in public computer codes, allowing for an efficient and accurate determination of the Higgs production cross section. Indeed, in ref. [13] we described the implementation of our results in the `POWHEG-BOX` framework, which matches NLO-QCD computations of matrix elements with parton-shower Monte Carlo generators such as `PYTHIA` or `HERWIG`. In addition to the total cross section for Higgs-boson production in gluon fusion, the code allows us compute also the rapidity and transverse-momentum distributions of the produced Higgs boson. Furthermore, our results were implemented in the public code `SusHi` [41], which computes the total and differential cross sections for Higgs production in gluon fusion and bottom-quark annihilation in the SM and in the MSSM.

The situation in other SUSY extensions of the SM is much less advanced than the one in the MSSM. Even in the simplest, next-to-minimal SUSY extension of the SM (NMSSM), where the addition of a gauge-singlet field to the Higgs sector allows to reduce the fine-tuning problem of the MSSM, the accuracy of the theoretical predictions for the Higgs-boson masses has until recently been stuck to the level that for the MSSM had been achieved in the mid-1990s, and radiative corrections to Higgs production and decay processes have only been studied at one-loop accuracy (if at all). For example, when I co-authored a study of the NMSSM with gauge-mediated SUSY breaking [3] in 2007, the dominant one-loop corrections to the Higgs masses controlled by the top and bottom Yukawa couplings had been computed in the effective-potential approximation, i.e. neglecting the external momentum in the self-energies, while the remaining one-loop and two-loop corrections were available only in a leading-logarithmic approximation. In ref. [8] we took a few steps towards bridging the accuracy gap between the NMSSM and MSSM calculations. In particular, we provided a full one-loop calculation of the self-energies and tadpoles of the neutral Higgs bosons of the NMSSM, and we computed the two-loop corrections to the neutral Higgs boson masses controlled by the strong gauge coupling in the effective-potential approximation. We showed that both classes of corrections can induce shifts of a few GeV in the light Higgs-boson masses, and they can also sizably affect the mixing between singlet and MSSM-like Higgs scalars. Our results were later implemented in public codes [42, 43] for the computation of the NMSSM mass spectrum, and they have become a standard ingredient of many phenomenological analyses of the NMSSM.

Independently of the direct searches for new particles at high-energy colliders, BSM physics could manifest itself through its effect on a number of well-measured low-energy observables. In particular, the contribution of new particles could induce large deviations from the SM predictions in processes that are suppressed in the SM, such as flavor-violating or CP-violating transitions. Extensions of the SM with broken SUSY, such as the MSSM and the NMSSM, do indeed suffer from what is known as the *flavor problem*. If the SUSY-breaking mass and interaction terms for the superpartners of the SM fermions had a generic structure in flavor space, and if the superparticles had masses of at most a few TeV (to avoid an excessive amount of fine tuning in the EWSB), processes such as meson-antimeson transitions would receive very large contributions from loops involving superparticles, which is strongly

ruled out by the good agreement between the SM predictions and the experimental measurements of these processes. A natural solution to the flavor problem is the so-called Minimal Flavor Violation (MFV) hypothesis, according to which the flavor-violating structure of the SUSY-breaking terms is linked to the known structure of the Yukawa couplings, so that, just as in the SM, all flavor-violating interactions are controlled by the CKM matrix. In such MFV scenarios, the superparticle contributions to low-energy flavor observables are at most comparable to the SM contributions, and the generally good agreement between measurements and SM predictions translates into constraints on the parameter space of the different SUSY models.

The rare flavor-violating inclusive decay $B \rightarrow X_s \gamma$ is particularly well-suited as a precision test of the SM and its extensions, thanks to its low sensitivity to non-perturbative effects. The SM prediction for the branching ratio $\text{BR}[B \rightarrow X_s \gamma]$, which includes most of the NNLO QCD contributions as well as the leading non-perturbative and electroweak effects, has an uncertainty of about 7% and agrees within 1σ with the current experimental world average. In extensions of the SM, however, the theoretical accuracy of the prediction for $\text{BR}[B \rightarrow X_s \gamma]$ is not at the same level as in the SM, and even a complete NLO calculation is available only for some specific models. For what concerns the MSSM with MFV, we computed in ref. [1] the contribution of two-loop diagrams involving gluinos to the Wilson coefficients for the $b \rightarrow s\gamma$ transition, thus completing the NLO calculation of $\text{BR}[B \rightarrow X_s \gamma]$ in that model. We had to overcome several hurdles, related to the large number of diagrams and, more conceptually, to the fact that the MFV condition is affected by radiative corrections and must be imposed on the squark-mixing matrices after renormalization. Later, we presented in ref. [9] a NLO calculation of the Wilson coefficients for $b \rightarrow s\gamma$ in a two-Higgs-doublet model (THDM) in which the second Higgs doublet is a color octet, the so-called Manohar-Wise model [44].

We made our results available to the public in the computer code `SusyBSG` [4], which provides the state-of-the-art calculation of $\text{BR}[B \rightarrow X_s \gamma]$ in the MSSM with MFV as well as in several versions of the THDM. Since its publication in 2007, the code has been repeatedly updated and expanded, and it has been used by many groups to analyze the constraints from flavor physics on the MSSM parameter space. In particular, I co-authored a study of flavor violation in the MSSM with anomaly-mediated SUSY breaking [7], in which we used `SusyBSG` to show that $B \rightarrow X_s \gamma$ provided the most stringent constraints on the parameter space of the model.

This dissertation is organized as follows: in the next chapter I will summarize the structure of SUSY extensions of the SM, namely the MSSM and the NMSSM, provide a brief overview of different patterns of SUSY breaking and discuss some issues on the renormalization of the input parameters that are common to all calculations of higher-order corrections in SUSY models. In chapter 3 I will review the results of refs. [6, 10, 12, 13, 14] on the production of MSSM Higgs bosons in gluon fusion. In chapter 4 I will review the results of ref. [8] on the radiative corrections to the Higgs boson masses in the NMSSM. In chapter 5 I will review the calculation of $\text{BR}[B \rightarrow X_s \gamma]$ in the MSSM with MFV, refs. [1, 4]. Finally, in chapter 6 I will briefly summarize the outlook of my future research.

Chapter 2

SUSY extensions of the SM

2.1 The Minimal Supersymmetric Standard Model

This section summarizes the particle spectrum of the MSSM. The purpose of the section is mainly to fix the notation, thus I will not discuss the important issue of radiative corrections in the Higgs sector, and I will skip information that is not relevant to the topics treated in the next chapters. For an exhaustive introduction to the MSSM, the reader is pointed to ref. [17].

Superpotential and SUSY-breaking Lagrangian: The SUSY-conserving masses and interactions of the quark, lepton and Higgs fields and of their superpartners are encoded in the *superpotential*, an analytic function of the quark and lepton *superfields* Q, U^c, D^c, L, E^c and of the Higgs superfields H_1 and H_2 . Assuming R -parity conservation, which forbids lepton- and baryon-number-violating interactions, the MSSM superpotential reads

$$W_{\text{MSSM}} = h_e H_1 L E^c + h_d H_1 Q D^c + h_u Q H_2 U^c + \mu H_1 H_2, \quad (2.1)$$

where sums over gauge and generation indices are understood (the $SU(2)$ -doublet superfields are contracted by the antisymmetric tensor ϵ_{ab} , with $\epsilon_{12} = 1$). The *soft SUSY-breaking* mass and interaction terms for the MSSM scalars (i.e., terms that break SUSY without inducing quadratic divergences through quantum corrections) are contained in the potential

$$V_{\text{soft}} = m_{H_1}^2 H_1^\dagger H_1 + m_{H_2}^2 H_2^\dagger H_2 + m_Q^2 Q^\dagger Q + m_L^2 L^\dagger L + m_U^2 \tilde{u}_R^* \tilde{u}_R + m_D^2 \tilde{d}_R^* \tilde{d}_R + m_E^2 \tilde{e}_R^* \tilde{e}_R \\ + \left(T_e H_1 L \tilde{e}_R^* + T_d H_1 Q \tilde{d}_R^* + T_u Q H_2 \tilde{u}_R^* + B_\mu H_1 H_2 + \text{h.c.} \right), \quad (2.2)$$

where for the scalar components of the quark and lepton superfields I define $\tilde{u}_R = U^{c*}$, $\tilde{d}_R = D^{c*}$, $\tilde{e}_R = E^{c*}$, $Q = (\tilde{u}_L, \tilde{d}_L)^T$ and $L = (\tilde{\nu}_L, \tilde{e}_L)^T$. Again, sums over gauge and generation indices are understood. Finally, the soft SUSY-breaking mass terms for the superpartners of the gauge bosons (the *gauginos*) are contained in the Lagrangian

$$\mathcal{L}_G = \frac{1}{2} \left(M_1 \tilde{b}\tilde{b} + M_2 \tilde{w}\tilde{w} + M_3 \tilde{g}\tilde{g} \right) + \text{h.c.}, \quad (2.3)$$

where the gauginos are two-component spinors and sums over gauge indices are once more understood. For simplicity, I will assume the parameter μ in eq. (2.1) and all the soft SUSY-breaking parameters in eqs. (2.2) and (2.3) to be real, thus neglecting any additional source of CP violation beyond the CKM matrix. Various conventions for the sign of the parameters μ in eq. (2.1) and B_μ in eq. (2.2) are used in the literature. I adopt here the convention used in my papers on the two-loop corrections to the MSSM Higgs masses [23]–[27] and production cross section [6, 10, 12, 14]. This is opposite to the convention prescribed by the *SUSY Les Houches Accord* (SLHA) [16, 5].

The Higgs sector: Keeping only the dependence on the neutral components of the Higgs doublets, the tree-level Higgs potential of the MSSM reads:

$$V_0 = m_1^2 |H_1^0|^2 + m_2^2 |H_2^0|^2 + B_\mu (H_1^0 H_2^0 + \text{h.c.}) + \frac{g^2 + g'^2}{8} (|H_1^0|^2 - |H_2^0|^2)^2, \quad (2.4)$$

where: $m_1^2 = m_{H_1}^2 + |\mu|^2$, $m_2^2 = m_{H_2}^2 + |\mu|^2$; g and g' are the $SU(2)_L$ and $U(1)_Y$ gauge couplings, respectively. Each neutral Higgs field can be decomposed into vacuum expectation value (v_{ev}) plus CP-even and CP-odd fluctuations as follows:

$$H_1^0 = v_1 + \frac{1}{\sqrt{2}}(S_1 + iP_1), \quad H_2^0 = v_2 + \frac{1}{\sqrt{2}}(S_2 + iP_2). \quad (2.5)$$

It is not restrictive to choose B_μ real and negative, so that v_1 and v_2 are real and positive. With the convention of eq. (2.5) for the normalization of the Higgs vevs, the squared masses of the gauge bosons are $m_W^2 = g^2 v^2/2$ and $m_Z^2 = (g^2 + g'^2) v^2/2$, where $v \equiv (v_1^2 + v_2^2)^{1/2} \approx 174$ GeV. The masses of the up-type quarks are $m_u = h_u v_2$, and the masses of the down-type quarks and charged leptons are $m_{d,e} = h_{d,e} v_1$ (here, e.g., h_u denotes one of the three eigenvalues of the corresponding matrix of Yukawa couplings).

The mass matrix for the CP-odd bosons is diagonalized by an angle β such that $\tan \beta = v_2/v_1$. One of the two eigenstates, G^0 , plays the role of the neutral would-be-Goldstone boson; the other, A , is a physical pseudoscalar with tree-level squared mass

$$m_A^2 = -\frac{B_\mu}{\cos \beta \sin \beta}. \quad (2.6)$$

The mass matrix for the charged components of the Higgs doublets is also diagonalized by the angle β . One of the two eigenstates, G^\pm , plays the role of the charged would-be-Goldstone boson; the other, H^\pm , is a physical charged scalar with tree-level squared mass $m_{H^\pm}^2 = m_A^2 + m_W^2$.

To determine the masses of the CP-even bosons, the minimum conditions of the tree-level Higgs potential V_0 can be used to replace m_1^2 and m_2^2 with combinations of m_A^2 and $\tan \beta$. The resulting tree-level mass matrix, in the (S_1, S_2) basis, is

$$\mathcal{M}_0 = \begin{pmatrix} m_A^2 \sin^2 \beta + m_Z^2 \cos^2 \beta & -(m_A^2 + m_Z^2) \sin \beta \cos \beta \\ -(m_A^2 + m_Z^2) \sin \beta \cos \beta & m_A^2 \cos^2 \beta + m_Z^2 \sin^2 \beta \end{pmatrix}. \quad (2.7)$$

The tree-level matrix \mathcal{M}_0 is diagonalized by an angle α given by

$$\tan 2\alpha = \left(\frac{m_A^2 + m_Z^2}{m_A^2 - m_Z^2} \right) \tan 2\beta, \quad (2.8)$$

and the two eigenstates of \mathcal{M}_0 are denoted as h and H , with $m_h < m_H$. There is an upper bound on the tree-level mass of the lightest eigenstate, $m_h^2 < m_Z^2 \cos^2 2\beta$.

In the MSSM the role of the SM Higgs boson is shared between the scalars h and H . In particular, the couplings of the two scalars to massive vector bosons and to SM fermions are

$$g_{hVV} = \frac{\sqrt{2}m_V^2}{v} \sin(\beta - \alpha), \quad g_{huu} = \frac{1}{\sqrt{2}} \frac{\cos \alpha}{\sin \beta} \frac{m_u}{v}, \quad g_{hdd,hee} = -\frac{1}{\sqrt{2}} \frac{\sin \alpha}{\cos \beta} \frac{m_{d,e}}{v}, \quad (2.9)$$

$$g_{HVV} = \frac{\sqrt{2}m_V^2}{v} \cos(\beta - \alpha), \quad g_{Huu} = \frac{1}{\sqrt{2}} \frac{\sin \alpha}{\sin \beta} \frac{m_u}{v}, \quad g_{Hdd,Hee} = \frac{1}{\sqrt{2}} \frac{\cos \alpha}{\cos \beta} \frac{m_{d,e}}{v}. \quad (2.10)$$

In the so-called *decoupling limit*, $m_A \gg m_Z$, the mixing angle in the CP-even sector simplifies to $\alpha \approx \beta - \pi/2$. As a result, the tree-level mass of the lightest scalar becomes $m_h \approx m_Z |\cos 2\beta|$, and its couplings to gauge bosons, quarks and leptons in eq. (2.9) become SM-like. On the other hand, the mass of the heaviest scalar becomes $m_H \approx m_A$, the couplings of H to two gauge bosons vanish and the couplings of H to two up-type (down-type) SM fermions are suppressed (enhanced) by $\tan \beta$. Therefore, in this limit, the Higgs sector of the MSSM reduces to a SM-like Higgs boson with tree-level mass $m_h < m_Z$, and a heavy and mass-degenerate multiplet (H, A, H^\pm) decoupled from the gauge sector. However, radiative corrections mediated by quark and squark loops can lift the mass of the SM-like Higgs boson up to the value $m_h \approx 125$ GeV suggested by the recent LHC results.

The sfermion sector: The Yukawa couplings (h_e, h_d, h_u) in eq. (2.1), as well as the mass terms $(m_Q^2, m_L^2, m_U^2, m_D^2, m_E^2)$ and the trilinear interaction terms (T_e, T_d, T_u) in eq. (2.2), are 3×3 matrices in generation space. The Higgs vevs induce additional mass terms for the superpartners of the SM fermions (the *sfermions*). In particular, the trilinear interaction terms in eq. (2.2) induce a mixing between the superpartners of the right-handed and left-handed SM fermions. The physical up-type and down-type squarks (as well as the physical charged sleptons, which I will not discuss here) are the eigenstates of the resulting 6×6 mass matrices.

In the so-called super-CKM basis, the quark fields are rotated in such a way that Yukawa couplings in eq. (2.1) are flavor-diagonal, and the squarks are rotated in parallel to their superpartners. A strict interpretation of the minimal-flavor-violation condition, which we adopted in our calculation of $\text{BR}[B \rightarrow X_s \gamma]$ [1, 4], consists in assuming that all the soft SUSY-breaking matrices for the squark masses and interactions in eq. (2.2) are flavor-diagonal in the super-CKM basis. In this case, the only source of flavor violation in the squark sector is the CKM matrix, as in the quark sector. However, for the mass matrices of the up-type and down-type squarks to be simultaneously flavor-diagonal in the super-CKM basis, the soft SUSY-breaking mass matrix for the left-squark doublets m_Q^2 must be not only diagonal, but also proportional to identity matrix.

If the strict MFV condition is satisfied, or if – as will be the case in the calculations of Higgs-boson properties in chapters 3 and 4 – one simply neglects any intergenerational mixing, the squark mass matrices are block-diagonal for each generation. In this case the only mixing to be taken into account is the one between the superpartners of the left-handed and the right-handed squarks. The trilinear Higgs-squarks interactions are usually decomposed as the product of two flavor-diagonal matrices, $T_q = h_q A_q$ (where $q = u, d$), and the mass matrices for the third-generation squarks, in the $(\tilde{q}_L, \tilde{q}_R)$ basis, read

$$\mathcal{M}_{\tilde{t}} = \begin{pmatrix} m_Q^2 + m_t^2 + (\frac{1}{2} - \frac{2}{3} \sin^2 \theta_W) m_Z^2 \cos 2\beta & m_t (A_t + \mu \cot \beta) \\ m_t (A_t + \mu \cot \beta) & m_U^2 + m_t^2 + \frac{2}{3} \sin^2 \theta_W m_Z^2 \cos 2\beta \end{pmatrix}, \quad (2.11)$$

$$\mathcal{M}_{\tilde{b}} = \begin{pmatrix} m_Q^2 + m_b^2 - (\frac{1}{2} - \frac{1}{3} \sin^2 \theta_W) m_Z^2 \cos 2\beta & m_b (A_b + \mu \tan \beta) \\ m_b (A_b + \mu \tan \beta) & m_D^2 + m_b^2 - \frac{1}{3} \sin^2 \theta_W m_Z^2 \cos 2\beta \end{pmatrix}, \quad (2.12)$$

where the soft SUSY-breaking parameters m_Q, m_U, m_D, A_t and A_b are understood as the (3,3) entries of the corresponding diagonal matrices in flavor space, and θ_W is the Weinberg angle. The stop and sbottom mass matrices are diagonalized by the mixing angles θ_t and θ_b , respectively, and the resulting mass eigenstates are denoted as $(\tilde{t}_1, \tilde{t}_2)$ and $(\tilde{b}_1, \tilde{b}_2)$, respectively. The relations between the squark masses, mixing angle and left-right mixing terms read

$$\sin 2\theta_t = \frac{2 m_t X_t}{m_{\tilde{t}_1}^2 - m_{\tilde{t}_2}^2}, \quad \sin 2\theta_b = \frac{2 m_b X_b}{m_{\tilde{b}_1}^2 - m_{\tilde{b}_2}^2}, \quad (2.13)$$

where $X_t \equiv A_t + \mu \cot \beta$ and $X_b \equiv A_b + \mu \tan \beta$.

The chargino/neutralino sector: The charged components of the superpartners of the Higgs bosons, the *higgsinos*, mix with the charged *winos*, $\tilde{w}^\pm = (\tilde{w}^1 \mp i\tilde{w}^2)/\sqrt{2}$. In the formalism of two-component spinors, the Lagrangian contains the mass terms

$$- \begin{pmatrix} -i\tilde{w}^- & \tilde{h}_1^- \end{pmatrix} \begin{pmatrix} M_2 & g v_2 \\ g v_1 & -\mu \end{pmatrix} \begin{pmatrix} -i\tilde{w}^+ \\ \tilde{h}_2^+ \end{pmatrix} + \text{h.c.} . \quad (2.14)$$

The above mass matrix, \mathcal{M}_{χ^\pm} , is diagonalized by two unitary matrices U and V such that $U^* \mathcal{M}_{\chi^\pm} V^\dagger = \text{diag}(m_{\chi_1^\pm}, m_{\chi_2^\pm})$, and the two-component *chargino* states, ordered by increasing mass, are

$$\chi_i^+ = V_{ij} \psi_j^+, \quad \chi_i^- = U_{ij} \psi_j^-, \quad (2.15)$$

where ψ^+ stands for $(-i\tilde{w}^+, \tilde{h}_2^+)$ and ψ^- for $(-i\tilde{w}^-, \tilde{h}_1^-)$. Under our simplifying assumptions all the entries of the chargino mass matrix in eq. (2.14) are real. In this case U and V become real matrices, as long as the chargino mass terms are allowed to take on negative signs.

The neutral components of the higgsinos, \tilde{h}_1^0 and \tilde{h}_2^0 , mix with the neutral gauginos \tilde{b} and \tilde{w}^0 . In the two-component formalism, the Lagrangian contains the mass terms

$$-\frac{1}{2} \begin{pmatrix} -i\tilde{b} & -i\tilde{w}^0 & \tilde{h}_1^0 & \tilde{h}_2^0 \end{pmatrix} \begin{pmatrix} M_1 & 0 & -g'v_1/\sqrt{2} & g'v_2/\sqrt{2} \\ 0 & M_2 & g'v_1/\sqrt{2} & -g'v_2/\sqrt{2} \\ -g'v_1/\sqrt{2} & g'v_1/\sqrt{2} & 0 & \mu \\ g'v_2/\sqrt{2} & -g'v_2/\sqrt{2} & \mu & 0 \end{pmatrix} \begin{pmatrix} -i\tilde{b} \\ -i\tilde{w}^0 \\ \tilde{h}_1^0 \\ \tilde{h}_2^0 \end{pmatrix}. \quad (2.16)$$

The above mass matrix is diagonalized by a single unitary matrix N such that

$$\chi_i^0 = N_{ij} \psi_j^0, \quad (2.17)$$

where ψ^0 stands for $(-i\tilde{b}, -i\tilde{w}^0, \tilde{h}_1^0, \tilde{h}_2^0)$ and χ_i^0 are the *neutralino* mass eigenstates ordered by increasing mass. Again, we take all the entries of the neutralino mass matrix in eq. (2.16) as real and allow the neutralino mass terms to take on negative signs, so that N is a real matrix.

Finally, being a color octet, the gluino does not mix with any other fermion and is not affected by EWSB. At tree level the gluino mass coincides with the soft SUSY-breaking term, i.e., $m_{\tilde{g}} = M_3$.

2.2 The Next-to-Minimal Supersymmetric Standard Model

The NMSSM provides an elegant solution to the so-called μ *problem* of the MSSM, i.e. the question of how to relate the higgsino mass parameter μ in the superpotential, eq. (2.1), to the other mass parameters in the soft SUSY-breaking scalar potential, eq. (2.2). Indeed, since μ enters the SUSY-conserving part of the Lagrangian, its natural value would be around the high boundary scale at which the MSSM is embedded in a larger theory. One possible solution to the problem, known as *Giudice-Masiero mechanism*, consists in assuming that μ is in fact generated by SUSY-breaking effects together with the soft terms. In the NMSSM, on the other hand, μ arises as the vev of the scalar component of an additional chiral superfield S , singlet with respect to the SM gauge group and coupled to the MSSM Higgs superfields H_1 and H_2 through a superpotential term $\lambda SH_1 H_2$. In this case, an effective higgsino mass parameter is generated as $\mu_{\text{eff}} = \lambda \langle S \rangle$, where $\langle S \rangle$ is in turn determined by the soft SUSY-breaking mass and interaction terms for the singlet. The scalar and pseudoscalar components of the singlet superfield mix with the MSSM Higgs fields of matching parity, while the fermion component (singlino) mixes with the MSSM higgsinos. The new superpotential term also induces a quartic Higgs-scalar interaction controlled by the new coupling λ , which can bring the additional benefit of increasing the tree-level prediction for the mass of the lightest Higgs boson. This allows for a smaller contribution to the Higgs mass from radiative corrections involving top quarks and stop squarks, thus reducing the so-called *little hierarchy problem* of the MSSM, i.e. the need for the stop masses to be substantially larger than the weak scale, which brings back a degree of fine tuning in the EWSB conditions. In this section I will only summarize how the Higgs sector of the NMSSM differs from the one of the MSSM. For a comprehensive review of the NMSSM the reader is pointed to ref. [20].

In the NMSSM, the superpotential mass term for the MSSM Higgs doublets in eq. (2.1) is replaced by a trilinear singlet-doublet interaction, plus a cubic interaction term for the singlet

$$\mu H_1 H_2 \longrightarrow \lambda S H_1 H_2 + \frac{\kappa}{3} S^3. \quad (2.18)$$

The corresponding term in the soft SUSY-breaking potential V_{soft} , eq. (2.2), is replaced as

$$B_\mu H_1 H_2 \longrightarrow \lambda A_\lambda S H_1 H_2 + \frac{\kappa}{3} A_\kappa S^3, \quad (2.19)$$

and V_{soft} contains an additional mass term for the singlet, $m_S^2 S^* S$. For simplicity the new parameters λ , κ , A_λ and A_κ are all assumed to be real. Note also that the convention for the sign of λ in eqs. (2.18) and (2.19) is the opposite of the one prescribed by the SLHA [5] and adopted in ref. [8]. Additional terms which would be allowed by gauge symmetry, such as MSSM-like μ and B_μ terms and terms linear or quadratic in S , are forbidden by a Z_3 symmetry acting on the superfields H_1 , H_2 and S .

The neutral components of the Higgs fields can be decomposed into their vevs plus their CP-even and CP-odd fluctuations as

$$H_i^0 = v_i + \frac{1}{\sqrt{2}} (S_i + iP_i) \quad (i = 1, 2), \quad S = v_s + \frac{1}{\sqrt{2}} (S_3 + iP_3). \quad (2.20)$$

Using the minimization conditions of the tree-level scalar potential to replace the soft SUSY-breaking Higgs masses $m_{H_1}^2$, $m_{H_2}^2$ and m_S^2 with combinations of the Higgs vevs and the trilinear couplings, the tree-level mass matrix for the CP-even fields reads

$$\left(\begin{array}{ccc} \bar{g}^2 v_1^2 - \lambda v_s \frac{v_2}{v_1} A_\Sigma & (2\lambda^2 - \bar{g}^2) v_1 v_2 + \lambda v_s A_\Sigma & 2\lambda^2 v_1 v_s + \lambda v_2 (A_\Sigma + \kappa v_s) \\ (2\lambda^2 - \bar{g}^2) v_1 v_2 + \lambda v_s A_\Sigma & \bar{g}^2 v_2^2 - \lambda v_s \frac{v_1}{v_2} A_\Sigma & 2\lambda^2 v_2 v_s + \lambda v_1 (A_\Sigma + \kappa v_s) \\ 2\lambda^2 v_1 v_s + \lambda v_2 (A_\Sigma + \kappa v_s) & 2\lambda^2 v_2 v_s + \lambda v_1 (A_\Sigma + \kappa v_s) & -\lambda A_\lambda \frac{v_1 v_2}{v_s} + \kappa v_s (A_\kappa + 4\kappa v_s) \end{array} \right), \quad (2.21)$$

where for brevity we define $A_\Sigma = A_\lambda + \kappa v_s$ and $\bar{g}^2 = (g^2 + g'^2)/2$. The CP-even mass matrix is diagonalized by an orthogonal matrix R^S , such that

$$h_i = R_{ij}^S S_j, \quad (2.22)$$

where h_i , with $i = 1, 2, 3$, are the CP-even mass eigenstates ordered by increasing mass. The upper bound on the lightest-scalar mass is weaker than in the MSSM, thanks to an additional contribution controlled by the singlet-doublet superpotential coupling:

$$m_{h_1}^2 < m_Z^2 \cos^2 2\beta + \lambda^2 v^2 \sin^2 2\beta, \quad (2.23)$$

where again we define $v^2 \equiv v_1^2 + v_2^2$. Note however that the second term on the r.h.s. in eq. (2.23) is significant only for small or moderate $\tan\beta$, which in turn suppresses the first term. Large values of λ are thus required for m_{h_1} to be significantly larger than m_Z at tree level.

The tree-level mass matrix for the CP-odd fields reads

$$\left(\begin{array}{ccc} -\lambda v_s \frac{v_2}{v_1} A_\Sigma & -\lambda v_s A_\Sigma & -\lambda v_2 (A_\Sigma - 3\kappa v_s) \\ -\lambda v_s A_\Sigma & -\lambda v_s \frac{v_1}{v_2} A_\Sigma & -\lambda v_1 (A_\Sigma - 3\kappa v_s) \\ -\lambda v_2 (A_\Sigma - 3\kappa v_s) & -\lambda v_1 (A_\Sigma - 3\kappa v_s) & -4\lambda\kappa v_1 v_2 - \lambda A_\lambda \frac{v_1 v_2}{v_s} - 3\kappa A_\kappa v_s \end{array} \right). \quad (2.24)$$

The CP-odd mass matrix is in turn diagonalized by an orthogonal matrix R^P , such that

$$a_i = R_{ij}^P P_j , \quad (2.25)$$

where a_i stands for (G^0, A_1, A_2) . Here, G^0 is the neutral would-be-Goldstone boson, while A_1 and A_2 are two physical pseudoscalars, ordered by increasing mass.

In the neutralino sector, the *singlino* \tilde{s} mixes with the neutral components of the MSSM higgsinos \tilde{h}_1^0 and \tilde{h}_2^0 , which in turn mix with the neutral gauginos \tilde{b} and \tilde{w}^0 . In the formalism of two-component spinors, the Lagrangian contains the mass terms

$$-\frac{1}{2} \begin{pmatrix} -i\tilde{b} & -i\tilde{w}^0 & \tilde{h}_1^0 & \tilde{h}_2^0 & \tilde{s} \end{pmatrix} \begin{pmatrix} M_1 & 0 & -g' v_1/\sqrt{2} & g' v_2/\sqrt{2} & 0 \\ 0 & M_2 & g v_1/\sqrt{2} & -g v_2/\sqrt{2} & 0 \\ -g' v_1/\sqrt{2} & g v_1/\sqrt{2} & 0 & \lambda v_s & \lambda v_2 \\ g' v_2/\sqrt{2} & -g v_2/\sqrt{2} & \lambda v_s & 0 & \lambda v_1 \\ 0 & 0 & \lambda v_2 & \lambda v_1 & 2\kappa v_s \end{pmatrix} \begin{pmatrix} -i\tilde{b} \\ -i\tilde{w}^0 \\ \tilde{h}_1^0 \\ \tilde{h}_2^0 \\ \tilde{s} \end{pmatrix} , \quad (2.26)$$

The neutralino mass matrix is diagonalized by a unitary matrix N , such that

$$\chi_i^0 = N_{ij} \psi_j^0 , \quad (2.27)$$

where ψ^0 stands for $(-i\tilde{b}, -i\tilde{w}^0, \tilde{h}_1^0, \tilde{h}_2^0, \tilde{s})$ and χ_i^0 are the neutralino mass eigenstates ordered by increasing mass. Under our simplifying assumptions all the entries of the neutralino mass matrix in eq. (2.26) are real. In this case N becomes a real matrix, as long as the neutralino mass terms are allowed to take on negative signs.

Finally, the charged-Higgs and chargino sectors of the NMSSM are not directly affected by the presence of the singlet superfield. The expressions for the corresponding mass matrices are the same as in the MSSM, once we identify

$$\tan \beta \equiv \frac{v_2}{v_1} , \quad \mu \equiv \lambda v_s , \quad B_\mu \equiv \lambda v_s A_\Sigma + \lambda^2 v_1 v_2 . \quad (2.28)$$

In particular, the chargino mass matrix is as in eq. (2.14), and the charged-Higgs mass is

$$m_{H^\pm}^2 = -\frac{B_\mu}{\cos \beta \sin \beta} + m_W^2 . \quad (2.29)$$

If $\lambda \ll 1$ and $v_s \gg v$ the singlet and the singlino decouple from the Higgs and higgsino sectors of the MSSM, respectively, leaving behind effective μ and B_μ terms as in eq. (2.28). Note that in this limit $B_\mu \approx \lambda \kappa v_s^2$ is driven to large values, unless $\kappa \ll 1$ as well.

2.3 Patterns of supersymmetry breaking

Until superparticles are actually discovered, the only information available on their masses and couplings comes in the form of exclusion bounds. The latter arise both from direct searches for superparticles at high-energy colliders and from indirect constraints such as flavor-violating observables, electroweak precision observables and the prediction for the Higgs-boson mass and couplings. An important aspect of (N)MSSM phenomenology consists in translating the experimental information on the superparticles (or lack thereof) into bounds on the SUSY-breaking parameters of the considered model. Moreover, in any computation of particle properties (such as, e.g., mass or production cross section of Higgs bosons) it is necessary to choose a representative set of SUSY-breaking parameters to assess the importance of the newly-computed contributions.

The soft SUSY-breaking Lagrangian in eqs. (2.2) and (2.3) contains more than a hundred independent parameters, making a general analysis of the parameter space overly complicated. However, if the soft SUSY-breaking mass and interaction terms for the sfermions had a generic structure in flavor space, diagrams with sfermion exchange would induce unacceptably large contributions to flavor-violating processes such as $\mu \rightarrow e\gamma$ decay or $K^0-\bar{K}^0$ mixing, unless the sfermion masses are much larger than the TeV scale. Similarly, generic complex phases in the soft SUSY-breaking terms would induce unacceptably large CP-violating effects. It is therefore reasonable to assume that the soft SUSY-breaking mass and interaction terms for squarks and sleptons are, at least approximately, real and flavor-universal, leading to the minimal-flavor-violation scenario described earlier.

Indeed, MFV scenarios can occur naturally. In most realizations of SUSY breaking, SUSY is spontaneously broken in a *hidden sector* of particles that do not couple directly to squarks and sleptons, but share with them some interaction that eventually transmits the breaking of SUSY to the *visible sector*. If the mediating interaction is flavor blind, the resulting soft SUSY-breaking terms for squarks and sleptons are flavor-universal at the energy scale characteristic of the process that breaks SUSY. Some amount of flavor violation still arises via the renormalization-group (RG) evolution of the soft terms down to the weak scale. However, being controlled by the same Yukawa couplings that induce flavor violation in the quark sector, these effects are not unacceptably large. Two flavor-blind mediating interactions that are commonly considered in the literature are gravity and the ordinary gauge interactions of the SM. A third well-studied mechanism, also involving supergravity, is *anomaly mediation*. Each of these mechanisms is characterized by a small number of independent parameters at the SUSY-breaking scale, and predicts a distinctive pattern of soft terms at the weak scale. Therefore, assuming a specific mechanism of SUSY breaking allows to substantially simplify the analysis of SUSY models. Public computer codes, such as `SoftSusy` [31], `SuSpect` [32] and `SPheno` [33], can then be used to perform the RG evolution of the soft terms between the SUSY-breaking scale and the weak scale and compute the mass spectrum of the model.

In the rest of this section I briefly review the most popular mechanisms of SUSY breaking. I also discuss the alternative approach of setting “by hand” a specific pattern of soft terms at the weak scale, without referring to an underlying SUSY-breaking mechanism at a higher scale.

Gravity mediation: In this class of models it is assumed that the breaking of SUSY is transmitted to the visible sector by interactions (in particular, gravity) that manifest themselves at the Planck scale. The typical scale of the soft SUSY-breaking terms for the MSSM superpartners is $m_{\text{soft}} \sim F/M_P$, where F has dimensions of a squared mass and parameterizes the breaking of SUSY in the hidden sector. In a particularly constrained class of models known as “minimal supergravity” (mSUGRA) or “constrained MSSM” (CMSSM), it is assumed that the interactions that communicate the breaking of SUSY to the visible sector are flavor-blind and insensitive to the gauge quantum numbers of the superparticles. In this case the soft SUSY-breaking masses and trilinear interactions in eqs. (2.2) and (2.3) have universal boundary conditions at the scale M_P :

$$M_1 = M_2 = M_3 = m_{1/2} , \quad (2.30)$$

$$m_{H_1}^2 = m_{H_2}^2 = m_0^2 , \quad m_Q^2 = m_L^2 = m_U^2 = m_D^2 = m_E^2 = m_0^2 I_3 , \quad (2.31)$$

$$T_u = A_0 h_u , \quad T_d = A_0 h_d , \quad T_e = A_0 h_e , \quad (2.32)$$

where I_3 in eq. (2.31) represents the identity in flavor space. The soft SUSY-breaking parameters can then be evolved down to the weak scale via the RG equations of the MSSM, allowing to determine the full mass spectrum of the superpartners from the three Planck-scale parameters $m_{1/2}$, m_0 and A_0 in eqs. (2.30)–(2.32), plus the parameters μ and B_μ and the known values of the various gauge and Yukawa couplings.

In practice, the boundary conditions in eqs. (2.30)–(2.32) are usually imposed at the lower scale $M_{\text{GUT}} \approx 2 \times 10^{16}$ GeV at which the gauge couplings unify, and above which the MSSM is presumably embedded in a grand-unified theory (GUT). Moreover, since any valid choice of GUT-scale parameters must reproduce the measured masses of the SM gauge bosons, it is convenient to exploit the minimization conditions of the Higgs potential at the weak scale, and trade the two parameters B_μ and μ^2 for the vevs v_1 and v_2 , or, equivalently, for the parameters v (which can be extracted from the SM masses) and $\tan \beta$. The CMSSM/mSUGRA scenarios are then characterized by just five input parameters beyond those already present in the SM: universal GUT-scale masses for the scalars (m_0^2) and for the gauginos ($m_{1/2}$), a universal trilinear coupling A_0 , plus $\tan \beta$ and the sign of μ .

In a less-constrained category of models inspired by gravity-mediated SUSY breaking, known as non-universal-Higgs-mass (NUHM) models, the soft SUSY-breaking Higgs masses $m_{H_1}^2$ and $m_{H_2}^2$ are not required to be equal to the sfermion masses at the GUT scale. This allows for two additional input parameters, which are usually chosen as the weak-scale values of μ and B_μ .

In the NMSSM with minimal gravity mediation the GUT-scale boundary conditions on the soft SUSY-breaking terms involving the singlet are $m_S^2 = m_0^2$ and $A_\lambda = A_\kappa = A_0$. The model contains the additional superpotential couplings λ and κ , while μ and B_μ are no longer independent input parameters. In practice, however, the NMSSM with fully universal GUT-scale boundary conditions turns out to be very constrained, and only finely-tuned regions in the parameter space lead to the correct EWSB. It is therefore convenient (and rather common in the literature) to relax the universality

conditions, assuming, e.g., that the mechanism of SUSY breaking treats the singlet differently from the other superfields. In that case, some of the soft SUSY-breaking terms (e.g., m_S^2 or A_k) can be considered as independent parameters at the GUT scale, and possibly traded for weak-scale input parameters such as the singlet vev v_s .

Gauge mediation: In this class of models the breaking of SUSY still happens in a hidden sector, but there is a set of *messenger* superfields that couple both to the SUSY-breaking sector and to the ordinary gauge sector of the MSSM. One-loop diagrams with gaugino-messenger interactions induce soft SUSY-breaking mass terms for the gauginos, while two-loop diagrams with both gaugino-messenger and gauge-boson-messenger interactions induce soft SUSY-breaking mass terms for the MSSM sfermions and the Higgs bosons. Since the gauge interactions are flavor-blind, the induced sfermion masses are flavor-universal.

In the simplest model of gauge-mediated SUSY breaking the messengers belong to one fundamental and one antifundamental multiplet of $SU(5)$, and are characterized by a mass scale M_m and a SUSY-breaking scale F , such that the messenger fermions have masses of order M_m and the messenger scalars have square masses of order $M_m^2 \pm F$. At the scale M_m , the SUSY-breaking masses for the three MSSM gauginos and for the scalars (the latter denoted collectively as ϕ) read

$$M_i = c_i \frac{\alpha_i}{4\pi} \frac{F}{M_m} \quad (i = 1, 2, 3) , \quad (2.33)$$

$$m_\phi^2 = 2 \left(\frac{F}{M_m} \right)^2 \sum_{i=1}^3 \left(\frac{\alpha_i}{4\pi} \right)^2 c_i C_i(\phi) , \quad (2.34)$$

where: $\alpha_i = g_i^2/(4\pi)$, with the gauge couplings ordered as (g', g, g_s) ; the constants c_i are $(5/3, 1, 1)$; $C_i(\phi)$ is the quadratic Casimir invariant of the field ϕ for the gauge group with coupling α_i . Eqs. (2.33) and (2.34) are valid for $F \ll M_m^2$, but they can be easily generalized to the case of larger F , or to the case of a more complicated messenger sector. It can be seen that the gaugino and scalar masses are of the same order in the loop expansion, since the gaugino masses are of $\mathcal{O}(\alpha_i)$ and the *squared* scalar masses are of $\mathcal{O}(\alpha_i^2)$. The trilinear interaction terms $T_{u,d,e}$ are generated only at two loops, thus they are suppressed with respect to the scalar and gaugino masses and they can be approximately considered equal to zero.

The MSSM with gauge-mediated SUSY breaking is therefore rather constrained. Once the structure of the messenger sector (i.e., number and gauge representation of the messenger multiplets) is fixed, the mass spectrum depends only on F and M_m , plus the parameters μ and B_μ which are usually traded for v and $\tan \beta$ at the weak scale. The evolution of the SUSY-breaking parameters from the messenger scale M_m down to the weak scale generates some degree of flavor mixing in the sfermion masses, as well as non-zero values for the trilinear terms, but these effects are generally small. Incidentally, the small value of A_t at the weak scale suppresses the contribution from stop loops to the lightest Higgs-boson mass, making it difficult to accommodate $m_h \approx 125$ GeV in gauge mediation.

Treating v and $\tan\beta$ as independent inputs instead of μ and B_μ does, however, hide a problem specific to models such as gauge mediation in which the soft terms are generated through loop effects. If the “ μ problem” of the MSSM described at the beginning of section 2.2 is addressed by the Giudice-Masiero mechanism, the generic prediction $B_\mu/\mu \sim F/M$ holds, where F and M are the SUSY-breaking parameter and the mass of the mediating field, respectively, for the considered mechanism of SUSY breaking. In gravity-mediated models, where $m_{\text{soft}} \sim F/M$, the prediction is not problematic, as it just implies that $B_\mu \sim m_{\text{soft}}^2$ when $\mu \sim m_{\text{soft}}$. On the other hand, as appears from eqs. (2.33) and (2.34), in gauge-mediated models the soft terms are suppressed by a loop factor, $m_{\text{soft}} \sim \alpha/4\pi \times F/M$. In these models, the prediction of the Giudice-Masiero mechanism implies that B_μ is two or three orders of magnitude larger than m_{soft}^2 , requiring an unnatural fine tuning in the Higgs sector.

For models that suffer from this so-called “ B_μ problem”, the option of extending the Higgs sector by a singlet S whose vev generates both μ and B_μ at the right size – see eq. (2.28) – seems particularly appealing. However, in the NMSSM with gauge mediation the specific form of the soft terms does not allow for a correct pattern of EWSB with an acceptable mass spectrum. The main difficulty lies in generating a sufficiently large vev for the singlet, which requires either a large and negative m_S^2 or large trilinear terms A_λ and A_κ . Indeed, the gauge-singlet nature of S means that it does not acquire a SUSY-breaking mass term through eq. (2.34), and as mentioned above the trilinear SUSY-breaking terms are not generated at leading order in the gauge couplings. In a paper of mine with Delgado and Giudice [3] we studied the structure and phenomenology of a model that circumvents this problem. By coupling the singlet directly to the messenger fields in the superpotential, a negative m_S^2 and non-vanishing trilinears can be generated, at the price of just one additional parameter (the singlet-messenger coupling ξ).

Anomaly mediation: In the conventional framework of gravity mediation, the breaking of SUSY arises in a hidden sector and is then transmitted to the visible sector by direct (but Planck-scale-suppressed) gravitational interactions between hidden-sector and visible-sector superfields. The resulting soft SUSY-breaking terms are of the order of the *gravitino* mass, $m_{\text{soft}} \sim m_{3/2} \sim F/M_P$. In addition to these direct effects, the breaking of SUSY is communicated to the visible sector by quantum effects involving only supergravity. This mechanism is known as “anomaly mediation” because the SUSY-breaking effects are associated to the anomaly of the conformal invariance of supergravity. The anomaly-mediated effects are always present whenever SUSY is broken, but, being due to quantum corrections, they are suppressed by a loop factor with respect to the effects of direct gravity mediation, i.e., $m_{\text{soft}} \sim \alpha/4\pi \times m_{3/2}$. Therefore, anomaly mediation becomes relevant only when there are no direct interactions between the visible sector and the hidden sector – as can be the case, e.g., in extra-dimensional models in which the two sectors live in separate *branes*.

The anomaly-mediated SUSY-breaking terms for the gaugino and scalar masses and for the trilinear interactions are

$$M_i = \frac{1}{g_i} m_{3/2} \frac{dg_i}{d\ln Q} \quad (i = 1, 2, 3) , \quad (2.35)$$

$$m_\phi^2 = \frac{1}{2} m_{3/2}^2 \frac{d\gamma_\phi}{d\ln Q}, \quad (2.36)$$

$$T_{u,d,e} = -m_{3/2} \frac{dh_{u,d,e}}{d\ln Q}, \quad (2.37)$$

where γ_ϕ is the anomalous dimension for the generic scalar ϕ (a matrix in flavor space in the case of squarks and sleptons) and Q is the renormalization scale. The conditions in eqs. (2.35)–(2.37) are RG-invariant to all orders in perturbation theory, thus they can be imposed at any value of Q . They are also extremely constraining, since the only free parameters in anomaly-mediated models are the gravitino mass $m_{3/2}$ and the parameters μ and B_μ which as usual can be traded for v and $\tan\beta$ at the weak scale. Indeed, this class of models is so constrained that it is already ruled out, because eq. (2.36) results in a negative squared mass for the sleptons. Several approaches proposed in the literature to solve this so-called “tachionic slepton problem” rely on the combination of anomaly mediation with other sources of SUSY breaking. A pragmatic (although not necessarily motivated) shortcut consists in adding a common mass parameter m_0^2 for all the scalars at the GUT scale. In this case, the mass spectrum of the model at the weak scale depends on only four parameters in addition to the SM ones: $m_{3/2}$, m_0^2 , $\tan\beta$ and $\text{sign}(\mu)$.

Another peculiar aspect of anomaly-mediated models is that the soft SUSY-breaking masses and trilinear interactions for squarks and sleptons are not flavor-diagonal at any renormalization scale. However, the flavor mixing in the soft terms arises from combinations of matrices of Yukawa couplings, therefore it is not substantially larger than the mixing in the quark sector. In a paper of mine with Allanach, Hiller and Jones [7] we investigated the flavor structure of models with anomaly mediation. We showed that the deviations from flavor-diagonality in the soft masses are in general suppressed, in particular for small or moderate values of $\tan\beta$, and we investigated how this conclusion is affected by different solutions to the tachionic slepton problem. We also studied the constraints on the parameter space of the model resulting from several low-energy flavor observables, the most important of which turned out to be the $B \rightarrow X_s \gamma$ branching ratio.

The “phenomenological (N)MSSM”: Referring to a specific mechanism of SUSY breaking at a high boundary scale reduces drastically the number of independent input parameters, and simplifies the phenomenological analysis of SUSY models. However, this simplification comes at a price: the models are so constrained that potentially interesting regions of the (N)MSSM parameter space might be difficult to access. A typical example is the region with $|X_t|/M_S \approx \sqrt{6}$, in which the corrections to the light Higgs boson mass arising from stop loops are maximized (here $M_S \equiv \sqrt{m_{\tilde{t}_1} m_{\tilde{t}_2}}$, and $X_t = A_t + \mu \cot\beta$ is the left-right mixing term in the stop mass matrix). The RG evolution of A_t and the RG evolution of the soft SUSY-breaking stop masses are correlated, with the result that $|X_t|/M_S < 1$ at the weak scale, unless the trilinear Higgs-stop coupling is very large already at the high scale. This is never the case in gauge-mediated and anomaly-mediated models, while in gravity-mediated models this requires A_0 to be considerably larger than both $m_{1/2}$ and m_0 .

An alternative approach, which makes it easier to study specific corners of the parameter space, consists in fixing directly the soft SUSY-breaking terms at the weak scale, without referring to the underlying mechanism of SUSY breaking. Of course, some simplifying assumptions still need to be made, to avoid dealing with more than a hundred independent parameters. Given the absence of large deviations from the predictions of the SM for CP-violating and flavor-violating processes, it is convenient to assume that all the soft-SUSY breaking terms are real and flavor-diagonal at the weak scale. Furthermore, the soft terms involving sfermions of the first two generations are often assumed to be the same at the weak scale. When flavor-mixing effects are not important, the latter is usually a good approximation also for models in which the soft terms are evolved down from universal boundary conditions, because the deviations from flavor universality are driven only by the Yukawa couplings, which are very small for the first two generations. With this set of simplifying assumptions, the mass spectrum of the MSSM is described by 22 weak-scale parameters beyond those already present in the SM: three gaugino masses (M_1, M_2, M_3); five soft SUSY-breaking masses (m_Q, m_U, m_D, m_L, m_E) and three trilinear couplings (A_t, A_b, A_τ) for the third-generation sfermions; eight equivalent parameters for the first-two-generation sfermions; the superpotential parameter μ ; two additional parameters in the Higgs sector, usually chosen as $\tan\beta$ and m_A (indeed, the minimum conditions of the scalar potential are used to trade the soft masses $m_{H_1}^2$ and $m_{H_2}^2$ for the vevs v_1 and v_2 , with the combination $v_1^2 + v_2^2$ fixed by the gauge boson masses, and B_μ is traded for m_A). This 22-parameter framework is sometimes referred to as “phenomenological MSSM”, or pMSSM.

In the case of the NMSSM, μ and m_A are not independent parameters, because μ and B_μ are induced by the vev of the singlet (moreover, m_A would be ill-defined, because the MSSM-like pseudoscalar mixes with the CP-odd component of the singlet). In addition to the 19 independent soft terms for gauginos and sfermions, the weak-scale input parameters of the “phenomenological NMSSM” are the superpotential couplings λ and κ , the soft SUSY-breaking trilinear interactions A_λ and A_κ , and two additional parameters that can be chosen as $\tan\beta$ and the singlet vev v_s (here the minimum conditions of the scalar potential are used to trade the three soft masses $m_{H_1}^2, m_{H_2}^2$ and m_S^2 for the vevs v_1, v_2 and v_s).

Split supersymmetry: In this scenario of SUSY breaking all of the MSSM scalars, with the exception of a SM-like Higgs, are assumed to be much heavier than the weak scale, while gauginos and higgsinos are light. This is inspired by the fact that most of the problematic aspects of SUSY models (such as, e.g., the flavor problem) are connected to the presence of new light scalars, while most of the advantages (e.g., unification of gauge couplings and neutralino candidate for Dark Matter) are due to the presence of new light fermions. Of course, taking the sfermions much heavier than the weak scale reintroduces fine tuning in the EWSB, undermining the solution to the hierarchy problem which was the original motivation for SUSY. However, it can be argued that an even larger fine tuning exists anyway in the cosmological constant (which is 120 orders of magnitude smaller than its “natural” scale M_P^4), and perhaps both problems can be solved together by another still-unknown mechanism.

In phenomenological studies of split SUSY, the heavy scalars are integrated out at a common mass scale M_S . The effective theory valid below M_S contains the SM particles plus gluino, charginos and neutralinos, and it is fine-tuned and non supersymmetric. However, SUSY dictates the values of the Higgs-higgsino-gaugino couplings and of the Higgs quartic coupling at the high boundary scale, making the scenario extremely predictive. Indeed, the mass spectrum of split SUSY can be determined from just six parameters in addition to the SM ones: the heavy scalar mass M_S ; the angle β that rotates the two Higgs doublets of the MSSM into a light SM-like Higgs and a heavy Higgs (the latter is integrated out at the high scale together with the sfermions); the gaugino masses M_1 , M_2 and M_3 ; the higgsino mass parameter μ . The number of independent inputs can be further reduced by assuming a specific pattern (e.g., universality) for the three gaugino masses at the GUT scale.

A typical prediction of split SUSY is a long lifetime for the gluino, which can lead to peculiar signatures at colliders (indeed, the gluino decays can only proceed via the exchange of heavy virtual squarks and are therefore very suppressed). In an old paper of mine with Gambino and Giudice [15] we presented a one-loop computation of the gluino decay widths, dealing in particular with the resummation of large corrections enhanced by $\ln(M_S/m_{\tilde{g}})$ that are characteristic of split SUSY. In a subsequent paper of mine with Bernal and Djouadi [2] we performed a comprehensive phenomenological analysis of the split-SUSY scenario, based on a full one-loop determination of the Higgs, chargino and neutralino masses. In particular, we considered scenarios where the gaugino masses are non-universal at the GUT scale, which leads to features that are not present in the case of GUT-scale universality. We discussed the constraints from collider searches and high-precision measurements, the cosmological constraints on the relic abundance of the neutralino candidate for Dark Matter, and the gluino lifetime. We then analyzed the decays of the Higgs boson (in particular decays into and contributions of SUSY particles), of charginos and neutralinos (in particular decays into Higgs bosons and photons) and of gluinos, and highlighted the effect of the different boundary conditions on the gaugino masses.

2.4 Input parameters and renormalization schemes

When the theoretical prediction for an observable is computed beyond the leading order in perturbation theory, it becomes necessary to specify a renormalization scheme for the parameters entering the lower-order terms in the calculation. For example, in the NLO-QCD (i.e., two-loop) calculation of the cross section for Higgs production in gluon fusion, the parameters entering the LO (i.e., one-loop) Higgs-gluon-gluon amplitude that are subject to $\mathcal{O}(\alpha_s)$ corrections require a renormalization prescription.

In the computation of radiative corrections within the SM, it is natural to choose the renormalization conditions in such a way that the fundamental parameters of the model (e.g., the top Yukawa coupling in the Lagrangian) are connected to experimentally measured quantities (e.g., the pole mass of the top quark). Such set of renormalization conditions is often called “on-shell” (OS) scheme, referring to the fact that the amplitudes entering the counterterms are evaluated with the external particles on their mass shell. On the other hand, in SUSY extensions of the SM it is not (yet?) possi-

ble to connect all of the fundamental parameters of the model to experimentally measured quantities. Until superpartners of the SM particles and an extended Higgs sector are discovered, the parameters of the soft SUSY-breaking Lagrangian, as well as (in the MSSM case) μ and $\tan\beta$, remain essentially free parameters. In such a situation, the choice of whether to connect the Lagrangian parameters to measurable (but yet unmeasured) quantities such as the superparticle masses, or rather to define them as *running* (i.e., renormalization-scale dependent and, strictly speaking, unphysical) parameters, is essentially a matter of convenience, depending on the kind of analysis that is being performed on the model's parameter space.

When the parameters of the soft SUSY-breaking Lagrangian are obtained via RG evolution from a set of high-energy boundary conditions, as in the gravity-mediation and gauge-mediation scenarios described in the previous section, they are naturally expressed in the modified minimal-subtraction scheme known as $\overline{\text{DR}}$, which is based on dimensional reduction (DRED) and preserves the supersymmetric Ward identities and the supersymmetric relations among couplings. In this case, it is convenient to take all the parameters of the Lagrangian as they come from the RG evolution, and perform the calculations directly in the $\overline{\text{DR}}$ scheme. In particular, the loop integrals are regularized in $4-2\epsilon$ dimensions using DRED, and the counterterms for the parameters entering the lower-order contributions contain only divergent terms (i.e., poles in $1/\epsilon$) that are necessary to cancel the divergences of the loop integrals. In the calculation of a physical observable, the implicit scale dependence of the running parameters entering the lower-order terms is compensated for by an explicit scale dependence of the higher-order terms, in such a way that the final result is scale independent up to the perturbative order considered in the calculation.

If, on the other hand, we do not refer to a set of high-energy boundary conditions for the parameters of the soft SUSY-breaking Lagrangian, but rather take them as input directly at the weak scale, we may choose to express them in terms of yet-unmeasured physical observables. Due to the relative simplicity of the renormalization procedure in the $\overline{\text{DR}}$ scheme, it is convenient to first perform the calculation of a physical observable in that scheme, then translate the result to the desired scheme, which we denote as R . To this purpose, we express the parameters $x_i^{\overline{\text{DR}}}$ entering the lower-order terms as $x_i^{\overline{\text{DR}}} = x_i^R + \delta x_i$, and expand perturbatively the lower-order terms around the x_i^R , i.e. the parameters renormalized in the scheme R . If all of the x_i^R are connected to physical observables, and are therefore scale independent, the effect of the resulting shifts in the higher-order terms will be to cancel their dependence on the scale. Indeed, the explicit scale independence of the whole result in such an OS scheme usually provides a first non-trivial check of the correctness of a calculation.

In the calculations of two-loop SUSY-QCD corrections that will be presented in this dissertation, the δx_i are one-loop shifts of $\mathcal{O}(\alpha_s)$, and the parameters that require a renormalization prescription are the quark masses and the parameters entering the squark mass matrices and the Higgs-squark couplings. Below I discuss in some detail the OS renormalization of the top/stop and bottom/sbottom sectors, while the special case of the renormalization of the flavor-mixing matrix for the down-type squarks, relevant to the calculation of $\text{BR}[B \rightarrow X_s \gamma]$, will be discussed separately in chapter 5.

OS scheme for the top/stop sector: The top mass m_t enters the calculations of two-loop QCD corrections in SUSY extensions of the SM both as the proper mass for the top quark and as a proxy for the Higgs-boson coupling to top quarks and to stop squarks, h_t (indeed, the two are related at tree level by $m_t = h_t v_2$, and the vev v_2 is not subject to $\mathcal{O}(\alpha_s)$ corrections). In the OS scheme, m_t is defined as the pole of the renormalized propagator for the top quark, and the corresponding shift with respect to the $\overline{\text{DR}}$ definition is

$$\delta m_t = \text{Re} \widehat{\Sigma}_t(m_t), \quad (2.38)$$

where $\widehat{\Sigma}_t(m_t)$ is the finite part of the top self-energy computed at an external momentum equal to the top mass.

Among the other parameters entering the Higgs-stop couplings and the stop mass matrix, see eq. (2.11), those that receive $\mathcal{O}(\alpha_s)$ corrections are the soft SUSY-breaking masses m_Q and m_U and the trilinear coupling A_t . However, in the OS scheme commonly adopted for the calculation of radiative corrections in the MSSM the renormalization conditions are imposed directly on the two stop-mass eigenvalues, $m_{\tilde{t}_1}$ and $m_{\tilde{t}_2}$, and on the stop mixing angle θ_t . The renormalized m_Q , m_U and A_t – which usually remain the actual input parameters – are then interpreted as the parameters that would enter a fictitious tree-level stop mass matrix that is diagonalized by the OS stop mixing angle and whose eigenvalues are the OS stop masses. As for the top mass, the OS stop masses are defined as the poles of the renormalized stop propagator (which in this case is a 2×2 matrix), and the shifts with respect to the $\overline{\text{DR}}$ definition are

$$\delta m_{\tilde{t}_1}^2 = \text{Re} \widehat{\Pi}_{11}(m_{\tilde{t}_1}^2), \quad \delta m_{\tilde{t}_2}^2 = \text{Re} \widehat{\Pi}_{22}(m_{\tilde{t}_2}^2), \quad (2.39)$$

where $\widehat{\Pi}_{ii}(m_{\tilde{t}_i}^2)$ denotes the finite parts of the diagonal terms of the stop self-energy computed at an external momentum equal to the corresponding stop mass.

An OS definition for the stop mixing angle is somewhat less obvious because, differently from the case of the stop masses, θ_t is not directly a physical observable. The divergent part of the counterterm for the stop mixing angle is fixed by the requirement that it cancels the divergence of the anti-hermitian part of the stop wave-function renormalization (WFR) matrix. A straightforward OS prescription consists in requiring that the counterterm cancels also the finite part of the anti-hermitian WFR. The resulting shift with respect to the $\overline{\text{DR}}$ definition is

$$\delta \theta_t = \frac{1}{2} \frac{\widehat{\Pi}_{12}(m_{\tilde{t}_1}^2) + \widehat{\Pi}_{12}(m_{\tilde{t}_2}^2)}{m_{\tilde{t}_1}^2 - m_{\tilde{t}_2}^2}, \quad (2.40)$$

where $\widehat{\Pi}_{12}(q^2)$ denotes the finite part of the off-diagonal self-energy of the stops.

The top/stop contributions to physical observables such as the Higgs mass and production cross section can generally be expressed in terms of the five parameters m_t , $m_{\tilde{t}_1}$, $m_{\tilde{t}_2}$, θ_t and A_t , plus other parameters (such as, e.g., μ and $\tan \beta$) that are not subject to $\mathcal{O}(\alpha_s)$ corrections. However, those parameters are not all independent, since they are related to each other by the definition of the stop mixing angle in eq. (2.13). If the OS renormalization conditions for the four parameters m_t , $m_{\tilde{t}_1}$, $m_{\tilde{t}_2}$

and θ_t are fixed by eqs. (2.38)–(2.40), the OS trilinear coupling A_t can be treated as a function of the other parameters, and its shift with respect to the $\overline{\text{DR}}$ definition becomes

$$\delta A_t = \left(\frac{\delta m_{\tilde{t}_1}^2 - \delta m_{\tilde{t}_2}^2}{m_{\tilde{t}_1}^2 - m_{\tilde{t}_2}^2} - \frac{\delta m_t}{m_t} + 2 \cot 2\theta_t \delta\theta_t \right) X_t. \quad (2.41)$$

OS scheme for the bottom/sbottom sector: A proper OS definition for the parameters entering the bottom/sbottom sector involves several complications. The main ones are related to the fact that the SUSY contributions to the shift δm_b between the pole bottom mass and its $\overline{\text{DR}}$ equivalent contain terms enhanced by $\tan\beta$. If we proceed in analogy with the renormalization of the stop sector, i.e., we define the OS bottom and sbottom masses and the sbottom mixing angle via conditions equivalent to those in eqs. (2.38)–(2.40), and derive δA_b from the other shifts as in eq. (2.41), it is easy to see that δA_b contains terms of $\mathcal{O}(\alpha_s \mu^2 \tan^2 \beta / m_{\tilde{g}})$. As a result, the Higgs masses and couplings computed in this “naive” OS scheme are subject to huge radiative corrections when $\tan\beta \gtrsim 30$, putting the validity of the perturbative expansion into question.

A possible solution to this problem was proposed in ref. [25] in the context of the calculation of the two-loop $\mathcal{O}(\alpha_b \alpha_s)$ corrections to the MSSM Higgs masses, then extended in ref. [27] to cover also the case of the Yukawa corrections, and finally revisited in ref. [10] in the context of the calculation of the cross section for Higgs boson production in gluon fusion. The solution requires that we retain only the leading terms in an expansion in the small bottom mass m_b , and that we differentiate the coupling that controls the Higgs-sbottom interactions, which we denote as h_b , from the coupling that controls the Higgs-bottom Yukawa interaction, which we denote as h_b^Y . At the tree level, of course, the two couplings coincide and are related to the bottom mass by $m_b = h_b^Y v_1 = h_b v_1$, but beyond tree level it is possible to impose renormalization conditions separately on h_b , h_b^Y and m_b . In the two-loop calculation of the Higgs masses, only the definition of h_b matters, because h_b^Y and m_b affect only corrections that are not sufficiently enhanced by powers of $\tan\beta$ to compensate for their suppression by powers of m_b . In the two-loop calculation of the cross section, on the other hand, a one-loop definition is required also for h_b^Y and m_b , as will be discussed in chapter 3.

Focusing here on the parameters that determine the sbottom masses and couplings, those requiring a one-loop definition are m_Q , m_D , h_b and A_b . Three of those parameters can be traded for $m_{\tilde{b}_1}$, $m_{\tilde{b}_2}$ and θ_b , which allow for OS definitions analogous to those adopted in the stop sector:

$$\delta m_{\tilde{b}_1}^2 = \text{Re} \widehat{\Pi}_{11}(m_{\tilde{b}_1}^2), \quad \delta m_{\tilde{b}_2}^2 = \text{Re} \widehat{\Pi}_{22}(m_{\tilde{b}_2}^2), \quad \delta\theta_b = \frac{1}{2} \frac{\widehat{\Pi}_{12}(m_{\tilde{b}_1}^2) + \widehat{\Pi}_{12}(m_{\tilde{b}_2}^2)}{m_{\tilde{b}_1}^2 - m_{\tilde{b}_2}^2}. \quad (2.42)$$

The OS definitions for h_b and A_b , on the other hand, differ from those adopted in the stop sector. Instead of relating h_b to the pole bottom mass and treating A_b as a function of the other parameters, we consider two quantities that are function of both h_b and A_b :

$$\tilde{X}_b = h_b v_1 (A_b + \mu \tan\beta), \quad \tilde{Y}_b = \frac{h_b}{\sqrt{2}} \sin\beta (A_b - \mu \cot\beta). \quad (2.43)$$

These quantities allow for a natural interpretation: at tree level, $\tilde{X}_b \equiv h_b v_1 X_b$ is the off-diagonal term in the sbottom mass matrix, see eq. (2.12), while \tilde{Y}_b is proportional to the coefficient of the trilinear interaction ($\tilde{b}_1 \tilde{b}_2^* A$). The relation between \tilde{X}_b and θ_b in eq. (2.13), together with the OS definitions for the sbottom masses and mixing angle in eq. (2.42), can immediately be translated into a prescription for \tilde{X}_b :

$$\delta \tilde{X}_b = \frac{1}{2} \cos 2\theta_b \left[\hat{\Pi}_{12}(m_{\tilde{b}_1}^2) + \hat{\Pi}_{12}(m_{\tilde{b}_2}^2) \right] + \tilde{X}_b \frac{\hat{\Pi}_{11}(m_{\tilde{b}_1}^2) - \hat{\Pi}_{22}(m_{\tilde{b}_2}^2)}{m_{\tilde{b}_1}^2 - m_{\tilde{b}_2}^2}. \quad (2.44)$$

The shift in \tilde{Y}_b could be defined via a physical process such as, e.g., one of the decays $\tilde{b}_1 \rightarrow \tilde{b}_2 A$ or $A \rightarrow \tilde{b}_1 \tilde{b}_2^*$, but this definition would suffer from the problem of infrared (IR) singularities associated with gluon radiation. To overcome this problem, and given our current ignorance of the MSSM mass spectrum, we find it less restrictive to define $\delta \tilde{Y}_b$ in terms of the ($\tilde{b}_1 \tilde{b}_2^* A$) proper vertex, at appropriately chosen external momenta and including suitable wave function corrections, so that the resulting combination is IR finite and gauge independent. Denoting the proper vertex $\tilde{b}_1 \tilde{b}_2^* A$ as $i\Lambda(p_1^2, p_2^2, p_A^2)$, we define

$$\begin{aligned} \delta \tilde{Y}_b &= -\frac{i}{2} \left[\Lambda(m_{\tilde{b}_1}^2, m_{\tilde{b}_1}^2, 0) + \Lambda(m_{\tilde{b}_2}^2, m_{\tilde{b}_2}^2, 0) \right] \\ &+ \frac{\tilde{Y}_b}{2} \frac{\hat{\Pi}_{11}(m_{\tilde{b}_1}^2) + \hat{\Pi}_{22}(m_{\tilde{b}_1}^2) - \hat{\Pi}_{11}(m_{\tilde{b}_2}^2) - \hat{\Pi}_{22}(m_{\tilde{b}_2}^2)}{m_{\tilde{b}_1}^2 - m_{\tilde{b}_2}^2}, \end{aligned} \quad (2.45)$$

whose IR finiteness and gauge independence were explicitly shown in ref. [25]. Finally, the shifts of the parameters h_b and A_b are related to those of \tilde{X}_b and \tilde{Y}_b by ¹

$$\delta h_b = \frac{\sin \beta}{\mu v} \left(\delta \tilde{X}_b - \delta \tilde{Y}_b v \cot \beta \right), \quad \delta A_b = \frac{\sqrt{2}}{h_b^2 \mu v} \left(\tilde{X}_b \delta \tilde{Y}_b - \tilde{Y}_b \delta \tilde{X}_b \right), \quad (2.46)$$

and the explicit evaluation of δh_b and δA_b shows that they are both free of $\tan \beta$ -enhanced terms.

In any phenomenological analysis of the MSSM, we will need to make use of the experimental information on the bottom mass to determine the numerical value of the OS Higgs-sbottom coupling h_b . To this effect, several steps are necessary: we take as input the SM bottom mass in the $\overline{\text{MS}}$ scheme, $m_b(m_b)_{\text{SM}}^{\overline{\text{MS}}}$, as determined from the Υ masses; we evolve it up to some reference scale Q_0 of the order of the weak scale by means of suitable renormalization group equations; finally, we convert the SM mass to the $\overline{\text{DR}}$ scheme, thus obtaining $\overline{m}_b \equiv m_b(Q_0)_{\text{SM}}^{\overline{\text{DR}}}$. Including the SUSY threshold corrections, we can then extract the corresponding running mass in the MSSM:

$$\hat{m}_b \equiv m_b(Q_0)_{\text{MSSM}}^{\overline{\text{DR}}} = \frac{\overline{m}_b (1 + \delta_b)}{1 + \epsilon_b \tan \beta}, \quad (2.47)$$

where δ_b denotes terms in the SUSY contribution to the bottom self-energy that are not enhanced by

¹Note that the normalization of the parameter v differs by a factor $\sqrt{2}$ from the one adopted in refs. [10, 25, 27].

$\tan\beta$ and, to $\mathcal{O}(\alpha_s)$,

$$\epsilon_b = \frac{\alpha_s C_F}{4\pi} \frac{2\mu m_{\tilde{g}}}{m_{\tilde{b}_1}^2 - m_{\tilde{b}_2}^2} \left(\frac{m_{\tilde{b}_1}^2}{m_{\tilde{g}}^2 - m_{\tilde{b}_1}^2} \ln \frac{m_{\tilde{b}_1}^2}{m_{\tilde{g}}^2} - \frac{m_{\tilde{b}_2}^2}{m_{\tilde{g}}^2 - m_{\tilde{b}_2}^2} \ln \frac{m_{\tilde{b}_2}^2}{m_{\tilde{g}}^2} \right), \quad (2.48)$$

where $C_F = 4/3$ is a color factor. The OS-renormalized Higgs-sbottom coupling h_b is then obtained from \widehat{m}_b by subtracting the shift computed in eq. (2.46):

$$h_b = \frac{\widehat{m}_b}{v_1} - \delta h_b. \quad (2.49)$$

By including $\epsilon_b \tan\beta$ in the denominator of the r.h.s. of eq. (2.47), we “resum” in \widehat{m}_b – and hence in h_b – the $\tan\beta$ -enhanced threshold corrections to the relation between the mass and the Yukawa coupling of the bottom quarks, to all orders in an expansion in powers of $\alpha_s \tan\beta$ [45, 46].

An additional complication is due to the fact that the $SU(2)$ symmetry of the soft SUSY-breaking Lagrangian relates the parameter m_Q^2 in the upper-left entry of the sbottom mass matrix, eq. (2.12), to the corresponding parameter in the upper-left entry of the stop mass matrix, eq. (2.11). In our OS scheme, denoting the parameter in the sbottom mass matrix as $m_{Q,\tilde{b}}^2$ and the one in the stop mass matrix as $m_{Q,\tilde{t}}^2$, we have

$$m_{Q,\tilde{b}}^2 = m_{Q,\tilde{t}}^2 + \delta m_{Q,\tilde{t}}^2 - \delta m_{Q,\tilde{b}}^2, \quad (2.50)$$

where, for $\tilde{q} = (\tilde{t}, \tilde{b})$,

$$\delta m_{Q,\tilde{q}}^2 = \cos^2\theta_q \delta m_{\tilde{q}_1}^2 + \sin^2\theta_q \delta m_{\tilde{q}_2}^2 - (m_{\tilde{q}_1}^2 - m_{\tilde{q}_2}^2) \sin 2\theta_q \delta\theta_q - 2m_q \delta m_q. \quad (2.51)$$

In practice, we take $m_{Q,\tilde{t}}$ as the actual input parameter, and compute $m_{Q,\tilde{b}}$ by means of eqs. (2.50) and (2.51). Finally, we write the sbottom mass matrix in terms of the OS-renormalized parameters $m_{Q,\tilde{b}}$, m_D , h_b and A_b , and diagonalize it to obtain the actual values of the sbottom masses and mixing angle.

Our OS scheme for the sbottom sector, first outlined in ref. [25], has been subject of further study by other groups, in the context of the calculation of two-loop corrections to the Higgs masses [47] and of the one-loop corrections to stop decays into a sbottom and a charged Higgs or W boson [48]. The authors of refs. [47, 48] also considered other schemes that avoid the occurrence of $\tan\beta$ -enhanced counterterm contributions, in particular a scheme in which h_b and A_b are defined as $\overline{\text{DR}}$ -renormalized quantities and θ_b is treated as a function of the other parameters. It turns out that, apart from some pathological points of the parameter space, the results obtained in the “ $\tan\beta$ -conscious” schemes are in good agreement with each other. The calculation of the Higgs boson masses and mixing angle implemented in the public computer code `FeynHiggs` [30] also relies on our OS scheme for the sbottom sector. If the Higgs masses and mixing computed by `FeynHiggs` are in turn used as input of another calculation – such as, e.g., the calculation of the Higgs production cross section – consistency requires that the same scheme for the renormalization of the sbottom parameters be used in both calculations (or, in alternative, that the input parameters for the sbottom sector be appropriately translated to the different scheme used in the downstream calculation).

Chapter 3

Higgs-boson production in gluon fusion

The main mechanism for the production of the SM Higgs boson at the LHC is the loop-induced gluon fusion, where the coupling of the gluons to the Higgs is mediated by loops of quarks, primarily the top. The knowledge of this process in the SM is quite advanced, including the full NLO-QCD corrections; the NNLO-QCD corrections from top loops; soft-gluon resummation effects; the first-order EW corrections; estimates of the NNNLO-QCD corrections and of the mixed QCD-EW corrections. Nevertheless, the theoretical uncertainty of the SM calculation, estimated at 15% for the production of a Higgs boson with mass around 125 GeV [34, 35, 36], remains significant.

In the MSSM the couplings of the neutral Higgs bosons to gluons are mediated primarily by top and bottom quarks and their supersymmetric partners, the stop and sbottom squarks. As in the SM, gluon fusion is one of the most important mechanisms for Higgs production. However, for the bosons whose couplings to down-type fermions are enhanced by $\tan\beta$, the production in bottom-quark annihilation can also be important (or even dominant) in specific regions of the MSSM parameter space.

The cross section for MSSM Higgs boson production in gluon fusion is currently known at the NLO (although approximate calculations of NNLO effects exist). The contributions arising from diagrams with quarks and gluons, with full dependence on the Higgs and quark masses, can be obtained from the corresponding SM results [49, 50] with an appropriate rescaling of the Higgs-quark couplings. The contributions arising from diagrams with squarks and gluons were first computed under the approximation of vanishing Higgs mass in ref. [51], and the full Higgs-mass dependence was included in later calculations [52, 53, 54, 55]. On the other hand, a full calculation of the two-loop diagrams with quarks, squarks and gluinos – which can involve up to five different particle masses – is still missing. Calculations based on a combination of analytic and numerical methods were presented in refs. [37, 38], but neither explicit analytic formulae nor public computer codes have been made available so far.

Approximate results for the quark-squark-gluino contributions can however be obtained assuming the presence of some hierarchy between the Higgs boson mass and the masses of the particles running in the loops. If the Higgs boson is lighter than all the particles in the loops, it is reasonable to Taylor-

expand the result in powers of the Higgs mass, with the first term in the expansion corresponding to the so-called vanishing-Higgs-mass limit (VHML). This limit was adopted in ref. [39] for the calculation of the top-stop-gluino contributions to scalar production and in ref. [40] for the analogous calculation of pseudoscalar production. In refs. [6, 12] we reproduced the VHML result of refs. [39, 40], and we discussed the validity of the VHML approximation by considering the next term in the expansion in the Higgs mass.

While a Taylor expansion in the Higgs mass is indeed a viable approximation in the computation of the top-stop-gluino contributions to the production of the lightest scalar h , it might not be applicable to the production of the heaviest scalar H and of the pseudoscalar A , if their mass is comparable to the mass of the top quark. Moreover, a Taylor expansion in the Higgs mass is certainly useless in the calculation of the bottom-sbottom-gluino contributions, due to the presence of a light bottom quark. To overcome these limitations, in refs. [10, 12, 14] we provided results for the production of both scalars and pseudoscalars based on an asymptotic expansion in the superparticle masses, which does not assume any hierarchy between the Higgs-boson mass and the mass of the quark in the loop. In particular, we retained terms up to $\mathcal{O}(m_\phi^2/M^2)$, $\mathcal{O}(m_t^2/M^2)$, $\mathcal{O}(m_b/M)$ and $\mathcal{O}(m_Z^2/M^2)$, where m_ϕ denotes a Higgs boson mass and M denotes a generic superparticle mass. Such an expansion is applicable to both top-stop-gluino and bottom-sbottom-gluino contributions, as long as the squarks and the gluino are heavier than the considered Higgs boson and the top quark.

After a summary of general results on Higgs production in gluon fusion, I discuss in this chapter our calculations of the two-loop quark-squark-gluino contributions to the production of scalar [6, 10, 14] and pseudoscalar [12] Higgs bosons, as well as our implementation of the SUSY contributions in public codes for the computation of the Higgs-production cross section [13, 35, 36].

3.1 Higgs production via gluon fusion in the MSSM

Gluon-fusion cross section at NLO: The hadronic cross section for neutral Higgs boson production at center-of-mass energy \sqrt{s} can be written as

$$\sigma(h_1 + h_2 \rightarrow \phi + X) = \sum_{a,b} \int_0^1 dx_1 dx_2 f_{a,h_1}(x_1, \mu_F) f_{b,h_2}(x_2, \mu_F) \times \int_0^1 dz \delta\left(z - \frac{\tau_\phi}{x_1 x_2}\right) \hat{\sigma}_{ab}(z), \quad (3.1)$$

where $\phi = (h, H, A)$, $\tau_\phi = m_\phi^2/s$, μ_F is the factorization scale, $f_{a,h_i}(x, \mu_F)$, the parton density of the colliding hadron h_i for the parton of type a , ($a = g, q, \bar{q}$) and $\hat{\sigma}_{ab}$ the cross section for the partonic subprocess $ab \rightarrow \phi + X$ at the center-of-mass energy $\hat{s} = x_1 x_2 s = m_\phi^2/z$. The latter can be written in terms of the LO contribution $\sigma^{(0)}$ as

$$\hat{\sigma}_{ab}(z) = \sigma^{(0)} z G_{ab}(z). \quad (3.2)$$

The LO partonic cross section for the $gg \rightarrow \phi$ process can be written as

$$\sigma^{(0)} = \frac{G_\mu \alpha_s^2(\mu_R)}{128 \sqrt{2} \pi} \left| \mathcal{H}_\phi^{1\ell} \right|^2, \quad (3.3)$$

where G_μ is the muon decay constant, $\alpha_s(\mu_R)$ is the strong gauge coupling expressed in the $\overline{\text{MS}}$ renormalization scheme at the scale μ_R , and \mathcal{H}_ϕ is the form factor for the coupling of the neutral Higgs boson ϕ with two gluons, which we decompose in one- and two-loop parts as

$$\mathcal{H}_\phi = \mathcal{H}_\phi^{1\ell} + \frac{\alpha_s}{\pi} \mathcal{H}_\phi^{2\ell} + \mathcal{O}(\alpha_s^2). \quad (3.4)$$

The coefficient function $G_{ab}(z)$ in eq. (3.2) can in turn be decomposed, up to NLO terms, as

$$G_{ab}(z) = G_{ab}^{(0)}(z) + \frac{\alpha_s}{\pi} G_{ab}^{(1)}(z) + \mathcal{O}(\alpha_s^2), \quad (3.5)$$

with the LO contribution given only by the gluon-fusion channel:

$$G_{ab}^{(0)}(z) = \delta(1-z) \delta_{ag} \delta_{bg}. \quad (3.6)$$

The NLO terms include, besides the gg channel, also the one-loop induced gq and $q\bar{q}$ channels:

$$\begin{aligned} G_{gg}^{(1)}(z) &= \delta(1-z) \left[C_A \frac{\pi^2}{3} + \beta_0 \ln \left(\frac{\mu_R^2}{\mu_F^2} \right) + 2 \text{Re} \left(\frac{\mathcal{H}_\phi^{2\ell}}{\mathcal{H}_\phi^{1\ell}} \right) \right] \\ &+ P_{gg}(z) \ln \left(\frac{\hat{s}}{\mu_F^2} \right) + C_A \frac{4}{z} (1-z+z^2)^2 \mathcal{D}_1(z) + C_A \mathcal{R}_{gg}, \end{aligned} \quad (3.7)$$

$$G_{q\bar{q}}^{(1)}(z) = \mathcal{R}_{q\bar{q}}, \quad G_{qg}^{(1)}(z) = P_{qg}(z) \left[\ln(1-z) + \frac{1}{2} \ln \left(\frac{\hat{s}}{\mu_F^2} \right) \right] + \mathcal{R}_{qg}, \quad (3.8)$$

where the LO Altarelli-Parisi splitting functions are

$$P_{gg}(z) = 2C_A \left[\mathcal{D}_0(z) + \frac{1}{z} - 2 + z(1-z) \right], \quad P_{gq}(z) = C_F \frac{1+(1-z)^2}{z}. \quad (3.9)$$

In the equations above, $C_A = N_c$ and $C_F = (N_c^2 - 1)/(2N_c)$ (N_c being the number of colors), $\beta_0 = (11C_A - 2N_f)/6$ (N_f being the number of active flavors) is the one-loop β -function of the strong coupling in the SM, and

$$\mathcal{D}_i(z) = \left[\frac{\ln^i(1-z)}{1-z} \right]_+. \quad (3.10)$$

The two-loop virtual contributions to $gg \rightarrow \phi$, regularized by the infrared-singular part of the contributions from one-loop gluon-fusion diagrams with the emission of a real gluon, $gg \rightarrow \phi g$, are contained in the first line of eq. (3.7). The second line of that equation contains instead the non-singular contributions from real gluon emission. Eq. (3.8) contains the contributions due to the one-loop quark-antiquark annihilation channel, $q\bar{q} \rightarrow \phi g$, and to the one-loop quark-gluon scattering channel, $gq \rightarrow q\phi$. General expressions for the functions \mathcal{R}_{gg} , $\mathcal{R}_{q\bar{q}}$, \mathcal{R}_{qg} entering eqs. (3.7) and (3.8) are available. They can be found in ref. [54] for the case of scalar production and in ref. [12] for the case of pseudoscalar production (see also ref. [49] for an earlier computation of the quark contributions in both cases).

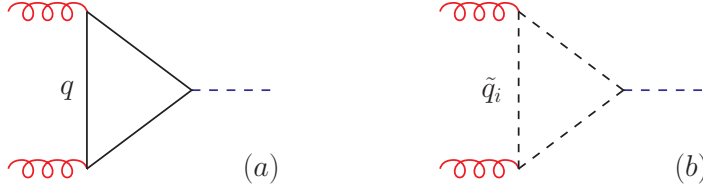


Figure 3.1: Examples of one-loop diagrams for $gg \rightarrow \phi$ involving a quark or a squark.

Form factors for scalar Higgs production: The form factors for the production of the lightest and heaviest scalar mass eigenstates can be decomposed as

$$\mathcal{H}_h = T_F (-\sin \alpha \mathcal{H}_1 + \cos \alpha \mathcal{H}_2) , \quad \mathcal{H}_H = T_F (\cos \alpha \mathcal{H}_1 + \sin \alpha \mathcal{H}_2) , \quad (3.11)$$

where $T_F = 1/2$ is a color factor, α is the mixing angle in the CP-even Higgs sector and \mathcal{H}_i ($i = 1, 2$) are the form factors for the coupling of the neutral, CP-even component of the Higgs doublet H_i with two gluons. Focusing on the contributions involving the third-generation quarks and squarks, and exploiting the structure of the Higgs-quark-quark and Higgs-squark-squark couplings, we can write to all orders in the strong interaction [6]

$$\mathcal{H}_1 = \lambda_t [m_t \mu s_{2\theta_t} F_t + m_Z^2 s_{2\beta} D_t] + \lambda_b [m_b A_b s_{2\theta_b} F_b + 2m_b^2 G_b + 2m_Z^2 c_\beta^2 D_b] , \quad (3.12)$$

$$\mathcal{H}_2 = \lambda_b [m_b \mu s_{2\theta_b} F_b - m_Z^2 s_{2\beta} D_b] + \lambda_t [m_t A_t s_{2\theta_t} F_t + 2m_t^2 G_t - 2m_Z^2 s_\beta^2 D_t] . \quad (3.13)$$

In the equations above $\lambda_t = 1/\sin \beta$ and $\lambda_b = 1/\cos \beta$, and the parameters μ , A_q (for $q = t, b$) and θ_q are defined in section 2.1 (note that in this section I use the notation $s_\varphi \equiv \sin \varphi$, $c_\varphi \equiv \cos \varphi$ for a generic angle φ). The functions F_q and G_q appearing in eqs. (3.12) and (3.13) denote the contributions controlled by the third-generation Yukawa couplings, while D_q denotes the contribution controlled by the electroweak, D-term-induced Higgs-squark-squark couplings. The latter can be decomposed as

$$D_q = \frac{I_{3q}}{2} \tilde{G}_q + c_{2\theta_t} \left(\frac{I_{3q}}{2} - Q_q s_{\theta_W}^2 \right) \tilde{F}_q , \quad (3.14)$$

where I_{3q} denotes the third component of the electroweak isospin of the quark q , and Q_q denotes its electric charge.

The one-loop parts of the form factors, $\mathcal{H}_i^{1\ell}$, contain contributions from diagrams involving quarks (figure 3.1a) or squarks (figure 3.1b). The functions entering $\mathcal{H}_i^{1\ell}$ are

$$F_q^{1\ell} = \tilde{F}_q^{1\ell} = \frac{1}{2} \left[\frac{1}{m_{\tilde{q}_1}^2} \mathcal{G}_0^{1\ell}(\tau_{\tilde{q}_1}) - \frac{1}{m_{\tilde{q}_2}^2} \mathcal{G}_0^{1\ell}(\tau_{\tilde{q}_2}) \right] , \quad (3.15)$$

$$G_q^{1\ell} = \frac{1}{2} \left[\frac{1}{m_{\tilde{q}_1}^2} \mathcal{G}_0^{1\ell}(\tau_{\tilde{q}_1}) + \frac{1}{m_{\tilde{q}_2}^2} \mathcal{G}_0^{1\ell}(\tau_{\tilde{q}_2}) + \frac{1}{m_q^2} \mathcal{G}_{1/2}^{1\ell}(\tau_q) \right] , \quad (3.16)$$

$$\tilde{G}_q^{1\ell} = \frac{1}{2} \left[\frac{1}{m_{\tilde{q}_1}^2} \mathcal{G}_0^{1\ell}(\tau_{\tilde{q}_1}) + \frac{1}{m_{\tilde{q}_2}^2} \mathcal{G}_0^{1\ell}(\tau_{\tilde{q}_2}) \right] , \quad (3.17)$$

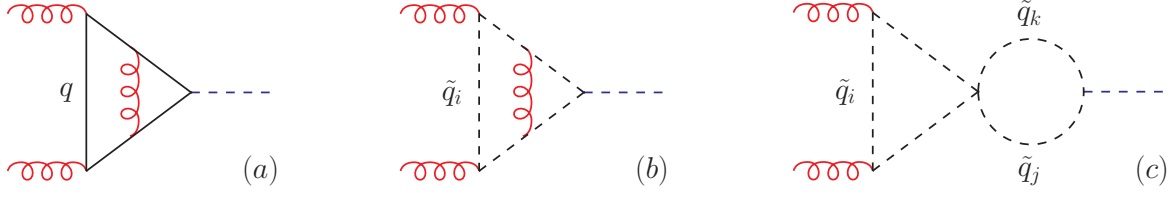


Figure 3.2: Examples of two-loop diagrams for $gg \rightarrow \phi$ that do not involve gluinos.

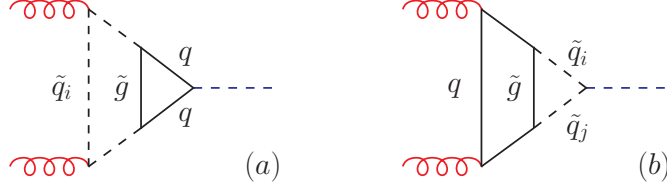


Figure 3.3: Examples of two-loop diagrams for $gg \rightarrow \phi$ involving gluinos.

where $\tau_k \equiv 4m_k^2/m_\phi^2$ (with $\phi = h, H$), and the functions $\mathcal{G}_0^{1\ell}$ and $\mathcal{G}_{1/2}^{1\ell}$ read

$$\mathcal{G}_0^{1\ell}(\tau) = \tau \left[1 + \frac{\tau}{4} \ln^2 \left(\frac{\sqrt{1-\tau}-1}{\sqrt{1-\tau}+1} \right) \right], \quad (3.18)$$

$$\mathcal{G}_{1/2}^{1\ell}(\tau) = -2\tau \left[1 - \frac{1-\tau}{4} \ln^2 \left(\frac{\sqrt{1-\tau}-1}{\sqrt{1-\tau}+1} \right) \right]. \quad (3.19)$$

It is useful to recall the behavior of $\mathcal{G}_0^{1\ell}$ and $\mathcal{G}_{1/2}^{1\ell}$ in the limit in which the Higgs boson mass is much smaller or much larger than the mass of the particle running in the loop. In the VHML, which can be applied to the top and squark contributions for the light-Higgs case,

$$\mathcal{G}_0^{1\ell} \rightarrow -\frac{1}{3}, \quad \mathcal{G}_{1/2}^{1\ell} \rightarrow -\frac{4}{3}, \quad (3.20)$$

while in the opposite case, i.e. $\tau \ll 1$, which is always relevant for the bottom contribution,

$$\mathcal{G}_0^{1\ell} \rightarrow \tau + \mathcal{O}(\tau^2), \quad \mathcal{G}_{1/2}^{1\ell} \rightarrow -2\tau + \frac{\tau}{2} \ln^2\left(\frac{-4}{\tau}\right) + \mathcal{O}(\tau^2). \quad (3.21)$$

The analytic continuations are obtained with the replacement $m_\phi^2 \rightarrow m_\phi^2 + i\epsilon$, thus the imaginary part of $\mathcal{G}_{1/2}^{1\ell}$ in eq. (3.21) can be recovered via the replacement $\ln(-4/\tau) \rightarrow \ln(4/\tau) - i\pi$.

The two-loop parts of the form factors, $\mathcal{H}_i^{2\ell}$, contain contributions from diagrams involving quarks, squarks, gluons and gluinos, such as the ones depicted in figures 3.2 and 3.3. The functions $F_q^{2\ell}$, $G_q^{2\ell}$, $\tilde{F}_q^{2\ell}$ and $\tilde{G}_q^{2\ell}$ entering the two-loop parts of eqs. (3.12) and (3.13) can be decomposed as

$$F_q^{2\ell} = Y_{\tilde{q}_1} - Y_{\tilde{q}_2} - \frac{4c_{2\theta_q}^2}{m_{\tilde{q}_1}^2 - m_{\tilde{q}_2}^2} Y_{c_{2\theta_q}^2}, \quad (3.22)$$

$$G_q^{2\ell} = Y_{\tilde{q}_1} + Y_{\tilde{q}_2} + Y_q, \quad (3.23)$$

$$\tilde{F}_q^{2\ell} = Y_{\tilde{q}_1} - Y_{\tilde{q}_2} + \frac{4 s_{2\theta_q}^2}{m_{\tilde{q}_1}^2 - m_{\tilde{q}_2}^2} Y_{c_{2\theta_q}^2}, \quad (3.24)$$

$$\tilde{G}_q^{2\ell} = Y_{\tilde{q}_1} + Y_{\tilde{q}_2}. \quad (3.25)$$

The various terms in eqs. (3.22)–(3.25) can be split in the contributions coming from diagrams with (s)quarks and gluons (g , figures 3.2a and 3.2b); with a quartic squark coupling ($4\tilde{q}$, figure 3.2c); with quarks, squarks and gluinos (\tilde{g} , figures 3.3a and 3.3b):

$$Y_x = Y_x^g + Y_x^{4\tilde{q}} + Y_x^{\tilde{g}} \quad (x = q, \tilde{q}_1, \tilde{q}_2, c_{2\theta_q}^2). \quad (3.26)$$

Furthermore, the term Y_q entering eq. (3.23) contains only contributions from diagrams with a Higgs-quark coupling, figures 3.2a and 3.3a, therefore $Y_q^{4\tilde{q}} = 0$. On the other hand, the terms $Y_{\tilde{q}_1}$, $Y_{\tilde{q}_2}$ and $Y_{c_{2\theta_q}^2}$ in eqs. (3.22)–(3.25) contain only contributions from diagrams with a Higgs-squark coupling, figures 3.2b, 3.2c, and 3.3b. Our computation of the quark-squark-gluino contributions to the terms Y_x in eq. (3.26) will be discussed in detail in section 3.2.

The contribution to the term Y_q arising from two-loop diagrams with quarks and gluons (figure 3.2a) has been computed for arbitrary values of the Higgs and quark masses [49, 50]. If the contribution of the one-loop diagram with a quark q to the form factors $\mathcal{H}_i^{1\ell}$ is expressed in terms of the quark mass renormalized in the $\overline{\text{DR}}$ scheme, the two-loop quark-gluon contribution reads:

$$2m_q^2 Y_q^g = C_F \left[\mathcal{F}_{1/2}^{(2\ell,a)}(x_q) + \left(\ln \frac{m_q^2}{Q^2} - \frac{1}{3} \right) \mathcal{F}_{1/2}^{(2\ell,b)}(x_q) \right] + C_A \mathcal{G}_{1/2}^{(2\ell,C_A)}(x_q), \quad (3.27)$$

where $C_F = 4/3$ and $C_A = 3$ are color factors, Q is the renormalization scale and exact expressions for $\mathcal{F}_{1/2}^{(2\ell,a)}$, $\mathcal{F}_{1/2}^{(2\ell,b)}$ and $\mathcal{G}_{1/2}^{(2\ell,C_A)}$ as functions of $x_q \equiv (\sqrt{1-\tau_q} - 1)/(\sqrt{1-\tau_q} + 1)$ are given in eqs. (2.12), (2.13) and (3.8) of ref. [53], respectively. If the one-loop quark contribution to the form factors is expressed in terms of the pole quark mass, the term multiplying $\mathcal{F}_{1/2}^{(2\ell,b)}$ in eq. (3.27) is replaced by $4/3$. In the VHML, i.e. for $\tau_q \rightarrow \infty$, the one-loop quark contribution and the two-loop quark-gluon contribution do not depend on the quark mass, and eq. (3.27) reduces to $2m_q^2 Y_q^g = C_F - 5C_A/3$.

The contributions to the terms $Y_{\tilde{q}_1}$, $Y_{\tilde{q}_2}$ and $Y_{c_{2\theta_q}^2}$ arising from two-loop diagrams with squarks and gluons (figure 3.2b) and from diagrams with a quartic squark coupling (figure 3.2c) can, to the accuracy required by our expansions, be computed in the VHML. If the parameters entering one-loop squark contributions to the form factors \mathcal{H}_i in eqs. (3.12) and (3.13) are expressed in the $\overline{\text{DR}}$ renormalization scheme at the scale Q , the two-loop contributions read [6]

$$Y_{\tilde{q}_1}^g = -\frac{1}{2m_{\tilde{q}_1}^2} \left(\frac{3C_F}{4} + \frac{C_A}{6} \right), \quad (3.28)$$

$$Y_{\tilde{q}_1}^{4\tilde{q}} = -\frac{C_F}{24} \left[\frac{c_{2\theta_q}^2 m_{\tilde{q}_1}^2 + s_{2\theta_q}^2 m_{\tilde{q}_2}^2}{m_{\tilde{q}_1}^4} + \frac{s_{2\theta_q}^2}{m_{\tilde{q}_1}^4 m_{\tilde{q}_2}^2} \left(m_{\tilde{q}_1}^4 \ln \frac{m_{\tilde{q}_1}^2}{Q^2} - m_{\tilde{q}_2}^4 \ln \frac{m_{\tilde{q}_2}^2}{Q^2} \right) \right], \quad (3.29)$$

$$Y_{c_{2\theta_q}^2}^{4\tilde{q}} = -\frac{C_F}{24} \left[\frac{(m_{\tilde{q}_1}^2 - m_{\tilde{q}_2}^2)^2}{m_{\tilde{q}_1}^2 m_{\tilde{q}_2}^2} - \frac{m_{\tilde{q}_1}^2 - m_{\tilde{q}_2}^2}{m_{\tilde{q}_2}^2} \ln \frac{m_{\tilde{q}_1}^2}{Q^2} - \frac{m_{\tilde{q}_2}^2 - m_{\tilde{q}_1}^2}{m_{\tilde{q}_1}^2} \ln \frac{m_{\tilde{q}_2}^2}{Q^2} \right]. \quad (3.30)$$

The term $Y_{c_{2\theta_q}^g}$ is zero, while the terms $Y_{\tilde{q}_2}^g$ and $Y_{\tilde{q}_2}^{4\tilde{q}}$ can be obtained by performing the substitutions $\tilde{q}_1 \leftrightarrow \tilde{q}_2$ in eqs. (3.28) and (3.29), respectively.

Form factors for pseudoscalar Higgs production: To fix the notation, the Lagrangian for the interactions of the pseudoscalar A with quarks and squarks reads

$$\mathcal{L} \supset \frac{i}{\sqrt{2}} h_t c_\beta A \bar{t} \gamma_5 t + \frac{i}{\sqrt{2}} h_b s_\beta A \bar{b} \gamma_5 b + \frac{i}{\sqrt{2}} \left(h_t c_\beta Z_t A \tilde{t}_1^* \tilde{t}_2 + h_b s_\beta Z_b A \tilde{b}_1^* \tilde{b}_2 - \text{h.c.} \right), \quad (3.31)$$

where $Z_t = A_t - \mu \tan \beta$ and $Z_b = A_b - \mu \cot \beta$. The fact that the pseudoscalar only couples to two different squark mass eigenstates, while gluons only couple to two equal eigenstates, implies that the form factor \mathcal{H}_A receives neither one-loop contributions from diagrams with squarks nor two-loop contributions from diagrams with squarks and gluons. However, contributions to $\mathcal{H}_A^{1\ell}$ do arise from the diagram in figure 3.1a involving top or bottom quarks. Also, contributions to $\mathcal{H}_A^{2\ell}$ arise from two-loop diagrams with quarks and gluons, figure 3.2a, as well as from two-loop diagrams with quarks, squarks and gluinos, figures 3.3a and 3.3b.

The one-loop form factor $\mathcal{H}_A^{1\ell}$ can be decomposed into top and bottom contributions as

$$\mathcal{H}_A^{1\ell} = T_F \left[\cot \beta \mathcal{K}^{1\ell}(\tau_t) + \tan \beta \mathcal{K}^{1\ell}(\tau_b) \right], \quad (3.32)$$

where

$$\mathcal{K}^{1\ell}(\tau) = \frac{\tau}{2} \ln^2 \left(\frac{\sqrt{1-\tau}-1}{\sqrt{1-\tau}+1} \right). \quad (3.33)$$

We recall the behavior of $\mathcal{K}^{1\ell}$ in the limit in which the pseudoscalar mass is much smaller or much larger than the mass of the particle running in the loop. In the VHML, which may apply to the top contribution if m_A is relatively small,

$$\mathcal{K}^{1\ell}(\tau) \longrightarrow -2, \quad (3.34)$$

while in the opposite case, i.e. $\tau \ll 1$, which is relevant for the bottom contribution,

$$\mathcal{K}^{1\ell}(\tau) \longrightarrow \frac{\tau}{2} \ln^2 \left(\frac{-4}{\tau} \right) + \mathcal{O}(\tau^2). \quad (3.35)$$

The two-loop form factor for pseudoscalar production can in turn be decomposed as

$$\mathcal{H}_A^{2\ell} = T_F \left[\cot \beta \left(\mathcal{K}_{t\tilde{g}}^{2\ell} + \mathcal{K}_{t\tilde{t}\tilde{g}}^{2\ell} \right) + \tan \beta \left(\mathcal{K}_{b\tilde{g}}^{2\ell} + \mathcal{K}_{b\tilde{b}\tilde{g}}^{2\ell} \right) \right], \quad (3.36)$$

where $\mathcal{K}_{q\tilde{g}}^{2\ell}$ denotes the quark-gluon contributions, and $\mathcal{K}_{q\tilde{q}\tilde{g}}^{2\ell}$ denotes the quark-squark-gluino contributions. If the one-loop form factor is expressed in terms of the running quark mass, renormalized in the $\overline{\text{DR}}$ scheme at the scale Q , the two-loop quark-gluon contribution reads

$$\mathcal{K}_{q\tilde{g}}^{2\ell} = C_F \left[\mathcal{E}_t^{(2\ell,a)}(x_q) + \left(\ln \frac{m_q^2}{Q^2} - \frac{1}{3} \right) \mathcal{E}_t^{(2\ell,b)}(x_q) \right] + C_A \mathcal{K}_t^{(2\ell,CA)}(x_q). \quad (3.37)$$

Expressions for the functions $\mathcal{E}_t^{(2\ell,a)}$, $\mathcal{E}_t^{(2\ell,b)}$ and $\mathcal{K}_t^{(2\ell,CA)}$, valid for arbitrary values of x_q , can be found in eqs. (4.6), (4.7) and (4.12) of ref. [53], respectively.

Gluonic and photonic Higgs decays: The results of our calculations for Higgs production in gluon fusion can be directly applied to the NLO computation of the gluonic decay widths of the Higgs bosons. At NLO in QCD, the decay width of a Higgs boson $\phi = (h, H, A)$ in two gluons reads

$$\Gamma(\phi \rightarrow gg) = \frac{G_\mu \alpha_s(\mu_R)^2 m_\phi^3}{16 \sqrt{2} \pi^3} \left| \mathcal{H}_\phi^{1\ell} \right|^2 \left(1 + \frac{\alpha_s}{\pi} \mathcal{C}^\phi \right), \quad (3.38)$$

where $\mathcal{C}^\phi = \mathcal{C}_{virt}^\phi + \mathcal{C}_{ggg}^\phi + \mathcal{C}_{gq\bar{q}}^\phi$ includes contributions from the two-loop virtual corrections and from the one-loop real radiation processes $\phi \rightarrow ggg$, $\phi \rightarrow gq\bar{q}$. The contribution of the two-loop virtual corrections is similar to the corresponding contribution to Higgs production, eq. (3.7)

$$\mathcal{C}_{virt}^\phi = C_A \frac{\pi^2}{3} + \beta_0 \ln \left(\frac{\mu_R^2}{m_\phi^2} \right) + 2 \operatorname{Re} \left(\frac{\mathcal{H}_\phi^{2\ell}}{\mathcal{H}_\phi^{1\ell}} \right), \quad (3.39)$$

while the contributions of the real radiation processes can be extracted from refs. [49, 54, 12]. In the VHML, they become

$$\mathcal{C}_{ggg}^\phi = -C_A \left(\frac{\pi^2}{3} - \frac{73}{12} \right), \quad \mathcal{C}_{gq\bar{q}}^\phi = -\frac{7}{6} N_f, \quad (3.40)$$

where N_f is the number of light quark species, with the quarks treated as massless particles.

As a byproduct of our calculations, we can also provide the explicit results for the two-loop QCD corrections to the quark/squark contributions to the photonic Higgs decay. The partial width for the decay of a neutral Higgs boson ϕ in two photons can be written as

$$\Gamma(\phi \rightarrow \gamma\gamma) = \frac{G_\mu \alpha_{em}^2 m_\phi^3}{128 \sqrt{2} \pi^3} |\mathcal{P}_\phi|^2, \quad (3.41)$$

where α_{em} is the electromagnetic coupling and \mathcal{P}_ϕ is defined, in analogy to the \mathcal{H}_ϕ in eq. (3.3), as the form factor for the coupling of the Higgs boson ϕ with two photons. At one loop, the form factors \mathcal{P}_h and \mathcal{P}_H receive contributions from all the electrically charged states of the MSSM (see, e.g., ref. [49] for the explicit results), and at least one of them is usually dominated by the contribution of the diagram involving the W boson. The form factor \mathcal{P}_A , on the other hand, receives one-loop contributions only from quarks and charginos. However, only the contributions involving quarks or squarks receive QCD corrections at two loops. We separate the one-loop part of the form factors and the two-loop QCD corrections as

$$\mathcal{P}_\phi = \mathcal{P}_\phi^{1\ell} + \frac{\alpha_s}{\pi} \mathcal{P}_\phi^{2\ell} + \dots, \quad (3.42)$$

where the ellipses stand for three-loop terms of $\mathcal{O}(\alpha_s^3)$ and for two-loop terms controlled by other coupling constants. To convert the two-loop form factors for the Higgs-gluon-gluon coupling, $\mathcal{H}_\phi^{2\ell}$, into the corresponding form factors for the Higgs-photon-photon coupling, $\mathcal{P}_\phi^{2\ell}$, it is sufficient to set $C_A = 0$ and $T_F = 1$ in our explicit formulae for $\mathcal{H}_\phi^{2\ell}$, and multiply the contributions involving the quark/squark q by $Q_q^2 N_c$, where Q_q is the electric charge and $N_c = 3$ is the number of colors.

3.2 Computation of the quark-squark-gluino contributions

In this section I describe the computations of refs. [6, 10, 12, 14] for the top-stop-gluino and bottom-sbottom-gluino contributions to the production of scalar and pseudoscalar Higgs bosons.

Taylor expansion and the low-energy theorem: The diagrams for the two-loop quark-squark-gluino contributions to the Higgs-gluon-gluon amplitude can depend on as much as five different masses (i.e., the masses of the quark, the two squarks and the gluino, plus the external momentum which, for on-shell Higgs production, corresponds to the Higgs mass). An exact analytic evaluation of such diagrams is, at the moment, beyond our computational ability, but an approximation can be obtained by Taylor-expanding in the external momentum the integrands of the loop integrals. The results can then be expressed in terms of vacuum integrals, i.e., integrals of diagrams with vanishing external momenta, for which exact evaluations exist [56]. However, such an approximation is valid only if the Higgs mass is below the lowest threshold encountered in the diagrams, thus it cannot be applied to diagrams involving bottom quarks. For what concerns the top-stop-gluino contributions, the approximation is good for the production of h (due to the upper bound on its mass in the MSSM), while for H and A it is valid only in specific regions of the parameter space.

The zeroth-order term in the Taylor expansion, which corresponds to the result in the VHML, can be obtained without even computing explicitly the Higgs-gluon-gluon vertex diagrams. The starting point of our derivation is the low-energy theorem (LET) for Higgs interactions [57, 58], relating the amplitude $\mathcal{M}(X, \phi)$ for a generic particle configuration X plus an external Higgs boson ϕ of vanishing momentum to the corresponding amplitude without the external Higgs boson, $\mathcal{M}(X)$. The LET can be stated as follows: the amplitude $\mathcal{M}(X, \phi)$ can be obtained by considering $\mathcal{M}(X)$ as a field-dependent quantity via the dependence of the relevant parameters (masses and mixing angles) on ϕ . The first term in the expansion of $\mathcal{M}(X)$ in the Higgs field, evaluated at the minimum of the Higgs potential, corresponds to $\mathcal{M}(X, \phi)$. Strictly speaking, in case $\mathcal{M}(X)$ contains infrared (IR) divergent terms the theorem applies to the IR-safe part of the two amplitudes. If ϕ represents a pseudoscalar Higgs boson and X a pair of vector bosons, an additional contribution to $\mathcal{M}(X, \phi)$ is induced by the axial-current anomaly. This contribution cannot be expressed in terms of derivatives of $\mathcal{M}(X)$ and must be computed explicitly.

To derive the CP-even Higgs-gluon-gluon form factors in the VHML we apply the LET, identifying $\mathcal{M}(X)$ with the gluon self-energy computed in the background-field gauge [59]. Then, the top/stop contributions to the form factors \mathcal{H}_i ($i = 1, 2$) are given by

$$\mathcal{H}_i \Big|_{m_\phi^2=0}^{\text{top/stop}} = \frac{2\pi\sqrt{2}v}{\alpha_s T_F} \frac{\partial \Pi^t(0)}{\partial S_i}, \quad (3.43)$$

where $v \approx 174$ GeV is the EWSB parameter, S_i ($i = 1, 2$) are the CP-even parts of the neutral components of the two MSSM Higgs doublets and $\Pi^t(q^2)$ denotes the top/stop contribution to the transverse part of the adimensional (i.e. divided by q^2) self-energy of the gluon. In analogy with the

procedure of ref. [23] for the calculation of the corrections to the Higgs-boson masses, the dependence of $\Pi^t(q^2)$ on the Higgs fields S_i can be identified through the field dependence of the top and stop masses and of the stop mixing angle. The gluon self-energy depends also on a fifth field-dependent parameter related to the phase difference between the top and stop fields. However, this parameter is relevant only when one consider derivatives with respect to the CP-odd fields, thus it can be ignored in our case. As in ref. [23], a lengthy but straightforward application of the chain rule allows us to express the functions F_t , G_t , \tilde{F}_t and \tilde{G}_t entering eqs. (3.12)–(3.14) as combinations of the derivatives of the gluon self-energy with respect to the top and stop masses and to the stop mixing angle. In particular, we find for the two-loop terms Y_x in eqs. (3.22)–(3.25)

$$Y_t = \frac{\partial \tilde{\Pi}}{\partial m_t^2}, \quad Y_{\tilde{t}_1} = \frac{\partial \tilde{\Pi}}{\partial m_{\tilde{t}_1}^2}, \quad Y_{\tilde{t}_2} = \frac{\partial \tilde{\Pi}}{\partial m_{\tilde{t}_2}^2}, \quad Y_{c_{2\theta_t}^2} = \frac{\partial \tilde{\Pi}}{\partial c_{2\theta_t}^2}, \quad (3.44)$$

where, to reduce clutter, we used the shortcut $\tilde{\Pi} \equiv (2/T_F)\Pi^{2\ell,t}(0)$, after decomposing the gluon self-energy in one- and two-loop parts as

$$\Pi(q^2) = \frac{\alpha_s}{\pi}\Pi^{1\ell}(q^2) + \left(\frac{\alpha_s}{\pi}\right)^2\Pi^{2\ell}(q^2) + \mathcal{O}(\alpha_s^3). \quad (3.45)$$

We computed the contributions to the gluon self-energy from the two-loop diagrams that involve top and/or stops with the help of **FeynArts** [60], using a version of the MSSM model file adapted to the background-field gauge. After isolating the transverse part of the self-energy with a suitable projector, we Taylor-expanded it in powers of the squared external momentum q^2 . The zeroth-order term of the expansion vanishes as a consequence of gauge invariance, while the first-order term corresponds indeed to $\Pi^{2\ell,t}(0)$. We evaluated the two-loop vacuum integrals using the approach of ref. [56], in which the results are expressed in terms of a “master function” $\Phi(m_1^2, m_2^2, m_3^2)$. Finally, we computed all the derivatives of $\tilde{\Pi}$ that enter eq. (3.44), exploiting a recursive relation for the derivatives of the function Φ given in appendix A of ref. [26].

We performed the two-loop computation using dimensional regularization (DREG) and modified minimal subtraction ($\overline{\text{MS}}$). However, it is convenient to express our results for the Higgs-production form factors in terms of parameters renormalized in the $\overline{\text{DR}}$ scheme, which is based on dimensional reduction (DRED) and preserves the supersymmetric Ward identities and relations. The conversion of the parameters from the $\overline{\text{MS}}$ scheme to the $\overline{\text{DR}}$ scheme was discussed in ref. [61]. In particular, the $\overline{\text{DR}}$ Higgs-quark-quark Yukawa couplings differ from their $\overline{\text{MS}}$ counterparts by a finite one-loop shift which, when inserted in the one-loop part of a calculation, induces an additional two-loop contribution. On the other hand, the couplings of the Higgs bosons to squarks, as far as strong corrections are concerned, are the same in both schemes, and they are related by supersymmetry to the corresponding $\overline{\text{DR}}$ Yukawa couplings. Specializing to our calculation, only the top contribution to $\mathcal{H}_2^{1\ell}$ is going to induce an additional two-loop contribution when the top Yukawa coupling is converted from its $\overline{\text{MS}}$ value to its $\overline{\text{DR}}$ value, while the stop contributions to $\mathcal{H}_1^{1\ell}$ and $\mathcal{H}_2^{1\ell}$ can be directly identified as expressed in terms of $\overline{\text{DR}}$ parameters. However, as can be seen from eqs. (3.13), (3.16) and (3.20), in the VHML the

top-quark contribution to $\mathcal{H}_2^{1\ell}$ goes to a constant, i.e. it does not actually depend on the top Yukawa coupling. Therefore, in this limit we need not introduce any additional contribution to the two-loop results obtained using DREG.

Our LET calculation does indeed yield the result of eq. (3.27), in the VHML, for the top-gluon contributions to the form factor, and the results of eqs. (3.28)–(3.30) for the stop-gluon and four-stop contributions. The formulae for the contributions of the two-loop diagrams that involve gluinos are somewhat longer, but they have been presented in explicit form in the appendix of ref. [6].

To test the validity of our LET approach, we also computed directly the two-loop top/stop contribution to the Higgs-gluon-gluon amplitude via a Taylor expansion in the external Higgs momentum up to terms of $\mathcal{O}(m_\phi^2/M^2)$ – where $\phi = h, H$, and M denotes generically the masses of the heavy particles in the loop (i.e. top, stops and gluino). In the calculation of the Higgs-gluon-gluon amplitude we followed the same strategy described above for the calculation of the two-loop gluon self-energy. The zeroth-order term in the Taylor expansion reproduces the result that we obtained via the LET, while the $\mathcal{O}(m_\phi^2/M^2)$ term in the expansion gives the first correction to the VHML. The analytic expressions for the $\mathcal{O}(m_\phi^2/M^2)$ corrections are very long and we did not report them. However, as will be described in section 3.3, we used those results to assess the validity of the Taylor expansion in the region where the Higgs mass is comparable to (or even larger than) the masses of the heavy particles running in the loops.

Asymptotic expansion in the SUSY masses: In the case of diagrams involving bottom quarks, as well as in the case of diagrams involving top quarks if the Higgs boson is sufficiently heavy, the evaluation of the quark-squark-gluino diagrams via a Taylor expansion in the Higgs mass is no longer viable. However, in regions of the MSSM parameter space where all of the SUSY particles are heavier than the Higgs boson and the quarks we can resort to an approximate evaluation of the diagrams via an asymptotic expansion in the heavy masses.

After generating with the help of `FeynArts` the two-loop diagrams involving quark, squark and gluino that contribute to the process $g(q_1) + g(q_2) \rightarrow \phi(q)$, we separate them in two classes: in class *A* the diagrams that can be evaluated via an ordinary Taylor expansion in powers of q^2/M^2 , and in class *B* the diagrams that require an asymptotic expansion. We recall that the Taylor expansion of a two-loop diagram in the external momentum q^2 is viable for values of q^2 up to the first physical threshold. In our case, diagrams with a physical threshold at $q^2 = 4m_q^2$, when Taylor-expanded in q^2 , exhibit an infrared (IR) divergent behavior as $m_q \rightarrow 0$. Thus, these diagrams belong to class *B*.

The Taylor expansion allows us to express the diagrams belonging to class *A* in terms of two-loop vacuum integrals that can be evaluated using the results of ref. [56]. To compute a diagram belonging to class *B*, on the other hand, we isolate the part that becomes infrared (IR) divergent when m_q and q^2 are sent to zero, and subtract it from the original diagram. The remainder, being by construction IR-safe, can be evaluated via a Taylor expansion in the same way as the class-*A* diagrams, while the IR-divergent part is evaluated separately, retaining its full dependence on m_q and q^2 .

The IR-divergent part of a diagram is isolated in the following way. We first note that in all the diagrams entering our calculation one can choose a routing of momenta such that the connecting propagators, i.e. the propagators that contain both integration momenta k_1 and k_2 , are always accompanied by a heavy mass M . Furthermore, only one subintegration, let us assume the one on k_2 , is IR divergent. Then, one can rewrite the connecting propagators using the identity

$$\frac{1}{(k_1 + k_2)^2 - M^2} = \frac{1}{k_1^2 - M^2} - \frac{k_2^2 + 2k_1 \cdot k_2}{[(k_1 + k_2)^2 - M^2](k_1^2 - M^2)}. \quad (3.46)$$

The first term on the r.h.s. of eq. (3.46) leads to a disconnected integral (product of two one-loop integrals) that contains the IR-divergent contributions present in the original diagram. This term can be evaluated exactly, i.e. for arbitrary q^2 , giving rise to the $\ln(q^2/m_q^2)$ terms that describe the physical threshold. The second term, instead, leads to a two-loop integral with improved infrared convergence in the k_2 integration and improved ultraviolet convergence in the k_1 integration. In general, a repeated application of eq. (3.46) allows us to construct the IR-divergent part of any diagram in terms of products of one-loop integrals with numerators that contain terms of the form $(k_i \cdot q_j)^m$, $(k_i \cdot k_j)^n$ ($i, j = 1, 2$) where m, n are generic powers. The Passarino-Veltman reduction method is then applied to eliminate the numerators and express the result in terms of the known one-loop scalar integrals [62]. Finally, one verifies explicitly that the IR-divergent part of the original diagram is canceled by the terms constructed via eq. (3.46), so that the result for the IR-safe part is free of any $\ln(q^2/m_q^2)$ or q^2/m_q^2 terms.

With the techniques described above, in refs. [10, 12] we obtained explicit analytic formulae for the gluino contributions to the two-loop terms Y_x in eqs. (3.22)–(3.25). In our general formula we retained only terms that contribute to the form factors \mathcal{H}_i up to $\mathcal{O}(m_q^2/M^2)$, $\mathcal{O}(m_\phi^2/M^2)$ or $\mathcal{O}(m_Z^2/M^2)$, where M denotes a generic superparticle mass, but we did not make any assumption on the ratio $\tau_q \equiv 4m_q^2/m_\phi^2$. Assuming that the contribution of the one-loop diagram with a quark q to the form factors $\mathcal{H}_i^{1\ell}$ is expressed in terms of the $\overline{\text{DR}}$ -renormalized quark mass, which we denote as \hat{m}_q , the quark-squark-gluino contributions to the term Y_q , arising from diagrams with a Higgs-quark coupling (figure 3.3a), read

$$2m_q^2 Y_q^{\tilde{g}} = \frac{4}{3} \mathcal{F}_{1/2}^{(2\ell, b)}(\tau_q) \frac{\delta m_q^{SUSY}}{m_q} - \frac{C_F}{4} \mathcal{G}_{1/2}^{1\ell}(\tau_q) \frac{m_{\tilde{g}}}{m_q} s_{2\theta_q} \left(\frac{m_{\tilde{q}_1}^2}{m_{\tilde{g}}^2 - m_{\tilde{q}_1}^2} \ln \frac{m_{\tilde{q}_1}^2}{m_{\tilde{g}}^2} - \frac{m_{\tilde{q}_2}^2}{m_{\tilde{g}}^2 - m_{\tilde{q}_2}^2} \ln \frac{m_{\tilde{q}_2}^2}{m_{\tilde{g}}^2} \right) + s_{2\theta_q} \frac{m_q}{m_{\tilde{g}}} \mathcal{R}_1 + \frac{m_q^2}{m_{\tilde{g}}^2} \mathcal{R}_2, \quad (3.47)$$

where δm_q^{SUSY} denotes the squark-gluino contribution to the quark self-energy, in units of α_s/π , expanded in powers of m_q up to terms of $\mathcal{O}(m_q^3)$. Ref. [12] contains explicit expressions for the quark-mass-suppressed terms \mathcal{R}_1 and \mathcal{R}_2 in the second line of eq. (3.47), as well as for the terms $Y_{\tilde{q}_i}^{\tilde{g}}$ and $Y_{c_{2\theta_q}^{\tilde{g}}}$ which arise from diagrams with a Higgs-squark coupling (figure 3.3b). As a check of the correctness of our procedure, we verified that by taking the limit $m_\phi \rightarrow 0$ in the results of our asymptotic expansion

we obtain for the top-stop-gluino contributions the same result that we would obtain by expanding the VHML results of ref. [6] in powers of m_t up to and including $\mathcal{O}(m_t^2/M^2)$.

Considering the hierarchy between the bottom mass and the other masses, we can choose to retain only terms up to $\mathcal{O}(m_b/M)$, $\mathcal{O}(m_b^2/m_\phi^2)$ or $\mathcal{O}(m_b^2/M^2)$ in the bottom-sbottom-gluino contributions. To this effect, it is sufficient to Taylor-expand to $\mathcal{O}(\tau_b)$ all the loop functions – such as, e.g., $\mathcal{G}_{1/2}^{1\ell}(\tau_b)$ – that enter our general formulae for the asymptotic expansion of the quark-squark-gluino contributions, and drop all the terms that contribute beyond the desired order in powers of m_b .

If the one-loop quark contribution to the form factors is expressed in terms of the pole quark mass, which we denote as M_q , the first term in the right-hand side of eq. (3.47) cancels out. Moreover, if the one-loop quark contribution expressed in terms of M_q is multiplied by the ratio \widehat{m}_q/M_q , the term $Y_q = Y_q^g + Y_q^{\tilde{g}}$ is further shifted as

$$2m_q^2 Y_q \longrightarrow 2m_q^2 Y_q - \mathcal{G}_{1/2}^{1\ell}(\tau_q) \frac{\delta m_q}{m_q}, \quad (3.48)$$

where δm_q is the total quark self-energy in units of α_s/π , i.e. it contains both a quark-gluon and a squark-gluino contribution. As a result of this shift, the terms enhanced by $m_{\tilde{g}}/m_q$ in the right-hand side of eq. (3.47) cancel out as well. This manipulation amounts to differentiating, in the one-loop contribution, between the parameter that describes the mass of the quark running in the loop – which is identified with the pole mass – and the parameter that describes the Yukawa coupling of the quark to the Higgs boson – which is identified with the $\overline{\text{DR}}$ mass. As will be discussed in section 3.4, the definition of the quark mass and of the Higgs-quark coupling entering the one-loop result has a crucial impact on the bottom-sbottom-gluino contributions, which, as appears from eq. (3.47), may contain terms enhanced by the large ratio $m_{\tilde{g}}/m_b$.

On-shell scheme for the squark parameters: As mentioned above, our explicit results for the two-loop form factors for scalar production have been derived under the assumption that the corresponding one-loop form factors are expressed in terms of $\overline{\text{DR}}$ -renormalized parameters at some scale Q . However, they can be easily adapted to a different renormalization scheme, such as, e.g., the OS scheme described in section 2.4 and implemented in the code `FeynHiggs` for the calculation of the Higgs boson masses and mixing angle. The effect on the two-loop form factors of the different definitions of the quark masses and Yukawa couplings entering the quark contributions to the one-loop form factors has already been discussed above. For what concerns the squark contributions, the conversion from the $\overline{\text{DR}}$ scheme to a generic scheme R results in a shift in the two-loop form factors:

$$\mathcal{H}_i^{2\ell} \longrightarrow \mathcal{H}_i^{2\ell} + \frac{\partial \mathcal{H}_i^{1\ell, \tilde{q}}}{\partial x_k} \delta x_k, \quad (3.49)$$

where x_k denote the parameters subject to $\mathcal{O}(\alpha_s)$ corrections that enter the squark contributions to the one-loop form factors, $\mathcal{H}_i^{1\ell, \tilde{q}}$, and $\delta x_k \equiv x_k^{\overline{\text{DR}}} - x_k^R$ in units of α_s/π . In the OS scheme of section 2.4, the parameters x_k correspond to $m_{\tilde{t}_i}^2$, θ_t , A_t and m_t in the stop sector, and to $m_{\tilde{b}_i}^2$, θ_b , A_b and h_b

in the sbottom sector (where we differentiate the Higgs-sbottom coupling h_b from the bottom mass and Yukawa coupling). The specific form of the shift in the two-loop form factors depends on the expansion (Taylor or asymptotic) used to simplify the loop integrals, and detailed formulae for the different cases can be found in refs. [6, 10, 14]. As a useful check of the consistency of our calculations, we verified that in each case the explicit dependence on the renormalization scale Q cancels out of the two-loop form factors when the one-loop form factors are fully expressed in terms of OS (and thus scale-independent) parameters.

Pseudoscalar production: We also computed the quark-squark-gluino contributions to the form factor for the production of the MSSM pseudoscalar A , using both a Taylor expansion and an asymptotic expansion in the heavy SUSY masses.

A non-trivial technical issue that arises in calculation of the form factor for pseudoscalar production is the treatment of the Dirac matrix γ_5 – an intrinsically four-dimensional object – within regularization methods defined in a number of dimensions $n_d = 4 - 2\epsilon$. The original calculation of the two-loop quark-gluon contributions of ref. [49] was performed in DREG, employing the 't Hooft-Veltman prescription [63] for the γ_5 matrix and introducing a finite multiplicative renormalization factor [64] to restore the Ward identities. In the context of supersymmetric models, it might be preferable to perform the calculation in DRED, which, differently from DREG, preserves supersymmetry. The latter method does not require the introduction of finite renormalization factors, but it involves additional subtleties concerning the treatment of the Levi-Civita symbol $\varepsilon_{\mu\nu\rho\sigma}$.

In our calculation of the quark-squark-gluino contributions we avoided all problems related to the treatment of γ_5 by employing the Pauli-Villars regularization (PVREG) method. Since all the diagrams contributing to the virtual NLO contributions to pseudoscalar production are at most logarithmically UV-divergent, PVREG can be implemented by subtracting from the original diagrams the same diagrams with some of the masses replaced by a PV mass regulator M_{PV} , and then taking the limit $M_{PV} \rightarrow \infty$ after the calculation of the loop integrals. In particular, in the evaluation of the quark-squark-gluino contributions to $\mathcal{H}_A^{2\ell}$, see eq. (3.36), the two-loop integrals are regularized by subtracting from each of them the same expression with $m_{q_1}^2$ and $m_{q_2}^2$ replaced by M_{PV}^2 . Being defined in four dimensions, the PVREG method respects both SUSY and the chiral symmetry, therefore no symmetry-restoring renormalization factors need to be introduced.

To start with, we tested our implementation of PVREG by computing the top-gluon contributions via an asymptotic expansion in the top quark mass, and recovering the result obtained in DREG in refs. [49, 53]. In our calculation, the IR divergences are regularized by giving a mass λ to the gluon, while the UV divergences are regularized by subtracting to any term a replica in which λ is replaced by M_{PV} . The final result is then obtained taking the limits $M_{PV} \rightarrow \infty$ and $\lambda \rightarrow 0$. The fact that this procedure gives the correct result is quite non-trivial, because it is known that, in general, regularizing the IR divergences via a fictitious gluon mass does not respect the non-abelian symmetry of $SU(3)$. However, we quantize the Lagrangian employing the background-field method (BFM) [59], so that the

external background gluons satisfy QED-like Ward identities. We also remark that within the BFM the renormalization of the strong gauge coupling is due only to the wave function renormalization of the external background gluons. Thus, the renormalization of α_s decouples completely from the rest of the calculation, and can be treated separately in the standard way. As a consequence, even if PVREG is used to regularize the loop integrals, the LO partonic cross section $\sigma^{(0)}$ can be directly expressed in terms of the running coupling $\alpha_s(\mu_R)$ as in eq. (3.3).

We then computed the top-stop-guino contribution $\mathcal{K}_{t\bar{t}\tilde{g}}^{2\ell}$ in eq. (3.36) via a Taylor expansion in the external Higgs momentum up to terms of $\mathcal{O}(m_A^2/m_t^2)$ and $\mathcal{O}(m_A^2/M^2)$, where M denotes generically the stop and guino masses. Such expansion should give a reasonable approximation to the full result when m_A is small compared to the other masses, and is anyway restricted to values of m_A below the lowest threshold encountered in the diagrams (this usually means $m_A < 2m_t$). In the limit of vanishing m_A we find that our result for $\mathcal{K}_{t\bar{t}\tilde{g}}^{2\ell}$ can be cast in an extremely compact form:

$$\mathcal{K}_{t\bar{t}\tilde{g}}^{2\ell} = \left(\frac{s_{2\theta_t}}{2} - \frac{m_t Z_t}{m_{\tilde{t}_1}^2 - m_{\tilde{t}_2}^2} \right) \left[f(m_{\tilde{g}}^2, m_t^2, m_{\tilde{t}_1}^2) - f(m_{\tilde{g}}^2, m_t^2, m_{\tilde{t}_2}^2) \right], \quad (3.50)$$

where

$$\begin{aligned} f(m_{\tilde{g}}^2, m_t^2, m_{\tilde{t}_i}^2) &= C_F \frac{m_{\tilde{g}}}{m_t \Delta} \left[m_{\tilde{t}_i}^2 (m_{\tilde{g}}^2 - m_t^2 + m_{\tilde{t}_i}^2) \ln \frac{m_{\tilde{t}_i}^2}{m_{\tilde{g}}^2} + m_{\tilde{t}_i}^2 (m_{\tilde{g}}^2 + m_t^2 - m_{\tilde{t}_i}^2) \ln \frac{m_{\tilde{t}_i}^2}{m_{\tilde{g}}^2} \right. \\ &\quad \left. + 2 m_{\tilde{g}}^2 m_{\tilde{t}_i}^2 \Phi(m_{\tilde{g}}^2, m_t^2, m_{\tilde{t}_i}^2) \right] \\ &+ C_A \frac{m_t}{m_{\tilde{g}} \Delta} \left[m_{\tilde{t}_i}^2 (m_{\tilde{t}_i}^2 - m_t^2 - m_{\tilde{g}}^2) \ln \frac{m_t^2}{m_{\tilde{g}}^2} + m_{\tilde{t}_i}^2 (m_t^2 - m_{\tilde{t}_i}^2 - m_{\tilde{g}}^2) \ln \frac{m_{\tilde{t}_i}^2}{m_{\tilde{g}}^2} \right. \\ &\quad \left. + m_{\tilde{g}}^2 (m_t^2 + m_{\tilde{t}_i}^2 - m_{\tilde{g}}^2) \Phi(m_{\tilde{g}}^2, m_t^2, m_{\tilde{t}_i}^2) \right], \end{aligned} \quad (3.51)$$

the function $\Phi(m_{\tilde{g}}^2, m_t^2, m_{\tilde{t}_i}^2)$ is given, e.g., in appendix A of ref. [26], and we introduced the shortcut $\Delta = m_t^4 + m_{\tilde{g}}^4 + m_{\tilde{t}_i}^4 - 2(m_t^2 m_{\tilde{g}}^2 + m_t^2 m_{\tilde{t}_i}^2 + m_{\tilde{g}}^2 m_{\tilde{t}_i}^2)$. As appears from eqs. (3.32) and (3.34), in the limit of vanishing m_A the one-loop top contribution to \mathcal{H}_A reduces to $-\cot \beta$, i.e., it does not actually depend on any parameter subject to $\mathcal{O}(\alpha_s)$ corrections. Therefore, the results in eqs. (3.50) and (3.51) do not depend on the renormalization scheme in which the calculation is performed. The contributions to $\mathcal{K}_{t\bar{t}\tilde{g}}^{2\ell}$ of the first order in the Taylor expansion in m_A^2 are too lengthy to be printed here, but in section 3.3 we will discuss their relevance in a representative region of the MSSM parameter space.

The two terms between parentheses in eq. (3.50) come from the diagrams with pseudoscalar-top and pseudoscalar-stop couplings in figures 3.3a and 3.3b, respectively. Inserting the explicit expressions for $s_{2\theta_t}$ and Z_t we find

$$\mathcal{K}_{t\bar{t}\tilde{g}}^{2\ell} = \frac{m_t \mu}{m_{\tilde{t}_1}^2 - m_{\tilde{t}_2}^2} (\cot \beta + \tan \beta) \left[f(m_{\tilde{g}}^2, m_t^2, m_{\tilde{t}_1}^2) - f(m_{\tilde{g}}^2, m_t^2, m_{\tilde{t}_2}^2) \right], \quad (3.52)$$

i.e., the explicit dependence of $\mathcal{K}_{t\bar{t}\tilde{g}}^{2\ell}$ on A_t drops out, leaving only a dependence on μ . This happens because the μ term breaks the axial U(1) Peccei-Quinn symmetry of the MSSM potential, thus violating

the Adler-Bardeen theorem [65] which would otherwise guarantee the cancellation of all contributions from irreducible diagrams beyond one loop.

Even when the superparticles are much heavier than the pseudoscalar, the validity of the result for $\mathcal{K}_{t\bar{t}\tilde{g}}^{2\ell}$ obtained via a Taylor expansion in m_A^2 becomes questionable if m_A is close to or even larger than m_t . Moreover, the Taylor expansion can certainly not be applied to the bottom-sbottom-gluino contributions. To cover these cases, we performed an asymptotic expansion of in the large superparticle masses. More specifically, we considered the case $(m_A, m_q) \ll M$ without assuming any hierarchy between m_A and m_q , and retained terms up to $\mathcal{O}(m_A^2/M^2)$ and $\mathcal{O}(m_q^2/M^2)$ in the expansion. Assuming that the contribution of the quark q to $\mathcal{H}_A^{1\ell}$ in eq. (3.32) is expressed in terms of the pole quark mass, we find

$$\begin{aligned} \mathcal{K}_{q\bar{q}\tilde{g}}^{2\ell} &= -\frac{C_F}{2} \mathcal{K}^{1\ell}(\tau_q) \frac{m_{\tilde{g}}}{m_q} \left(\frac{s_{2\theta_q}}{2} - \frac{m_q Z_q}{m_{\tilde{q}_1}^2 - m_{\tilde{q}_2}^2} \right) \left(\frac{m_{\tilde{q}_1}^2}{m_g^2 - m_{\tilde{q}_1}^2} \ln \frac{m_{\tilde{q}_1}^2}{m_g^2} - \frac{m_{\tilde{q}_2}^2}{m_g^2 - m_{\tilde{q}_2}^2} \ln \frac{m_{\tilde{q}_2}^2}{m_g^2} \right) \\ &\quad - \frac{m_q}{m_{\tilde{g}}} s_{2\theta_q} \mathcal{R}_1^A + \frac{2 m_q^2 Z_q}{m_{\tilde{g}} (m_{\tilde{q}_1}^2 - m_{\tilde{q}_2}^2)} \mathcal{R}_2^A + \frac{m_q^2}{m_{\tilde{g}}^2} \mathcal{R}_3^A - \frac{1}{2} \mathcal{K}^{1\ell}(\tau_q) \frac{m_A^2}{m_{\tilde{q}_1}^2 - m_{\tilde{q}_2}^2} \mathcal{R}_4^A, \end{aligned} \quad (3.53)$$

where the one-loop function $\mathcal{K}^{1\ell}(\tau)$ was defined in eq. (3.33), and explicit formulae for the terms \mathcal{R}_i^A are given in eqs. (31)–(34) of ref. [12]. Again, in the bottom-sbottom-gluino contribution we retain only the terms up to $\mathcal{O}(m_b/M)$ and $\mathcal{O}(m_b^2/m_A^2)$ (in particular, the terms \mathcal{R}_2^A , \mathcal{R}_3^A and \mathcal{R}_4^A give contributions of higher order in m_b and can be neglected).

As in the case of the form factor for scalar production, the terms enhanced by $m_{\tilde{g}}/m_q$ in eq. (3.53) cancel out if the one-loop contribution of the quark q is multiplied by \hat{m}_q/M_q , resulting in a shift of $\mathcal{K}_q^{2\ell} \equiv \mathcal{K}_{qg}^{2\ell} + \mathcal{K}_{q\bar{q}\tilde{g}}$ such that

$$\mathcal{K}_q^{2\ell} \longrightarrow \mathcal{K}_q^{2\ell} - \mathcal{K}^{1\ell}(\tau_q) \frac{\delta m_q}{m_q}. \quad (3.54)$$

On the other hand, since the squarks do not contribute to pseudoscalar production at one loop, it is not necessary to specify a renormalization prescription for the parameters in the stop and sbottom sector.

Comparison with other calculations: The two-loop top/stop contributions to the form factors for scalar and pseudoscalar Higgs production in the VHML had already been computed in refs. [39] and [40], respectively, using an OS renormalization scheme. However, the analytic results of those calculations were too long to be printed, and they were only made available in the form of a computer code, `evalcsusy.f`. We compared our results for scalar and pseudoscalar production in the VHML limit with those of `evalcsusy.f`, and found perfect numerical agreement after taking into account the different convention for the sign of the superpotential parameter μ , see eq. (2.1), the different normalization of the form factors and a different renormalization prescription for the stop mixing angle.

Indeed, in the calculation of ref. [39] the counterterm for θ_t is given by

$$\delta\theta_t = \frac{\Pi_{12}(q_0^2)}{m_{t_1}^2 - m_{t_2}^2}, \quad (3.55)$$

where q_0 is an arbitrary external momentum (a free input parameter of `evalcsusy.f`) chosen to be of the order of the stop masses. The divergent part of the counterterm is in fact compelled to have the form of eq. (2.40) – with the finite part of the self-energy replaced by the divergent part – by the requirement that it cancel the poles of the anti-hermitian part of the stop WFR matrix. The renormalization prescription given in eq. (3.55) does fulfill this requirement in the case of the QCD corrections, but only because the divergent part of the $\mathcal{O}(\alpha_s)$ contribution to $\Pi_{12}(q^2)$ does not depend on q^2 . In general, however, the prescription in eq. (3.55) does not cancel all the poles, unless $q_0^2 = (m_{t_1}^2 + m_{t_2}^2)/2$. Therefore, we found it preferable to stick to the “symmetrical” prescription for $\delta\theta_t$, eq. (2.40), which can be more naturally applied to other loop corrections. Moreover, the prescription in eq. (2.40) is the one implemented in `FeynHiggs`, and it should be adopted for consistency if that code is used to compute the Higgs boson masses and mixing angle.

Formulae for the two-loop SUSY contributions to the form factors for scalar production, based on an asymptotic expansion in the superparticle masses but restricted to the limit of zero squark mixing and degenerate superparticle masses, were provided in ref. [66]. They confirmed – in the simplified limit considered in that paper – the earlier results for the bottom/sbottom contributions given in our ref. [10] (again, after taking into account differences in the overall normalization and in the convention for the sign of μ). In our subsequent ref. [14] we checked that our results for the asymptotic expansion of the top/stop contributions also agree with those of ref. [66] in the simplified limit.

Finally, our use of a low-energy theorem to compute higher-order corrections to Higgs-related observables in the MSSM, see ref. [6], was subject to further investigation in two papers by other groups. The authors of ref. [67] showed that a LET analogous to the one in eq. (3.43) – with the gluon self-energy replaced by the bottom-quark self-energy – can be used to compute the two-loop SUSY-QCD corrections to the decay $h \rightarrow b\bar{b}$. Indeed, the results of such calculation can be expressed in terms of form factors analogous to the ones given by eqs. (3.12)–(3.13) and eqs. (3.15)–(3.17). The authors of ref. [68] discussed instead the application of the LET to the computation of the three-loop SUSY-QCD contributions to the form factors for Higgs production in gluon fusion. In that case there are additional complications related to the renormalization of couplings of the Higgs bosons to the so-called ϵ -scalars of DRED, and the LET of ref. [6] must be modified.

3.3 Stop contributions: comparing different expansions

The applicability of the Taylor expansion to the contributions of two-loop diagrams involving top quarks and stop squarks is restricted to Higgs masses below the first threshold encountered in the diagrams. Therefore, it depends first of all on the hierarchy between the Higgs mass and the top mass (indeed, both stops are heavier than the top, except in very special regions of the MSSM parameter

space). While the mass of lightest scalar h is always well below the threshold for real-top production, this is not necessarily the case for the heaviest scalar H and the pseudoscalar A , and we can expect that, for values of m_H and m_A close to (or even above) $2m_t$, the Taylor expansion will fail to approximate the correct result. On the other hand, we expect that the asymptotic expansion in the heavy superparticle masses, which does not assume a specific hierarchy between the Higgs mass and the top mass, will provide a reasonable approximation even above the real-top threshold, as long as the superparticles are sufficiently heavy. To put these expectations on a more quantitative ground, we compared the results of the Taylor expansion and those of the asymptotic expansion in a representative region of the parameter space, considering both scalar [14] and pseudoscalar [12] production.

Scalar production: The SM parameters entering our calculation include the Z -boson mass $m_Z = 91.1876$ GeV, the W -boson mass $m_W = 80.399$ GeV and the strong coupling constant $\alpha_s(m_Z) = 0.118$ [69]. For the pole mass of the top quark we take $M_t = 173.2$ GeV [70]. For the relevant SUSY parameters we choose

$$m_Q = m_U = \mu = 1 \text{ TeV}, \quad A_t = 2 \text{ TeV}, \quad m_{\tilde{g}} = 800 \text{ GeV}, \quad \tan\beta = 5, \quad (3.56)$$

where m_Q and m_U are the soft SUSY-breaking masses for the left and right stops, respectively. For a given value of the pseudoscalar mass m_A , the scalar masses m_h and m_H and the mixing angle α are computed including the leading one-loop corrections of $\mathcal{O}(\alpha_t)$ and the leading two-loop corrections of $\mathcal{O}(\alpha_s\alpha_t)$ [23].

Figure 3.4 shows the real part of the SUSY (i.e., all except top-gluon) contributions to the two-loop form factor for heaviest-Higgs production, $\mathcal{H}_H^{2\ell}$, as a function of m_H . Since, as mentioned above, m_H is not a free parameter in our calculation, its variation is obtained by varying m_A between 100 GeV and 500 GeV. For simplicity, in the computation of the form factor we neglected the small D-term-induced electroweak contributions. The left plot in figure 3.4 is obtained assuming that the parameters m_t , $m_{\tilde{t}_1}$, $m_{\tilde{t}_2}$ and θ_t entering the one-loop part of the form factor, $\mathcal{H}_H^{1\ell}$, are expressed in the $\overline{\text{DR}}$ renormalization scheme at the scale $Q = 1$ TeV. In this case we extract the $\overline{\text{DR}}$ top mass $m_t(Q)$ from the input value for the pole mass M_t by means of eq. (B2) of ref. [23], and we interpret the input parameters m_Q , m_U and A_t in eq. (3.56) directly as running parameters evaluated at the scale Q . The right plot, on the other hand, is obtained assuming that the parameters m_t , $m_{\tilde{t}_1}$, $m_{\tilde{t}_2}$ and θ_t entering $\mathcal{H}_H^{1\ell}$ are expressed in the OS scheme described in section 2.4. In this case we identify m_t directly with the pole mass M_t , and we interpret the input parameters m_Q , m_U and A_t in eq. (3.56) as the parameters that can be obtained by rotating the diagonal matrix of the physical stop masses by the “physical” angle θ_t , defined through eq. (2.40).

In each plot, the dashed (blue) line represents the result obtained in the VHML, as given in ref. [6], while the solid (red) line represents the result computed at the first order of a Taylor expansion in m_H^2 , i.e. it includes the effect of terms of $\mathcal{O}(m_H^2/m_t^2)$ and $\mathcal{O}(m_H^2/M^2)$ which were also computed in ref. [6] but proved too lengthy to be presented in analytic form. The dot-dashed (black) line represents

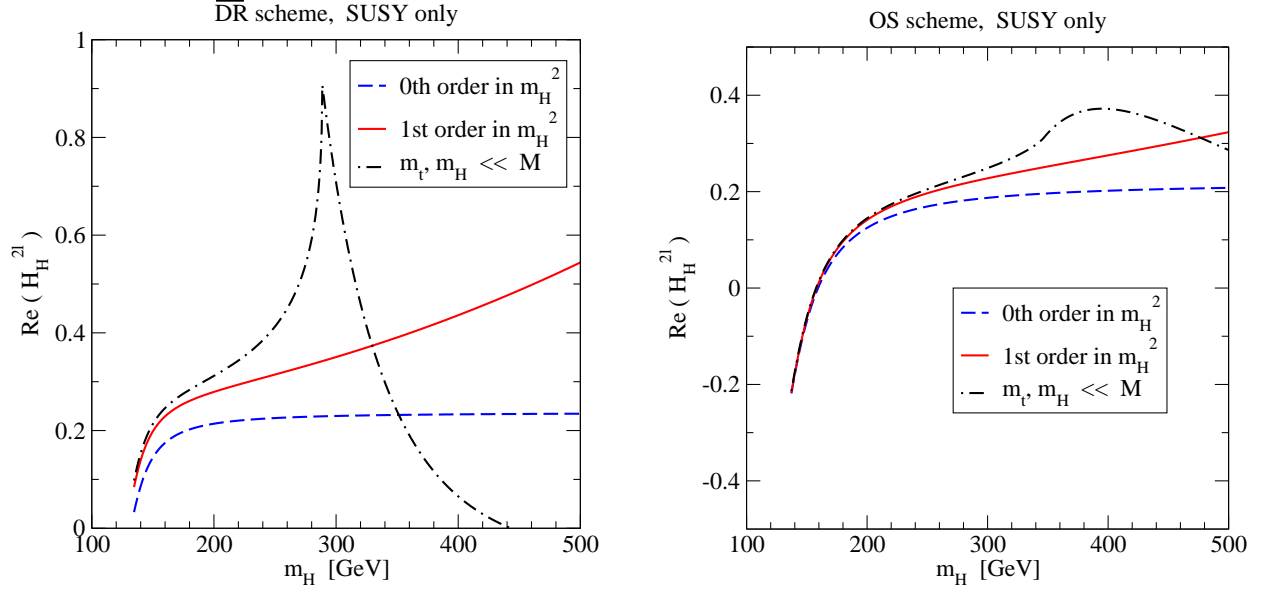


Figure 3.4: Real part of the SUSY contributions to $\mathcal{H}_H^{2\ell}$, plotted as a function of m_H . The choice of SUSY parameters and the meaning of the different curves are explained in the text. The plot on the left refers to the $\overline{\text{DR}}$ scheme, while the plot on the right refers to the OS scheme.

instead the result of the asymptotic expansion in the superparticle masses derived in ref. [14]. The latter is applicable when both m_t and m_H are smaller than the generic superparticle mass M , as is indeed the case here since $M \approx 1$ TeV, but it does not require any specific hierarchy between m_H and m_t .

The comparison between the dashed and solid lines shows that, as m_H increases, the effect of the terms of $\mathcal{O}(m_H^2/m_t^2)$ and $\mathcal{O}(m_H^2/M^2)$ becomes more and more relevant, and the VHML does not provide an accurate approximation to $\mathcal{H}_H^{2\ell}$. Furthermore, the comparison between the dot-dashed and solid lines shows that, even if the inclusion of the first-order terms pushes the validity of the Taylor expansion up to larger values of m_H , the Taylor expansion fails anyway when m_H gets close to the threshold for the production of a real top-quark pair in the loops. In that case one can use the result of our asymptotic expansion in M , provided that the latter is still considerably larger than m_H .

A few additional comments are in order concerning the comparison between the left ($\overline{\text{DR}}$) and right (OS) plots in figure 3.4. There is no reason to expect the plots to look similar to each other, first of all because the difference between the values of $\mathcal{H}_H^{2\ell}$ in the two schemes is compensated for, up to higher-order terms, by a shift in the value of the one-loop form factor, $\mathcal{H}_H^{1\ell}$, and also because the different interpretation of the input parameters in the two schemes means that, by using the numerical inputs in eq. (3.56) for both schemes, we are in fact considering two different points of the MSSM parameter space. This said, a striking difference between the two schemes is visible in the behavior of the asymptotic expansion (i.e., the dot-dashed line) around the threshold for the production of a real

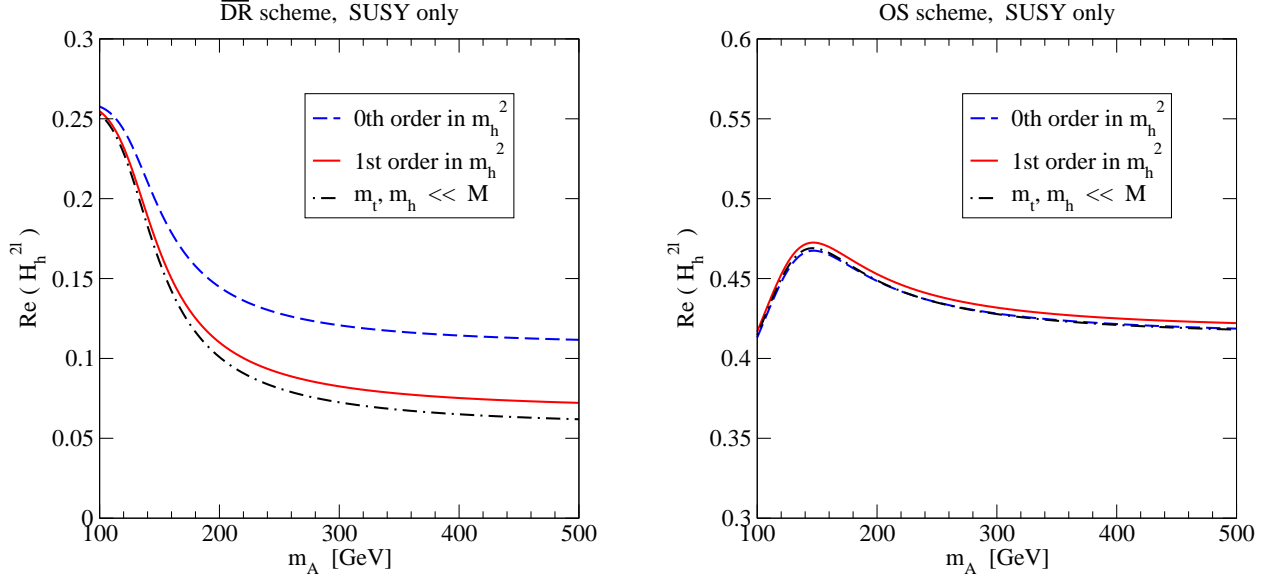


Figure 3.5: Real part of the SUSY contributions to $\mathcal{H}_h^{2\ell}$, plotted as a function of m_A . The choice of SUSY parameters and the meaning of the different curves are explained in the text. The plot on the left refers to the $\overline{\text{DR}}$ scheme, while the plot on the right refers to the OS scheme.

top-quark pair in the loops. The fact that in the $\overline{\text{DR}}$ plot the threshold is located at a lower value of m_H than in the OS plot is an artifact, due to lower value of the MSSM running top mass with respect to the pole top mass (indeed, for our choice of parameters $m_t(Q) = 144.3$ GeV). The much sharper behavior around the threshold of the dot-dashed line in the $\overline{\text{DR}}$ plot, on the other hand, can be traced back to the contribution of the first term in the right-hand side of eq. (3.47) for $Y_t^{\tilde{g}}$. That term reflects the fact that the running top mass of the MSSM (i.e., including the stop-gluino contribution) is used in the top-quark contribution to $\mathcal{H}_H^{1\ell}$, and it is canceled out if the pole top mass (or, for that matter, the running top mass of the SM) is used instead. Indeed, we checked that, in a “mixed” renormalization scheme in which the stop contributions to $\mathcal{H}_H^{1\ell}$ are expressed in term of running parameters (including the MSSM running top mass) but the top-quark contribution is expressed in terms of the pole top mass, the qualitative behavior of the dot-dashed line around the threshold would be similar to the one in the OS plot.

To conclude this discussion, we show in figure 3.5 the real part of the SUSY contributions to the two-loop form factor for lightest-Higgs production, $\mathcal{H}_h^{2\ell}$, as a function of the pseudoscalar mass m_A , which is varied in the same range used to produce figure 3.4. The meaning of the different curves is the same as in figure 3.4, and again the left plot is obtained assuming that the parameters entering the one-loop form factor $\mathcal{H}_h^{1\ell}$ are expressed in the $\overline{\text{DR}}$ scheme, while the right plot is obtained assuming that they are expressed in the OS scheme.

In the MSSM the mass of the lightest Higgs scalar h is bounded from above, and for large enough

values of the pseudoscalar mass it becomes independent of m_A , as do the couplings of h to the top quark and to the stops. Indeed, for the choice of SUSY parameters in eq. (3.56) our crude $\mathcal{O}(\alpha_t + \alpha_t \alpha_s)$ calculation of the Higgs mass yields $m_h < 123.8$ GeV in the $\overline{\text{DR}}$ plot and $m_h < 122.5$ GeV in the OS plot, and all the curves in figure 3.5 become essentially flat for $m_A > 250$ GeV. Due to the relative smallness of m_h no real-particle threshold is crossed, thus the result of the asymptotic expansion (dot-dashed line) is rather close to the result of the Taylor expansion at the first order in m_h^2 (solid line).

However, a comparison between the left and right plots of figure 3.5 shows that in the $\overline{\text{DR}}$ calculation the VHML result (dashed line) provides a less-than-perfect approximation to $\mathcal{H}_h^{2\ell}$, while in the OS calculation the effect of the terms proportional to m_h^2 is small, and the VHML result essentially overlaps with the other two results. This difference between the two schemes can again be traced to the contribution of the first term in the right-hand side of eq. (3.47), i.e. to the choice of renormalization scheme for the top mass entering the top-quark contribution to $\mathcal{H}_h^{1\ell}$. Even in this case we checked that, in a “mixed” scheme in which the top-quark contribution to $\mathcal{H}_h^{1\ell}$ is expressed in terms of the pole top mass while the stop contributions are expressed in terms of running parameters, the VHML would provide as good an approximation to $\mathcal{H}_h^{2\ell}$ as it does in the full OS scheme.

Pseudoscalar production: Since the squarks do not contribute to the one-loop form factor for pseudoscalar production, the only parameters entering $\mathcal{H}_A^{1\ell}$ in addition to the quark masses are $\tan\beta$ and m_A . Neither of those parameters is subject to one-loop $\mathcal{O}(\alpha_s)$ corrections, therefore we need not specify a renormalization scheme for them (although it is natural to consider m_A as the pole pseudoscalar mass). The remaining input parameters are $m_{\tilde{g}}$, μ , A_t , A_b and the soft SUSY-breaking mass terms for stop and sbottom squarks, m_Q , m_U and m_D . Since these parameters only enter the two-loop part of the form factor for pseudoscalar production, in this discussion we need not specify a renormalization scheme for them either. For simplicity, we will set all the SUSY-breaking parameters, as well as the supersymmetric mass parameter μ , to a common value M . Note however that the squark mass eigenstates differ from M , because of the supersymmetric (F-term and D-term) contributions to the squark mass matrices as well as of the left-right mixing terms.

Figure 3.6 shows the top-stop-gluino contribution to the two-loop form factor for pseudoscalar production, i.e., the term $\mathcal{K}_{t\tilde{t}\tilde{g}}^{2\ell}$ entering eq. (3.36), as a function of the common SUSY mass M , for $m_A = 150$ GeV and $\tan\beta = 2$. Even for the lowest value of M considered in the plot, $M = 100$ GeV, the stop and sbottom masses are above the threshold for real-particle production. The dashed line represents the result obtained in the limit of vanishing m_A , shown explicitly in eqs. (3.50) and (3.51), while the solid line represents the result computed at the first order of the Taylor expansion in the pseudoscalar mass, i.e. it includes the effect of terms of $\mathcal{O}(m_A^2/m_t^2)$ and $\mathcal{O}(m_A^2/M^2)$ which are too long to be presented in analytic form. In the computation of these additional terms we assumed that the $\mathcal{O}(m_A^2/m_t^2)$ part of the one-loop top contribution, see eq. (3.34), is expressed in terms of the pole top mass.

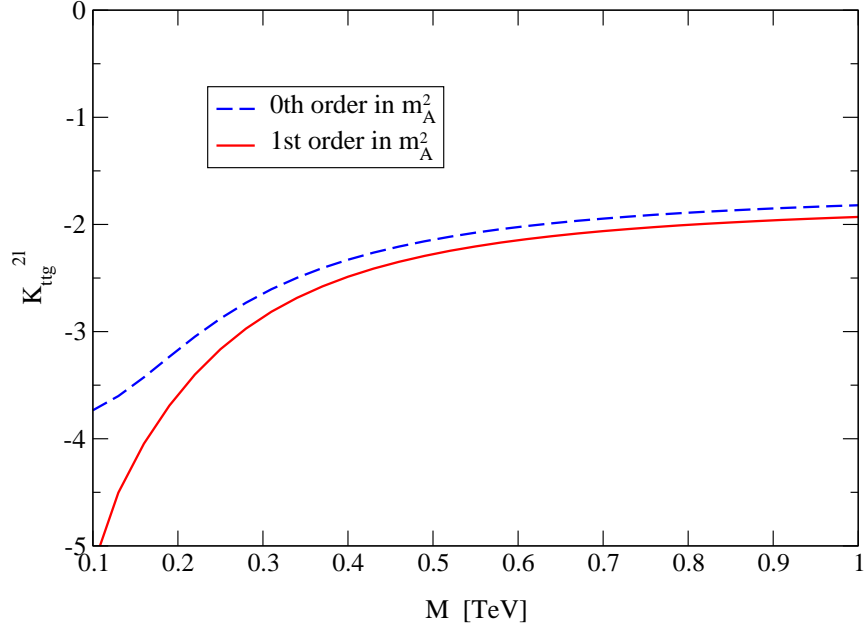


Figure 3.6: Top-stop-gluino contribution $\mathcal{K}_{t\bar{t}g}^{2\ell}$ as a function of a common SUSY mass M , for $m_A = 150$ GeV and $\tan\beta = 2$. The dashed line is the result in the limit of vanishing m_A , while the solid line includes the first-order term of a Taylor expansion in m_A^2 .

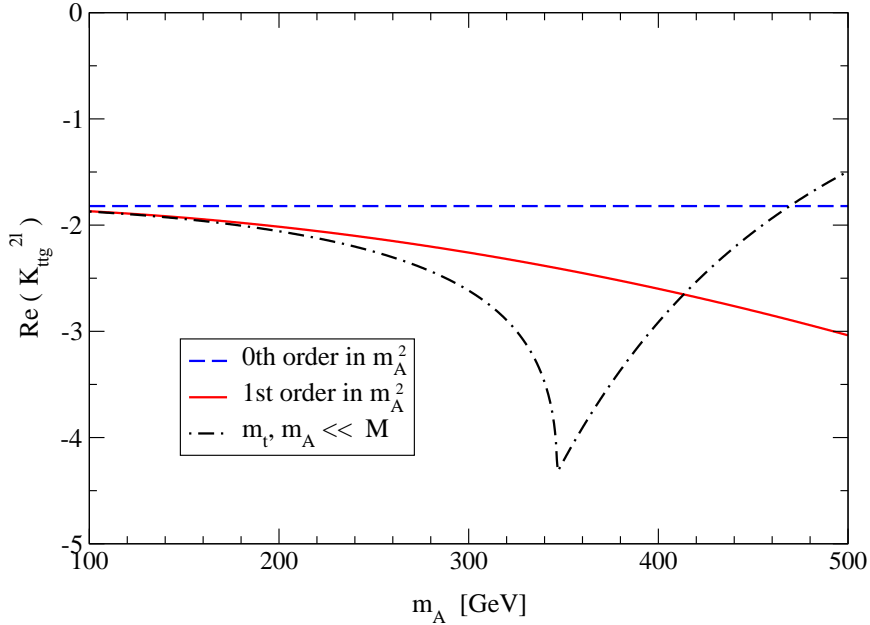


Figure 3.7: Real part of $\mathcal{K}_{t\bar{t}g}^{2\ell}$ as a function of m_A , for a common SUSY mass $M = 1$ TeV and $\tan\beta = 2$. The solid and dashed lines are as in figure 3.6 above, while the dot-dashed line is the result of an asymptotic expansion in M which does not assume a specific hierarchy between m_t and m_A .

It can be seen in figure 3.6 that the two-loop top-stop-gluino contribution $\mathcal{K}_{t\bar{t}g}^{2\ell}$ is of non-decoupling nature, i.e., it does not tend to zero when all the superparticle masses become large (note that we increase the superpotential parameter μ together with the SUSY-breaking parameters). In addition, the comparison between the solid and dashed lines shows that when the common SUSY mass M is close to m_A the combined effect of the terms of $\mathcal{O}(m_A^2/m_t^2)$ and $\mathcal{O}(m_A^2/M^2)$ can be as large as 20%–25% with respect to the result obtained for vanishing m_A . However, when M increases the effect of the terms of $\mathcal{O}(m_A^2/M^2)$ becomes quickly negligible. The remaining discrepancy between the solid and dashed lines for moderate to large values of M is due to the terms of $\mathcal{O}(m_A^2/m_t^2)$, and it amounts to a modest 6% for the value of m_A considered in this example.

To assess the importance of the terms of $\mathcal{O}(m_A^2/m_t^2)$ for larger values of m_A , we plot in figure 3.7 the real part of $\mathcal{K}_{t\bar{t}g}^{2\ell}$ as a function of the pseudoscalar mass, up to a value $m_A = 500$ GeV well above the threshold for real top-quark production. The common SUSY mass is set to the relatively large value $M = 1$ TeV, and $\tan\beta = 2$. As in figure 3.6, the dashed and solid lines represent the results obtained at the zeroth and first order of the Taylor expansion in m_A^2 , respectively. The comparison between those lines shows that when m_A approaches $2m_t$ the effect of the terms of $\mathcal{O}(m_A^2/m_t^2)$ gets as large as 30% with respect to the result obtained for vanishing m_A . However, it is natural to wonder whether a Taylor expansion in m_A^2 can give an accurate approximation to $\mathcal{K}_{t\bar{t}g}^{2\ell}$ for values of m_A close to or larger than m_t . To address this question, we show in figure 3.7 as a dot-dashed line the result of the asymptotic expansion in M . This result was derived under the assumption that both m_A and m_t are much smaller than M , which is indeed the case for $M = 1$ TeV, but it does not require any specific hierarchy between m_A and m_t . The comparison between the dot-dashed and solid lines shows that the Taylor expansion at the first order in m_A^2 provides a good description of the dependence of $\mathcal{K}_{t\bar{t}g}^{2\ell}$ on the ratio m_A/m_t up to values of m_A of the order of 250 GeV. On the other hand, when m_A reaches the threshold for real top production (i.e., at the cusp of the dot-dashed line) the result of the asymptotic expansion in M is roughly 80% larger in absolute value than the result at the first order of the Taylor expansion in m_A^2 , and a full 140% larger than the result obtained for vanishing m_A .

In summary, the behavior of the different expansions of the two-loop SUSY contributions to the form factor for pseudoscalar production follows qualitatively the case of heavy-scalar production discussed earlier. In particular, the compact result for $\mathcal{K}_{t\bar{t}g}^{2\ell}$ given in eqs. (3.50) and (3.51), which was derived for $m_A = 0$, can be safely applied only to scenarios in which m_A is smaller than m_t . While the inclusion of the terms proportional to m_A^2 pushes the validity of the Taylor expansion up to larger values of m_A , the expansion fails when m_A gets close to the threshold for real-top production. In that case one can use the result of the asymptotic expansion in M , provided that the latter is sufficiently larger than m_A . Comparing figures 3.4 and 3.7 we can also note that, when the one-loop top contribution is expressed in terms of the pole top mass, the behavior of the form factor for pseudoscalar production around the real-top threshold is much sharper than in the case of scalar production. This reflects the different threshold behavior of the functions $\mathcal{G}_{1/2}^{1\ell}(\tau)$ and $\mathcal{K}^{1\ell}(\tau)$ entering the leading terms in the form factors for scalar and pseudoscalar production, respectively.

3.4 Sbottom contributions: dealing with large corrections

In the calculation of the bottom/sbottom contributions, a judicious choice of the renormalization conditions on the parameters entering the one-loop form factors is required to avoid the occurrence of unphysically large contributions in the two-loop form factors. As discussed in section 2.4, the parameters that determine the couplings of the Higgs bosons to the bottom squarks cannot be renormalized in a way analogous to the one usually adopted in the stop sector. In addition, the presence of large contributions to the two-loop form factors depends on the definitions adopted for the Higgs-bottom coupling and for the bottom mass.

Indeed, specializing eq. (3.47) to the case of the bottom/sbottom contributions, assuming that the one-loop contribution to the form factors for scalar production is expressed in terms of the pole bottom mass, and neglecting suppressed terms, we find the following result for the contribution of bottom-sbottom-gluino diagrams with a Higgs-bottom coupling:

$$2m_b^2 Y_b^{\tilde{g}} = -\frac{C_F}{4} \mathcal{G}_{1/2}^{1\ell}(\tau_b) \frac{m_{\tilde{g}}}{m_b} s_{2\theta_b} \left(\frac{m_{b_1}^2}{m_{\tilde{g}}^2 - m_{b_1}^2} \ln \frac{m_{b_1}^2}{m_{\tilde{g}}^2} - \frac{m_{b_2}^2}{m_{\tilde{g}}^2 - m_{b_2}^2} \ln \frac{m_{b_2}^2}{m_{\tilde{g}}^2} \right) + s_{2\theta_b} \frac{m_b}{m_{\tilde{g}}} \mathcal{R}_1. \quad (3.57)$$

Similarly, the bottom-sbottom-gluino contribution to the form factor for pseudoscalar production, eq. (3.53), becomes:

$$\mathcal{K}_{b\tilde{b}\tilde{g}}^{2\ell} = -\frac{C_F}{2} \mathcal{K}^{1\ell}(\tau_b) \frac{m_{\tilde{g}}}{m_b} \left(\frac{s_{2\theta_b}}{2} - \frac{m_b Z_b}{m_{b_1}^2 - m_{b_2}^2} \right) \left(\frac{m_{b_1}^2}{m_{\tilde{g}}^2 - m_{b_1}^2} \ln \frac{m_{b_1}^2}{m_{\tilde{g}}^2} - \frac{m_{b_2}^2}{m_{\tilde{g}}^2 - m_{b_2}^2} \ln \frac{m_{b_2}^2}{m_{\tilde{g}}^2} \right) - s_{2\theta_b} \frac{m_b}{m_{\tilde{g}}} \mathcal{R}_1^A. \quad (3.58)$$

The equations above show that the bottom-sbottom-gluino contributions to the form factors for Higgs production contain terms enhanced by the large ratio $m_{\tilde{g}}/m_b$. Recalling the limiting behavior of the functions entering the one-loop form factors for small τ_b , eqs. (3.21) and (3.35), it is clear that those terms are in fact of $\mathcal{O}(m_b m_{\tilde{g}}/m_\phi^2)$, i.e., they still vanish as $m_b \rightarrow 0$ but they are enhanced by the ratio $m_{\tilde{g}}/m_\phi$. Such terms arise from two-loop diagrams in which the helicity flip on the fermion loop is achieved via a gluino mass insertion instead of a bottom mass insertion, and they by far dominate the new-physics contribution to the two-loop part of the form factors. Alternatively, inserting $s_{2\theta_b} = 2m_b(A_b + \mu \tan \beta)/(m_{b_1}^2 - m_{b_2}^2)$ in eqs. (3.57) and (3.58), the large two-loop contributions manifest themselves as terms enhanced by a factor $\Delta_b \equiv \epsilon_b \tan \beta$, where ϵ_b is defined in eq. (2.48). As mentioned in section 3.2, the contributions enhanced by $m_{\tilde{g}}/m_b$ (or Δ_b) cancel out of the two-loop form factors if the bottom contributions to the one-loop form factors are computed in terms of the pole bottom mass M_b , but they are further multiplied by \hat{m}_b/M_b , where \hat{m}_b is the $\overline{\text{DR}}$ mass given in eq. (2.47). This manipulation corresponds to adopting a $\overline{\text{DR}}$ renormalization for the coupling that controls the Higgs-bottom Yukawa interaction, denoted as h_b^Y in section 2.4.

A numerical example: We will now illustrate the effect of the two-loop bottom/sbottom contributions to the form factors for Higgs-boson production in a region of the MSSM parameter space characterized by large values of $\tan \beta$.

In addition to the input parameters used in section 3.3 for the numerical study of the top-stop-gluino contributions, we take $M_b = 4.49$ GeV for the pole mass of the bottom quark, corresponding to the SM running mass (in the $\overline{\text{MS}}$ scheme) $\overline{m}_b(m_b) = 4.16$ GeV [71]. For the parameters in the sbottom sector, $(h_b, m_{Q_{\tilde{b}}}, m_D, A_b)$, we adopt the OS scheme described in section 2.4, which avoids the occurrence of unphysically large two-loop corrections. In our numerical example all the relevant SUSY-breaking parameters, as well as the supersymmetric mass parameter μ , are set to a common value $M = 500$ GeV, and the physical pseudoscalar mass m_A is set to 150 GeV. The tree-level mass matrix for the CP-even Higgs bosons h and H can be expressed in terms of m_A and $\tan\beta$, in addition to m_z . Since we are considering a region of the parameter space where the bottom/sbottom contributions can be relevant, in the calculation of the Higgs masses and mixing angle α we include the one-loop $\mathcal{O}(\alpha_t + \alpha_b)$ and two-loop $\mathcal{O}(\alpha_t\alpha_s + \alpha_b\alpha_s)$ corrections as in refs. [23, 25].

To visualize the effect of the two-loop bottom/sbottom contributions, we define a factor K_ϕ , where $\phi = (h, H, A)$, containing the ratio of two-loop to one-loop form factors that enter eq. (3.7):

$$K_\phi = 1 + 2 \frac{\alpha_s}{\pi} \text{Re} \left(\frac{\mathcal{H}_\phi^{2\ell}}{\mathcal{H}_\phi^{1\ell}} \right). \quad (3.59)$$

In the left panel of figure 3.8 we plot as a function of $\tan\beta$ the factor K_h for the production of the light scalar h , in a fully OS scheme in which the bottom-quark contribution to the one-loop form factor is expressed in terms of the pole bottom mass. The one-loop form factors in the denominator of the term between parentheses in eq. (3.59) contain both the top/stop and bottom/sbottom contributions, computed under the approximations of eqs. (3.20) and (3.21). The lines in the plot correspond to different computations of the two-loop form factors in the numerator: the dotted line includes only the contributions of the top/stop sector computed in the VHML; the dashed line includes also the contribution of two-loop diagrams with bottom quarks and gluons; the solid line includes the full two-loop contribution of the bottom/sbottom sector computed in the asymptotic expansion; finally, the dot-dashed line is obtained by approximating the bottom/sbottom contribution (with the exception of the bottom-gluon diagrams) with just the terms enhanced by $m_{\tilde{g}}/m_b$ in eq. (3.57).

From the comparison between the dotted and dashed lines it can be seen that, in the OS renormalization scheme, the contribution to $\mathcal{H}_1^{2\ell}$ of the two-loop diagrams with bottom quarks and gluons is very small. This is due to a partial cancellation between the terms $C_F \mathcal{F}_{1/2}^{(2\ell,a)}$ and $C_A \mathcal{G}_{1/2}^{(2\ell,C_A)}$ entering the function Y_b^g in eq. (3.27), and to the fact that, in this scheme, the term $\mathcal{F}_{1/2}^{(2\ell,b)}$ is not enhanced by the potentially large logarithm of the ratio between the bottom mass and the renormalization scale. The solid line shows that the effect of the diagrams involving sbottoms can be very significant at large $\tan\beta$, more than doubling K_h . Indeed, in this scenario the coupling of the light Higgs boson to the (s)bottom is considerably enhanced with respect to its SM value when $\tan\beta$ gets large. However, the proximity between the solid and dot-dashed lines shows that this sizable effect is almost entirely due to the terms enhanced by $m_{\tilde{g}}/m_b$ in the contribution of the two-loop bottom-sbottom-gluino diagrams in which the light Higgs boson couples to the bottom quark.

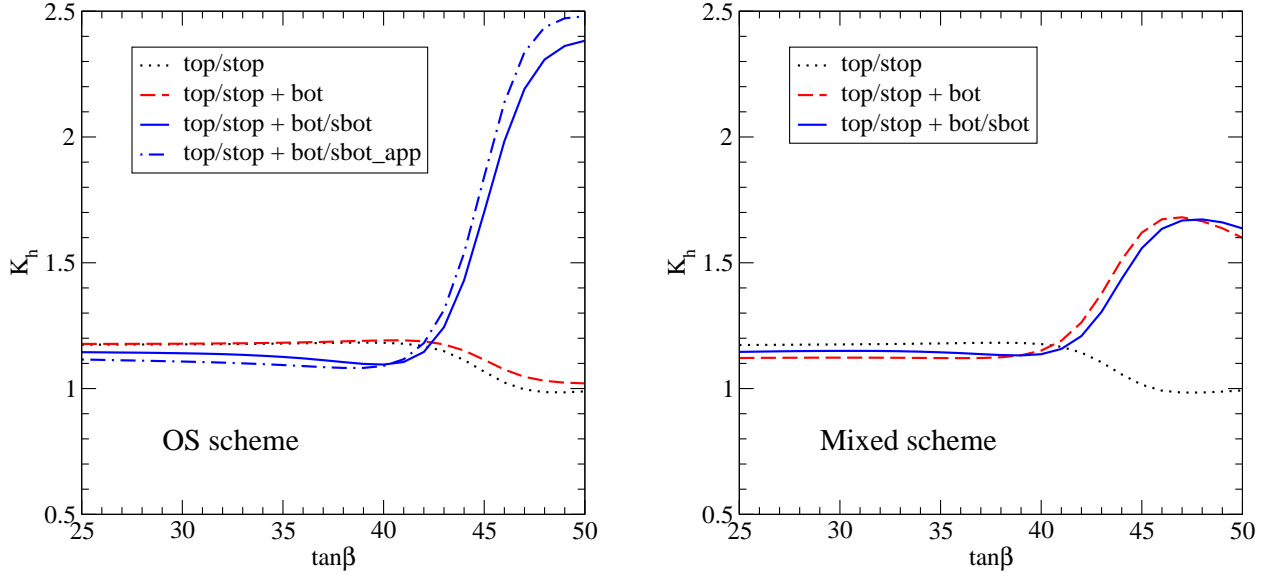


Figure 3.8: K factor for the production of a light Higgs boson h as a function of $\tan\beta$, for $m_A = 150$ GeV and all SUSY mass parameters equal to $M = 500$ GeV. For the meaning of the different lines see the text.

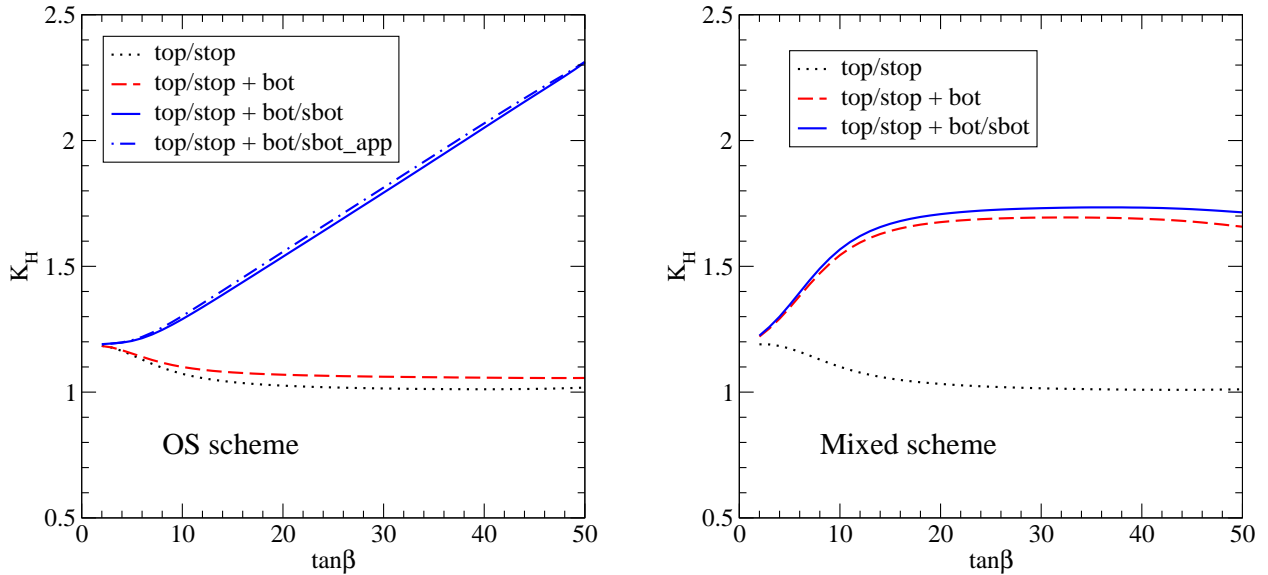


Figure 3.9: Same as figure 3.8 for the heavy Higgs boson H .

As discussed above, the terms enhanced by $m_{\tilde{g}}/m_b$ can be canceled out in a “mixed” renormalization scheme in which the Higgs-bottom Yukawa coupling h_b^Y is identified with the $\overline{\text{DR}}$ -renormalized MSSM bottom mass \hat{m}_b instead of the physical mass M_b . In the right panel of figure 3.8 we present the result of this manipulation, with \hat{m}_b evaluated at the scale $Q = m_h$. The input parameters and the meaning of the different lines are the same as for the plot in the left panel. The proximity between the dashed and solid lines shows that the contribution of the two-loop diagrams involving sbottoms is rather small in this renormalization scheme, at least for our choice of input parameters. However, K_h still shows a sizable increase at large $\tan\beta$. This is due to the fact that the shift in eq. (3.48) brings back a large logarithm, $\ln(m_b^2/m_h^2)$, in the contribution of the two-loop diagrams with bottom and gluon (this logarithm compensates the scale dependence of the running mass \hat{m}_b).

In figure 3.9 we show instead the factor K_H for the production of the heavy scalar H . The input parameters and the meaning of the lines in the left and right panels are the same as in figure 3.8. Since in this example the mass of the heavy Higgs boson is of the order of 150 GeV, i.e. well below any threshold for heavy-particle production, we expect the VHML to hold reasonably well even for H . From figure 3.9 it appears that the balance of the various contributions to K_H in the two different renormalization schemes is qualitatively similar to the one for K_h shown in figure 3.8: in the OS scheme the factor K_H receives a sizable contribution from the sbottom diagrams, largely dominated by the terms enhanced by $m_{\tilde{g}}/m_b$ in the diagrams controlled by the Higgs-bottom coupling; in the “mixed” scheme, on the other hand, the sbottom contribution is rather small, but there is a sizable contribution from the diagrams with bottom and gluon.

This said, the factor K_H shows a peculiar dependence on $\tan\beta$: for sufficiently large values of $\tan\beta$, it grows linearly in the OS scheme, while it reaches a plateau in the mixed scheme. This can be easily understood by recalling that, for moderate-to-large $\tan\beta$ and for our choice of m_A , the Yukawa coupling of the heavy MSSM Higgs to bottom quarks is enhanced by $\tan\beta$ with respect to the SM value, while the coupling to top quarks is suppressed by $\tan\beta$. Consequently, both the one-loop and the two-loop form factors in K_H are dominated by the contribution of the diagrams controlled by the Higgs-bottom coupling, with the result that the coupling itself cancels out in the ratio. However, the dominant contribution from the bottom-sbottom-gluino diagrams in the OS scheme contains an additional $\tan\beta$ -enhancement hidden in the product $s_{2\theta_b} m_{\tilde{g}}/m_b$, which explains the linear rise of K_H . On the other hand, the dominant contribution of the bottom-gluon diagrams in the mixed scheme possesses no further $\tan\beta$ -enhancement, which explains the plateau.

Finally, in figure 3.10 we show the factor K_A for the production of the pseudoscalar A , as a function of $\tan\beta$, setting again $m_A = 150$ GeV. The meaning of the lines in the left and right panels is the same as in figures 3.8 and 3.9, with the caveat that the contributions of the top/stop sector are computed at the first order of the Taylor expansion in m_A^2 instead of the VHML, and that we do not show the dot-dashed line in the left panel. The comparison between figures 3.10 and 3.9 shows that, for values of $\tan\beta$ larger than 10–15, the behavior of the bottom/sbottom contributions to pseudoscalar production – in both renormalization schemes – follows very closely the corresponding behavior in the

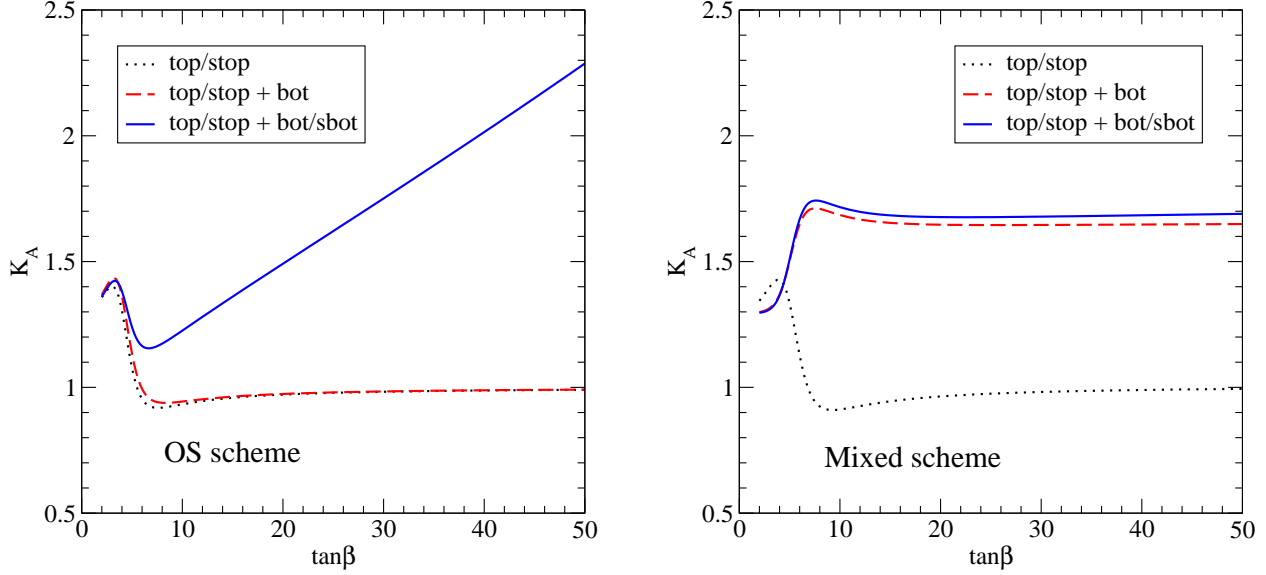


Figure 3.10: K factor for the production of a pseudoscalar Higgs A as a function of $\tan \beta$, for $m_A = 150$ GeV and all SUSY mass parameters equal to $M = 500$ GeV. The three lines show the effect of the different two-loop contributions, in the OS scheme (left panel) and in the “mixed” scheme (right panel).

case of heavy-scalar production. On the other hand, for small values of $\tan \beta$ the top/stop contributions to pseudoscalar production appear to be relatively larger, and to have a sharper dependence on $\tan \beta$, than the corresponding contributions to scalar production.

Comparison with the effective-Lagrangian approximation: It is well known that, in the MSSM, loop diagrams involving superparticles induce interactions between the quarks and the “wrong” Higgs doublets, i.e., interactions that are absent from the tree-level Lagrangian due to the requirement that the superpotential be a holomorphic function of the superfields [45]. Such non-holomorphic, loop-induced Higgs-quark interactions result in $\tan \beta$ -enhanced (or $\tan \beta$ -suppressed) corrections to the MSSM predictions for various physical observables. If all superparticles are considerably heavier than the Higgs bosons they can be integrated out of the Lagrangian, in which case the loop-induced corrections are *resummed* in effective Higgs-quark couplings. In particular, if g_b^ϕ denote the tree-level couplings of a neutral Higgs $\phi = (h, H, A)$ to bottom quarks (normalized to the SM value), the corresponding effective couplings \tilde{g}_b^ϕ read [46]

$$\tilde{g}_b^h = \frac{g_b^h}{1 + \Delta_b} \left(1 - \Delta_b \frac{\cot \alpha}{\tan \beta} \right), \quad \tilde{g}_b^H = \frac{g_b^H}{1 + \Delta_b} \left(1 + \Delta_b \frac{\tan \alpha}{\tan \beta} \right), \quad \tilde{g}_b^A = \frac{g_b^A}{1 + \Delta_b} (1 - \Delta_b \cot^2 \beta), \quad (3.60)$$

where, as mentioned earlier, $\Delta_b \equiv \epsilon_b \tan \beta$, with ϵ_b defined in eq. (2.48).

In the calculation of processes involving the Higgs-bottom couplings, it is often found that the $\tan\beta$ -enhanced corrections can be included to all orders in an expansion in powers of $\alpha_s \tan\beta$ by inserting the effective couplings of eq. (3.60) in the lowest-order result. A comparison with our explicit results for the two-loop form factors allows us to test the validity of that procedure in the case of the production of both CP-even and CP-odd Higgs bosons in gluon fusion.

We recall that the bottom-quark contributions $\mathcal{H}_\phi^{1\ell,b}$ to the one-loop form factors for the production of the Higgs boson $\phi = (h, H, A)$ read

$$\mathcal{H}_h^{1\ell,b} = -T_F \frac{\sin\alpha}{\cos\beta} \mathcal{G}_{1/2}^{1\ell}(\tau_b), \quad \mathcal{H}_H^{1\ell,b} = T_F \frac{\cos\alpha}{\cos\beta} \mathcal{G}_{1/2}^{1\ell}(\tau_b), \quad \mathcal{H}_A^{1\ell,b} = T_F \tan\beta \mathcal{K}^{1\ell}(\tau_b). \quad (3.61)$$

Assuming that $\mathcal{H}_\phi^{1\ell,b}$ are expressed in terms of the pole bottom mass, and that the Higgs-sbottom couplings are renormalized in a way that avoids the introduction of additional $\tan\beta$ -enhanced corrections, we find that the two-loop form factors read

$$\mathcal{H}_h^{2\ell} = \mathcal{H}_h^{1\ell,b} \left[-\frac{\pi}{\alpha_s} \Delta_b \left(1 + \frac{\cot\alpha}{\tan\beta} \right) + \frac{C_F}{4} \frac{A_b - \mu \cot\alpha}{m_{\tilde{g}}} s_{2\theta_b}^2 F \left(\frac{m_{\tilde{b}_1}^2}{m_{\tilde{g}}^2}, \frac{m_{\tilde{b}_2}^2}{m_{\tilde{g}}^2} \right) \right] + \dots, \quad (3.62)$$

$$\mathcal{H}_H^{2\ell} = \mathcal{H}_H^{1\ell,b} \left[-\frac{\pi}{\alpha_s} \Delta_b \left(1 - \frac{\tan\alpha}{\tan\beta} \right) + \frac{C_F}{4} \frac{A_b + \mu \tan\alpha}{m_{\tilde{g}}} s_{2\theta_b}^2 F \left(\frac{m_{\tilde{b}_1}^2}{m_{\tilde{g}}^2}, \frac{m_{\tilde{b}_2}^2}{m_{\tilde{g}}^2} \right) \right] + \dots, \quad (3.63)$$

$$\mathcal{H}_A^{2\ell} = -\mathcal{H}_A^{1\ell,b} \frac{\pi}{\alpha_s} \Delta_b (1 + \cot^2\beta) + \dots, \quad (3.64)$$

where the ellipses denote contributions suppressed by m_b/M or m_Z^2/M^2 , as well as all of the contributions from diagrams involving top and stop, and

$$F(x_1, x_2) = \frac{1}{1-x_1} \left(1 + \frac{\ln x_1}{1-x_1} \right) + \frac{1}{1-x_2} \left(1 + \frac{\ln x_2}{1-x_2} \right) - \frac{2}{x_1-x_2} \left(\frac{x_1}{1-x_1} \ln x_1 - \frac{x_2}{1-x_2} \ln x_2 \right). \quad (3.65)$$

In practice, the effective-Lagrangian approximation consists in rescaling the one-loop bottom contributions $\mathcal{H}_\phi^{1\ell,b}$ by the same factors that rescale the Higgs-bottom couplings g_b^ϕ in eq. (3.60). Expanding the rescaling factors to the first order in Δ_b it is easy to see that the effective-Lagrangian approximation does indeed reproduce the two-loop terms proportional to Δ_b in eqs. (3.62)–(3.64).

It is also interesting to consider the so-called decoupling limit of the MSSM, $m_A \gg m_Z$, in which $\cot\alpha \rightarrow -\tan\beta$ and the light scalar h has SM-like couplings to fermions and gauge bosons. Eq. (3.60) shows that in this limit the effective coupling of h to bottom quarks is equal to the tree-level coupling, therefore in the effective-Lagrangian approximation there are no $\tan\beta$ -enhanced contributions to $\mathcal{H}_h^{2\ell}$. Indeed, for $\cot\alpha \rightarrow -\tan\beta$ the terms proportional to Δ_b drop out of the two-loop form factor in eq. (3.62). However, eq. (3.62) also shows that in the decoupling limit $\mathcal{H}_h^{2\ell}$ contains additional $\tan\beta$ -enhanced contributions, controlled by the left-right sbottom mixing $X_b = (A_b + \mu \tan\beta)$, which are not reproduced by the effective-Lagrangian approximation. However, when the implicit dependence of the sbottom masses and mixing on the bottom mass is taken into account, such contributions turn out to be partially suppressed by powers of m_b . Indeed, taking for illustrative purposes the limit in

which the diagonal entries of the sbottom mass matrix as well as the squared gluino mass are all equal to M^2 , and expanding the form factor in powers of m_b , we find

$$\mathcal{H}_h^{2\ell} \supset -\mathcal{H}_h^{1\ell,b} \frac{C_F}{12} \frac{m_b^2 X_b^3}{M^5} + T_F \frac{2C_A + 25C_F}{18} \frac{m_b^2 X_b^2}{M^4} + \dots, \quad (3.66)$$

where the ellipses denote terms further suppressed by powers of m_b or m_z , as well as all of the contributions from diagrams involving top and stop. The first term in eq. (3.66) comes from the expansion of the terms proportional to $s_{2\theta_b}^2$ in eq. (3.62), while the second comes from the expansion of terms not shown in eq. (3.62). The contributions neglected by the effective-Lagrangian approximation can be relevant for values of X_b large enough to compensate for the suppression due to m_b . It should however be recalled that in the decoupling limit $\mathcal{H}_h^{1\ell,b}$ is not further enhanced by $\tan\beta$, therefore – differently from what happens in the case of the heavy Higgs bosons – the total form factor for h production can still be dominated by the top/stop contributions even for large values of $\tan\beta$.

The effective-Lagrangian approximation described above inspires possible variations of our “mixed” renormalization scheme in which the Higgs-bottom Yukawa coupling h_b^Y is treated differently from the mass of the bottom quark entering the loop. Indeed, in our numerical study we considered a $\overline{\text{DR}}$ prescription for the coupling:

$$h_b^{Y,\overline{\text{DR}}} = \frac{\widehat{m}_b}{v_1} = \frac{\overline{m}_b}{v_1} \frac{1 + \delta_b}{1 + \Delta_b}, \quad (3.67)$$

where \widehat{m}_b is the $\overline{\text{DR}}$ -renormalized (and scale-dependent) bottom mass in the MSSM, \overline{m}_b is the corresponding quantity in the SM and δ_b denotes the terms in the SUSY contribution to the bottom self-energy that are not enhanced by $\tan\beta$. The concomitant shift in the two-loop form factor, eq. (3.48), removes the terms proportional to Δ_b , but introduces both terms proportional to $\ln(m_b^2/Q^2)$ and terms proportional to $\ln(m_g^2/Q^2)$, where Q is the scale at which the running mass \widehat{m}_b is expressed. Consequently, for any reasonable choice of Q (earlier on we chose $Q = m_\phi$) the two-loop form factor contains large logarithms, resulting in the large K factors in the right panels of figures 3.8–3.10.

An alternative definition of the coupling, closer to the one adopted in the effective-Lagrangian approximation, is

$$h_b^{Y,\text{eff}} = \frac{M_b}{v_1} \frac{1}{1 + \Delta_b}. \quad (3.68)$$

In this case, the term $\delta m_b/m_b$ in eq. (3.48) is replaced by $-\Delta_b$, and the shift in the two-loop form factor removes only the terms proportional to Δ_b , without introducing any logarithmically enhanced contributions. Another option consists in replacing the pole mass M_b in eq. (3.68) with the SM running mass \overline{m}_b computed at $Q = m_b$ (as a result of this replacement, the two-loop form factor changes only by a small non-logarithmic term). While these schemes might seem preferable to the one in eq. (3.67) in that they lead to smaller two-loop form factors, it must be kept in mind that this is due to an accidental cancellation between terms proportional to C_F and terms proportional to C_A in the two-loop bottom-gluon contribution, eq. (3.27). There is no argument suggesting that such cancellation persists at higher orders in QCD, or that it is motivated by some physical property of the bottom contribution to the gluon-fusion process. For example, it was noticed already in ref. [49] that the

two-loop bottom-gluon contribution to the form factor for Higgs decay into two photons (obtained by setting $C_A = 0$ in the gluon-fusion result) is minimized when the bottom mass and Yukawa coupling are expressed in terms of \overline{m}_b computed at $Q = m_\phi/2$, even if the one-loop bottom contribution has exactly the same structure as the corresponding contribution to gluon fusion. Therefore, there is no obvious reason to favor one of the possible “mixed” schemes over the others, and it would seem reasonable to consider the difference between the results for the cross section obtained with the various schemes as a measure of the uncertainty associated with the uncomputed higher-order QCD corrections.

Finally, it is possible to follow the effective-Lagrangian approximation one step further, and absorb in the coupling of each Higgs boson ϕ with bottom quarks also the second term within parentheses in eq. (3.60). In this case, both the coupling $h_b^{Y,\phi}$ and the accompanying shift in the two-loop form factor depend on the Higgs boson under consideration. As appears from eq. (3.60), these additional terms – originating from two-loop diagrams in which the Higgs boson couples to squarks – are suppressed by powers of $\tan\beta$, and they are numerically relevant only for the light scalar h in the decoupling limit where $\cot\alpha \rightarrow -\tan\beta$.

3.5 Implementation in public codes

An important aspect of particle physics phenomenology consists in making the results of our calculations available to the physics community in the form of computer codes. In the absence of that, even sophisticated theoretical efforts such as the full two-loop calculations of Higgs production in the MSSM, see refs. [37, 38], remain of limited practical usefulness. In this spirit, the approximate results for the two-loop SUSY contributions to Higgs-boson production described in this chapter have been implemented in two independent public codes. Much of this “popularization” effort took place under the umbrella of the LHC Higgs Cross Section Working Group (LHC-HXSWG), a joint collaboration between ATLAS, CMS and the theory community aimed at producing agreements on cross sections, branching ratios and pseudo-observables relevant to SM and MSSM Higgs boson(s), and at facilitating the comparison and combination of results. The studies performed within the LHC-HXSWG were summarized in a series of CERN Yellow Reports [34, 35, 36].

The first implementation of our results for the SUSY contributions to gluon fusion, described in refs. [13, 35], was in the form of a module for the so-called POWHEG BOX [72], a framework for consistently matching NLO-QCD computations of matrix elements with parton-shower Monte Carlo generators, avoiding double counting and preserving the NLO accuracy of the calculation. In the context of that work, we also produced a POWHEG-BOX module for the gluon-fusion process in the SM, in which we improved on an earlier contribution by another group [73] by including the full dependence on the top-quark mass and the effect of bottom-quark loops through NLO. This module was later used by the ATLAS collaboration in the analysis that led to the discovery of the Higgs boson [21]. The second implementation of our results for the SUSY contributions, by a group including one of the authors of `evalcsusy.f`, was in the public code `SusHi` [41], which computes the total and differential

cross section for Higgs production in gluon fusion and bottom-quark annihilation in the SM and the MSSM.

In this section I summarize a study performed in collaboration with the authors of `SusHi` and included in the third LHC-HXSWG report [36]. In particular, I provide some detail on the implementation of the two-loop SUSY contributions to gluon fusion in the `POWHEG BOX` and in `SusHi` and compare the results of the two codes, both between each other and with the results of earlier calculations by the LHC-HXSWG. Since the calculations of the gluon-fusion cross section implemented in our `POWHEG-BOX` module and in `SusHi` largely coincide, the description that follows refers to both codes (unless explicitly stated). However, it is important to remark that the two codes serve rather different purposes: the `POWHEG BOX`, in conjunction with a Monte Carlo generator, allows to produce sets of events that can be used to study the kinematic distributions of the Higgs boson at NLO and at leading-logarithmic (LL) accuracy in QCD, taking also into account the effect of parton showers. However, this approach can prove rather inefficient when one is interested only in the computation of the total cross section. A dedicated code like `SusHi`, on the other hand, does allow for a fast calculation of the total cross section for Higgs production, but it cannot be used directly to generate event sets. Moreover, `SusHi` computes the differential distributions only at fixed order (i.e., NLO) in QCD, without resumming the logarithms of the form $\ln(p_T^\phi/m_\phi)$ which may spoil the perturbative convergence of the result for low values of the Higgs transverse momentum p_T^ϕ .

Contributions to the gluon-fusion cross section: At the LO, the partonic cross section for Higgs production via gluon fusion in the MSSM is induced by quark and squark loops, and we take into account only the contributions from the top/stop and bottom/sbottom sectors. For what concerns the first two generations, the quark contributions are negligible due to the smallness of the corresponding Yukawa couplings, while the squarks contribute only via terms suppressed by the ratio m_Z^2/M^2 , with significant cancellations among the different contributions in each generation (indeed, the total contribution vanishes for degenerate squark masses).

Virtual effects at the NLO in QCD include the gluonic corrections to the LO quark and squark contributions, as well as the mixed quark-squark-gluino contributions. While the gluonic corrections to the quark contributions are implemented for generic quark and Higgs masses [49, 50], for the two-loop contributions involving squarks we use the approximate results described in the previous sections, which are valid as long as the Higgs mass does not exceed the lowest threshold for squark production. In particular, for the production of the lightest scalar h we compute the contributions involving stops via the Taylor expansion in m_h^2 [6, 39], and those involving sbottoms via the asymptotic expansion in the SUSY masses [10]. For H and A production, on the other hand, we use the asymptotic expansion for both stop and sbottom contributions [12, 14]. In addition, we use the full results of refs. [49, 54] for the contributions to the NLO-QCD cross section that arise from one-loop diagrams involving the emission of real quarks and gluons.

As discussed in section 3.4, the existence of non-decoupling, $\tan\beta$ -enhanced SUSY corrections to

the bottom Yukawa coupling induces contributions to the gluon-fusion cross section that can become numerically dominant in regions of the MSSM parameter space characterized by large $\tan\beta$. We follow the effective-Lagrangian approach, and absorb these contributions in a redefinition of the Higgs-bottom Yukawa coupling as in eq. (3.68). As a consequence, we need to shift accordingly the formulae for the two-loop contributions, in order to avoid double counting.

In order to perform meaningful comparisons between the predictions of the SM and those of the MSSM, it is crucial that the MSSM calculation reproduce the SM result when the SUSY particles are heavy and the Higgs boson has SM-like couplings to quarks and gauge bosons. To this purpose, we must adapt to the MSSM calculation two higher-order contributions that have been computed only in the SM, i.e., the NNLO-QCD contributions induced by top-quark loops and the NLO electroweak (EW) contributions. In particular, we define

$$\sigma^{\text{MSSM}} = (1 + \delta_{\text{EW}}) \sigma_{\text{NLO}}^{\text{MSSM}} + g_{\phi tt}^2 \left(\sigma_{\text{NNLO}}^{\text{SM},t} - \sigma_{\text{NLO}}^{\text{SM},t} \right), \quad (3.69)$$

where δ_{EW} parameterizes the NLO-EW correction, $g_{\phi tt}$ is the factor that rescales the coupling of the MSSM Higgs boson ϕ to top quarks and the cross sections within parentheses include only the top contributions computed in the SM.

For the NNLO-QCD top-quark contributions entering eq. (3.69) we use known results computed in the VHML, both for the SM Higgs [74] and for the pseudoscalar [75]. The NLO-EW contributions to Higgs boson production in the SM have been computed in ref. [76]. For a SM Higgs boson sufficiently lighter than the top threshold, those contributions are well approximated by the contributions coming from two-loop diagrams in which the Higgs couples to EW gauge bosons, which in turn couple to the gluons via a loop of light quarks [77]. Considering only these contributions, we can approximate the EW correction as

$$\delta_{\text{EW}} \approx 2 g_{\phi VV} \alpha_{\text{em}} T_F \text{Re} \left(\frac{\mathcal{G}_{\text{lf}}^{2\ell}}{\mathcal{H}_{\phi}^{1\ell}} \right), \quad (3.70)$$

where $g_{\phi VV}$ is the factor that rescales the coupling of the MSSM Higgs boson ϕ to gauge bosons, the one-loop form factor $\mathcal{H}_{\phi}^{1\ell}$ is computed in the MSSM (i.e., it contains both the quark and squark contributions), and the explicit expression for the two-loop EW light-quark contribution $\mathcal{G}_{\text{lf}}^{2\ell}$ can be found in ref. [77].

The inclusion in the MSSM calculation of the additional contributions in eq. (3.69) allows us to properly account for the NNLO-QCD and the NLO-EW corrections to the production of the lightest scalar h in scenarios where the SUSY particles are heavy. For what concerns the other neutral Higgs bosons, their couplings to gauge bosons and to top quarks are suppressed in most of the parameter space, if not downright absent (in the case of the coupling of A to gauge bosons), therefore the additional contributions in eq. (3.69) are less important.

In the following we will compare our determination of the gluon-fusion cross section in the MSSM, eq. (3.69), with the one employed in the early stages of the activities of the LHC-HXSWG [34, 35]. In the latter, the NLO cross section $\sigma_{\text{NLO}}^{\text{MSSM}}$ was computed with the public code HIGLU [79], including only

the top- and bottom-quark contributions rescaled by the appropriate Higgs-quark effective couplings. The only SUSY effect included in the calculation was the $\tan\beta$ -enhanced correction to the effective Higgs-bottom couplings, i.e., the term Δ_b entering eq. (3.60), and the electroweak correction δ_{EW} was omitted.

Numerical examples: We are now ready to discuss the numerical effect of the different contributions that we have included in the computation of the cross section for Higgs production in gluon fusion. As a representative choice for the MSSM parameters, we take the “light stop” scenario introduced in ref. [78]:

$$m_Q = m_U = 500 \text{ GeV}, \quad \mu = -350 \text{ GeV}, \quad X_t = 1 \text{ TeV}, \quad m_{\tilde{g}} = 1.5 \text{ TeV}, \quad (3.71)$$

where m_Q and m_U denote the soft SUSY-breaking masses for the left and right stops, respectively, and $X_t = A_t + \mu \cot\beta$ (for the values of the remaining soft SUSY-breaking parameters see ref. [78]). This scenario corresponds to stop masses around 325 and 670 GeV, i.e. light enough to induce sizable contributions to the cross section but not (yet?) excluded by stop searches at the LHC. For the SM input parameters we adopt the standard values prescribed by the LHC-HXSWG (in particular, we set $M_t = 172.5$ GeV and $M_b = 4.75$ GeV). For each value of the pseudoscalar mass m_A and of $\tan\beta$, we use `FeynHiggs` [30] to compute the Higgs boson masses and mixing angle, as well as the $\tan\beta$ -enhanced correction to the Higgs-bottom coupling, Δ_b . To compute the total gluon-fusion cross section we use `SusHi`, and cross-check the results with a private code. It is useful to remark that the two-loop calculations of the Higgs-boson masses and production cross section implemented in `FeynHiggs` and `SusHi`, respectively, adopt the OS renormalization scheme for the parameters in the stop and sbottom sectors described in section 2.4. As a consequence, the numerical values of the parameters for the “light stop” scenario listed in eq. (3.71) can be passed to both codes as they are.

Figure 3.11 shows the contours in the $m_A - \tan\beta$ plane of equal ratio between the cross section for Higgs-boson production in gluon fusion computed by `SusHi` and the corresponding cross section computed as in the earlier LHC-HXSWG reports, refs. [34, 35]. In particular, the former includes the NLO-QCD calculation of both quark and squark contributions plus the dominant NNLO-QCD and NLO-EW effects adapted from the SM calculation, while the latter includes only the NLO-QCD calculation of quark contributions (supplemented with the $\tan\beta$ -enhanced SUSY corrections to the Higgs-bottom couplings) and the dominant NNLO-QCD effects from top-quark loops. The plot on the left in figure 3.11 refers to the production of the lightest scalar h , while the plot on the right refers to the production of the heaviest scalar H . The red lines superimposed to each plot are the contours of equal mass for the corresponding scalar (for H we only show the contours between 124 GeV and 128 GeV).

From the left plot in figure 3.11 it can be seen that, in the “light stop” scenario, the combined effect of the squark contributions and the NLO-EW corrections tends to suppress the cross section for h production, with a maximum effect of 8–10% in the region with m_A larger than roughly 150 GeV,

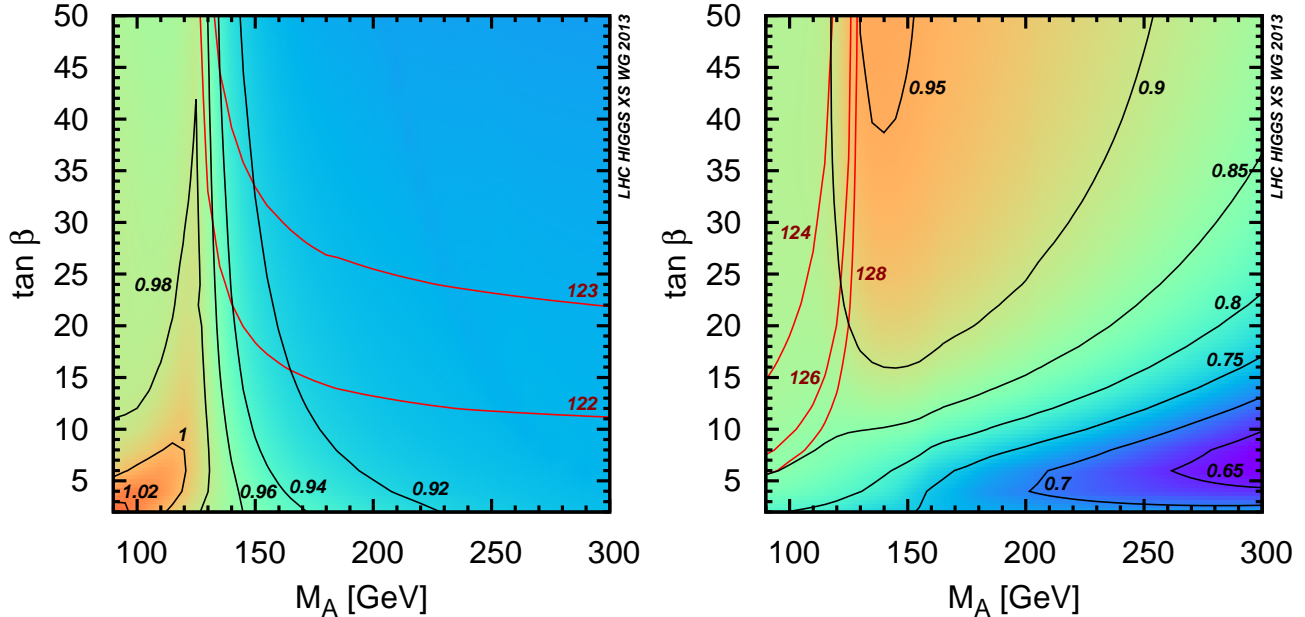


Figure 3.11: Ratio of the cross section for h (left) and H (right) production in gluon fusion in the “light stop” scenario as computed by `SusHi`, over the corresponding cross section computed omitting squark contributions and EW corrections.

where h has SM-like couplings to quarks and gauge bosons. It is useful to remark that this results from a partial compensation between the contributions of stop loops, which in this scenario can reduce the cross section of the lightest scalar by up to 14–16%, and the NLO-EW light-quark contributions, which increase by approximately 6% the cross section of a SM-like scalar with mass around 125 GeV [77].

The right plot in figure 3.11 shows that in the case of H production the relative effect of the squark contributions can be somewhat larger than in the case of h production (the NLO-EW light-quark contributions, on the other hand, become negligible for sufficiently large m_A , due to the vanishing couplings of H to gauge bosons). However, a suppression of the order of 35–40% is reached only in the lower-right corner of the plot, where m_A is large and $\tan\beta$ ranges between 5 and 10. In this region, the coupling of H to top quarks is suppressed while the coupling to bottom quarks is not sufficiently enhanced, resulting in very small gluon-fusion cross sections, of the order of tenths of a picobarn.

In regions of the MSSM parameter space where the Higgs coupling to bottom quarks is enhanced, the transverse-momentum distribution of a scalar produced via gluon fusion can be distorted with respect to the corresponding distribution of a SM Higgs boson. In order to investigate this effect, we consider the point in the “light-stop” scenario with $m_A = 130$ GeV and $\tan\beta = 40$, characterized by the fact that both scalars have non-standard couplings to quarks and masses in the vicinity of the LHC signal (indeed, `FeynHiggs` predicts $m_h = 122.4$ GeV and $m_H = 129.3$ GeV). This point is likely to be already excluded by the ATLAS and CMS searches for neutral Higgs bosons decaying into $\tau^+\tau^-$ pairs, but it can still provide a useful illustration of the expected size of this kind of effects.

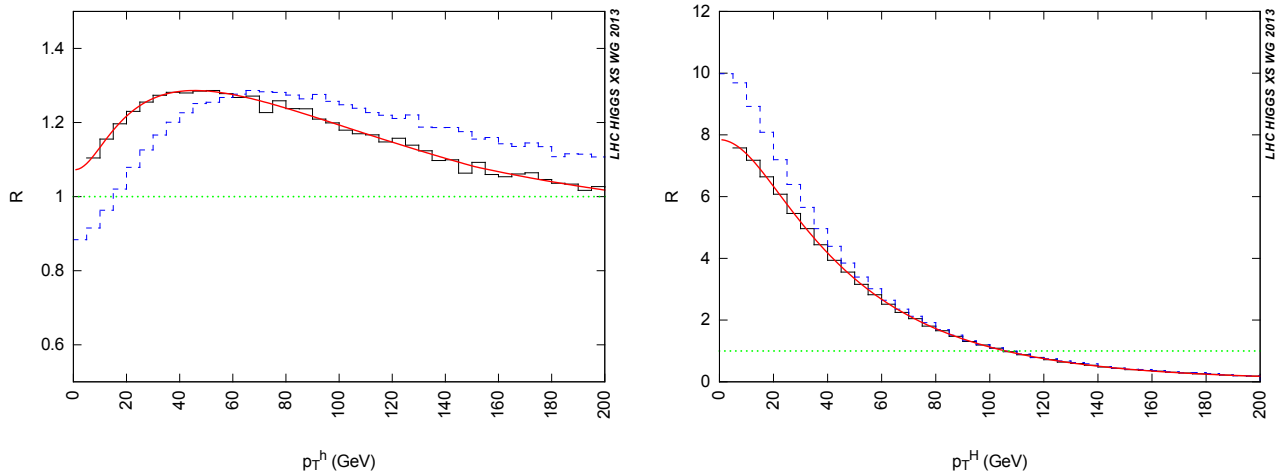


Figure 3.12: Ratio of the transverse-momentum distribution for the MSSM scalar h (left) or H (right) over the distribution for a SM Higgs with the same mass, in the “light stop” scenario with $m_A = 130$ GeV and $\tan\beta = 40$. The meaning of the different curves is explained in the text.

In figure 3.12 we show the ratio of the transverse-momentum distribution for a MSSM scalar produced via gluon fusion over the corresponding distribution for a SM Higgs with the same mass. The plot on the left refers to the lightest scalar h , while the plot on the right refers to the heaviest scalar H . In each plot, the continuous (red) line represents the ratio of distributions computed at NLO by `SusHi`, while the two histograms are computed with the `POWHEG` implementation of gluon fusion of ref. [13], modified by the adoption of the OS renormalization scheme for the squark parameters and the inclusion of the results of ref. [14] for the squark contributions to H production. In particular, the solid (black) histogram represents the ratio of distributions computed in a pure (i.e., fixed-order) NLO calculation, while in the dashed (blue) histogram the distributions are computed with the `POWHEG` method [72], in which the potentially large logarithms of the form $\ln(p_T^\phi/M_\phi^2)$ are resummed via the introduction of a Sudakov form factor and a parton-shower generator to describe multiple gluon emission (in this case, we use `PYTHIA` [80]).

The plots in figure 3.12 show that, in this point of the MSSM parameter space, the enhancement of the Higgs-bottom coupling results in both an enhancement of the total cross section and a distortion of the transverse-momentum distribution, in particular for the heaviest scalar H (note the difference in the scale between the left and the right plot). The comparison between the continuous line and the solid histogram shows a very good agreement between the result obtained with `SusHi` and the pure NLO result obtained with `POWHEG`. The effect of the resummation in `POWHEG` makes the transverse-momentum distribution of the Higgs boson harder. The comparison between the solid and dashed histograms shows that for h this effect is somewhat stronger than in the SM, while for H it is somewhat weaker.

Chapter 4

Higgs-boson masses in the NMSSM

Due to the crucial role of radiative corrections in pushing the prediction for the lightest-scalar mass above the tree-level bound $m_h < m_Z |\cos 2\beta|$, an impressive theoretical effort has been devoted in the past two decades to the precise determination of the Higgs sector of the MSSM. After the early realization [81] of the importance of the one-loop $\mathcal{O}(\alpha_t)$ corrections¹ involving top and stop, full one-loop computations of the MSSM Higgs masses have been provided [82, 83], leading logarithmic effects at two loops have been included via the renormalization-group method [84], and genuine two-loop corrections of $\mathcal{O}(\alpha_t\alpha_s)$ [85, 86, 87, 88, 23], $\mathcal{O}(\alpha_t^2)$ [85, 88, 24], $\mathcal{O}(\alpha_b\alpha_s)$ [25, 47] and $\mathcal{O}(\alpha_t\alpha_b + \alpha_b^2)$ [27] have been evaluated in the limit of zero external momentum. All of these corrections have been implemented in public computer codes [30, 31, 32, 33] for the calculation of the MSSM mass spectrum. In addition, a nearly complete two-loop calculation, including electroweak effects and part of the external momentum dependence, has been performed [89], and even the leading three-loop effects have been computed [90]. Finally, a vast literature is available on the dominant corrections to the MSSM Higgs masses in the presence of CP-violating phases in the soft SUSY-breaking parameters.

Until about four years ago, when our ref. [8] was published, the computation of the radiative corrections to the Higgs masses in the NMSSM was not quite as advanced as in the MSSM. The one-loop contributions from diagrams involving top/stop and bottom/sbottom loops had been computed [91] in the effective-potential approximation, i.e. neglecting the external momentum in the self-energies. For what concerns the one-loop contributions from diagrams involving chargino, neutralino or scalar loops (the contributions arising from gauge-boson loops are the same as in the MSSM) only the leading-logarithmic terms had been computed [92]. Similarly, among the two-loop contributions only the leading-logarithmic $\mathcal{O}(\alpha_t\alpha_s)$ and $\mathcal{O}(\alpha_t^2)$ terms – borrowed from the MSSM results under the simplifying assumption of fully degenerate SUSY masses – had been taken into account. All of these corrections were implemented in a public computer code, `NMHDECAY` [42], which computes masses, couplings and decay widths of the NMSSM Higgs bosons.

¹Here $\alpha_{t,b} = h_{t,b}^2/(4\pi)$, where h_t and h_b are the top and bottom Yukawa couplings, respectively. I follow the standard convention of denoting as $\mathcal{O}(\alpha_t)$ the one-loop corrections to the Higgs masses that are in fact proportional to $h_t^2 m_t^2$, i.e. $h_t^4 v_2^2$. Similar abuses of notation affect the other one- and two-loop corrections.

It is clear that, for a proper comparison between the MSSM and NMSSM predictions, and for a precise characterization of the scenarios in which the phenomenology of the NMSSM Higgs sector differs markedly from the MSSM case (for a review see ref. [93]), it would be desirable to compute the masses and mixings in the NMSSM Higgs sector with an accuracy comparable to that of the calculations implemented in the public codes for the MSSM mass spectrum. In ref. [8] we took a few steps in this direction. First of all, we provided explicit formulae for the full one-loop corrections to the mass matrices of the neutral CP-even and CP-odd Higgs bosons. In addition, we computed the two-loop $\mathcal{O}(\alpha_t\alpha_s + \alpha_b\alpha_s)$ corrections in the approximation of zero external momentum, adapting to the NMSSM case the effective-potential techniques (and, in part, the results) developed for the MSSM in refs. [23, 24, 27, 26]. To fully match the accuracy of the MSSM codes it would also be necessary to include the two-loop $\mathcal{O}(\alpha_t^2 + \alpha_t\alpha_b + \alpha_b^2)$ corrections. These corrections, however, cannot be straightforwardly adapted from the MSSM case and require a dedicated calculation.

In this chapter I present the results of ref. [8], and summarize some further developments on the precise calculation of the Higgs-boson masses in the NMSSM.

4.1 One-loop corrections to the Higgs mass matrices

This section describes the calculation of the one-loop corrections to the neutral Higgs boson masses in the NMSSM. We followed closely the approach² of the MSSM calculation of ref. [83], which is the one implemented in most public computer codes [31, 32, 33] that compute the mass spectrum of the MSSM. For simplicity, we neglected the Yukawa couplings of the first two generations, and we assumed all of the parameters in the NMSSM superpotential and soft SUSY-breaking Lagrangian to be real.

Including the one-loop corrections in the $\overline{\text{DR}}$ renormalization scheme, and using the minimization conditions of the scalar potential to replace the soft SUSY-breaking Higgs masses with combinations of the other parameters, the 3×3 mass matrices for the CP-even and CP-odd fields read

$$(\mathcal{M}_S^2)_{ij}^{\text{1loop}} = (\mathcal{M}_S^2)_{ij}^{\text{tree}} + \frac{1}{\sqrt{2}} \frac{\delta_{ij}}{v_i} T_i - \Pi_{s_i s_j}(p^2) \quad (4.1)$$

$$(\mathcal{M}_P^2)_{ij}^{\text{1loop}} = (\mathcal{M}_P^2)_{ij}^{\text{tree}} + \frac{1}{\sqrt{2}} \frac{\delta_{ij}}{v_i} T_i - \Pi_{p_i p_j}(p^2) \quad (4.2)$$

where: the tree-level mass matrices $(\mathcal{M}_S^2)^{\text{tree}}$ and $(\mathcal{M}_P^2)^{\text{tree}}$ are given in eqs. (2.21) and (2.24), respectively, and they are expressed in terms of $\overline{\text{DR}}$ -renormalized parameters; v_i stands for (v_1, v_2, v_s) ; T_i is the finite part of the one-loop tadpole diagram for the scalar S_i ; $\Pi_{s_i s_j}(p^2)$ and $\Pi_{p_i p_j}(p^2)$ are the finite parts of the one-loop self-energies for scalars and pseudoscalars, respectively; p^2 is the external momentum flowing in the self-energy. The explicit formulae for the scalar and pseudoscalar self-energies and for the scalar tadpoles are collected in appendix B of ref. [8]. We checked that, in the limit in which $\lambda \rightarrow 0$ while $\mu \equiv \lambda v_s$ is constant, our results for the 2×2 upper-left submatrix of $\Pi_{s_i s_j}$ and for

²Note that, differently from ref. [83], here the Higgs vevs are normalized in such a way that $(v_1^2 + v_2^2) \approx (174 \text{ GeV})^2$.

the tadpoles T_1 and T_2 coincide with the MSSM results of ref. [83], as does the pseudoscalar self-energy Π_{AA} that we can obtain by rotating the 2×2 upper-left submatrix of $\Pi_{p_i p_j}$ by an angle β .

The radiatively-corrected squared mass of the n -th scalar or (physical) pseudoscalar can be obtained by solving iteratively for the n -th eigenvalue of the corresponding mass matrix evaluated at an external momentum p^2 equal to the mass eigenvalue itself (we remark that this procedure includes in the results for the masses also contributions that are formally of higher order in the perturbative expansion). On the other hand, there is a well-known ambiguity in the definition of the radiatively-corrected mixing matrices R^S and R^P , because the rotations that diagonalize the radiatively-corrected mass matrices depend on the choice of external momentum in the self-energies. This ambiguity reflects the fact that the mixing matrices themselves are not physical observables. In our analysis we will define the radiatively-corrected mixing matrix as the one that diagonalizes the mass matrix at $p^2 = 0$. This corresponds to the result obtained in the effective-potential approximation.

The tree-level mass matrices entering eqs. (4.1) and (4.2) depend on the combination of gauge couplings $\bar{g}^2 = (g^2 + g'^2)/2$, on the NMSSM superpotential couplings λ and κ and the associated soft SUSY-breaking terms A_λ and A_κ , and on the three vevs v_1, v_2 and v_s . As long as no experimental information on the parameters of the NMSSM Higgs sector (nor on the validity of the NMSSM itself) is available, $\lambda, \kappa, A_\lambda, A_\kappa, v_s$ and the ratio of vevs $\tan \beta$ can be considered directly as $\overline{\text{DR}}$ -renormalized inputs at some reference scale Q . On the other hand, the $\overline{\text{DR}}$ values of $v^2 \equiv v_1^2 + v_2^2$, g and g' can be extracted from the experimentally known SM observables. For example, starting from the muon decay constant G_μ and the gauge-boson pole masses, we can make use of the relations

$$v^{-2} = 2\sqrt{2} G_\mu \left(1 - \frac{\Pi_{WW}^T(0)}{M_W^2} - \delta_{\text{VB}} \right), \quad (4.3)$$

$$\bar{g}^2 = v^{-2} M_Z^2 \left(1 + \frac{\Pi_{ZZ}^T(M_Z^2)}{M_Z^2} \right), \quad g^2 = 2 v^{-2} M_W^2 \left(1 + \frac{\Pi_{WW}^T(M_W^2)}{M_W^2} \right). \quad (4.4)$$

In eqs. (4.3) and (4.4), $\Pi_{VV}^T(p^2)$ ($V = Z, W$) denotes the finite and transverse part of the self-energy of the vector bosons, while δ_{VB} denotes the sum of vertex, box and wave-function-renormalization corrections to the muon decay amplitude. The explicit formulae for the vector-boson self-energies are collected in appendix B of ref. [8]. The SM contribution to δ_{VB} was computed long ago [94], and the SUSY contribution can be obtained from the MSSM results given in eqs. (C.13)–(C.22) of ref. [83], by simply extending the sum over the neutralinos to the five mass eigenstates of the NMSSM.

4.2 Two-loop corrections in the effective-potential approach

This section summarizes the computation of the two-loop corrections to the NMSSM Higgs mass matrices in the effective-potential approach. The effective potential for the neutral Higgs sector can be decomposed as $V_{\text{eff}} = V_0 + \Delta V$, where ΔV contains the radiative corrections. The 3×3 mass matrices for the CP-even and CP-odd fields can be decomposed as

$$(\mathcal{M}_S^2)_{ij}^{\text{eff}} = (\mathcal{M}_S^2)_{ij}^{\text{tree}} + (\Delta \mathcal{M}_S^2)_{ij}, \quad (\mathcal{M}_P^2)_{ij}^{\text{eff}} = (\mathcal{M}_P^2)_{ij}^{\text{tree}} + (\Delta \mathcal{M}_P^2)_{ij}, \quad (4.5)$$

and the radiative corrections to the mass matrices are

$$(\Delta\mathcal{M}_S^2)_{ij} = -\frac{1}{\sqrt{2}} \frac{\delta_{ij}}{v_i} \frac{\partial\Delta V}{\partial S_i} \Big|_{\min} + \frac{\partial^2\Delta V}{\partial S_i\partial S_j} \Big|_{\min}, \quad (4.6)$$

$$(\Delta\mathcal{M}_P^2)_{ij} = -\frac{1}{\sqrt{2}} \frac{\delta_{ij}}{v_i} \frac{\partial\Delta V}{\partial S_i} \Big|_{\min} + \frac{\partial^2\Delta V}{\partial P_i\partial P_j} \Big|_{\min}, \quad (4.7)$$

where v_i stands for (v_1, v_2, v_s) , and the derivatives of the correction ΔV are computed at the minimum of V_{eff} . The comparison between eqs. (4.6) and (4.7) and eqs. (4.1) and (4.2) highlights the correspondence between tadpoles, self-energies and derivatives of the effective potential. In the calculation of the MSSM Higgs boson masses it is customary to reorganize the corrections in such a way that $(\mathcal{M}_S^2)^{\text{tree}}$ is expressed in terms of the non-zero eigenvalue of $(\mathcal{M}_P^2)^{\text{eff}}$, which in the effective-potential approximation corresponds to the physical A -boson mass. In the case of the NMSSM this reorganization is not as practical, because there are two non-zero eigenvalues of $(\mathcal{M}_P^2)^{\text{eff}}$. While it is possible to absorb some of the radiative corrections in an “effective” trilinear coupling \widetilde{A}_λ , this parameter does not allow for a direct physical interpretation. Therefore, we refrain from this manipulation as well and leave eq. (4.6) as it stands. Throughout the calculation we assume that all the parameters entering both the tree-level and one-loop parts of the mass matrices are renormalized in the $\overline{\text{DR}}$ scheme at a renormalization scale that we denote by Q .

The $\mathcal{O}(\alpha_s)$ contribution to ΔV from two-loop diagrams involving top, stop, gluon and gluino is the same for the MSSM and for the NMSSM, and has been computed, e.g., in refs. [87, 23]. The corresponding $\mathcal{O}(\alpha_t\alpha_s)$ corrections to the mass matrices in eqs. (4.6) and (4.7) can in turn be computed by exploiting the Higgs-field dependence of the parameters appearing in ΔV . As detailed in ref. [23], if we neglect D-term contributions controlled by the electroweak gauge couplings the parameters in the top/top sector depend on the neutral Higgs fields only through two combinations:

$$X \equiv |X| e^{i\varphi} = h_t H_2^0, \quad \widetilde{X} \equiv |\widetilde{X}| e^{i\tilde{\varphi}} = h_t (A_t H_2^0 + \lambda S^* H_1^{0*}). \quad (4.8)$$

The top/stop $\mathcal{O}(\alpha_s)$ contribution to ΔV can be expressed in terms of five field-dependent parameters, which can be chosen as follows. The squared top and stop masses

$$m_t^2 = |X|^2, \quad m_{\tilde{t}_{1,2}}^2 = \frac{1}{2} \left[(m_Q^2 + m_U^2 + 2|X|^2) \pm \sqrt{(m_Q^2 - m_U^2)^2 + 4|\widetilde{X}|^2} \right], \quad (4.9)$$

a mixing angle $\bar{\theta}_t$, with $0 \leq \bar{\theta}_t \leq \pi/2$, which diagonalizes the stop mass matrix after the stop fields have been redefined to make it real and symmetric

$$\sin 2\bar{\theta}_t = \frac{2|\widetilde{X}|}{m_{\tilde{t}_1}^2 - m_{\tilde{t}_2}^2}, \quad (4.10)$$

and a combination of the phases of X and \widetilde{X} that we can choose as

$$\cos(\varphi - \tilde{\varphi}) = \frac{\text{Re}(\widetilde{X}) \text{Re}(X) + \text{Im}(\widetilde{X}) \text{Im}(X)}{|\widetilde{X}| |X|}. \quad (4.11)$$

A sixth parameter, the gluino mass $m_{\tilde{g}}$, does not depend on the Higgs background. In the following we will also refer to θ_t , with $-\pi/2 < \theta_t < \pi/2$, i.e. the usual field-independent mixing angle that diagonalizes the stop mass matrix at the minimum of the scalar potential.

With a lengthy but straightforward application of the chain rule for the derivatives of the effective potential, the corrections to the Higgs mass matrices in eqs. (4.6) and (4.7) can be expressed as ³

$$(\Delta\mathcal{M}_S^2)_{11} = \frac{1}{2} h_t^2 \mu^2 s_{2\theta_t}^2 F_3 - h_t^2 \tan\beta \frac{\mu A_t}{m_{\tilde{t}_1}^2 - m_{\tilde{t}_2}^2} F, \quad (4.12)$$

$$(\Delta\mathcal{M}_S^2)_{12} = h_t^2 \mu m_t s_{2\theta_t} F_2 + \frac{1}{2} h_t^2 A_t \mu s_{2\theta_t}^2 F_3 + h_t^2 \frac{\mu A_t}{m_{\tilde{t}_1}^2 - m_{\tilde{t}_2}^2} F, \quad (4.13)$$

$$(\Delta\mathcal{M}_S^2)_{22} = 2 h_t^2 m_t^2 F_1 + 2 h_t^2 A_t m_t s_{2\theta_t} F_2 + \frac{1}{2} h_t^2 A_t^2 s_{2\theta_t}^2 F_3 - h_t^2 \cot\beta \frac{\mu A_t}{m_{\tilde{t}_1}^2 - m_{\tilde{t}_2}^2} F, \quad (4.14)$$

$$(\Delta\mathcal{M}_S^2)_{13} = \frac{1}{2} h_t \lambda m_t \mu \cot\beta s_{2\theta_t}^2 F_3 + h_t \lambda m_t \frac{A_t + 2\mu \cot\beta}{m_{\tilde{t}_1}^2 - m_{\tilde{t}_2}^2} F, \quad (4.15)$$

$$(\Delta\mathcal{M}_S^2)_{23} = h_t \lambda m_t^2 \cot\beta s_{2\theta_t} F_2 + \frac{1}{2} h_t \lambda A_t m_t \cot\beta s_{2\theta_t}^2 F_3 + h_t \lambda \cot\beta \frac{m_t A_t}{m_{\tilde{t}_1}^2 - m_{\tilde{t}_2}^2} F, \quad (4.16)$$

$$(\Delta\mathcal{M}_S^2)_{33} = \frac{1}{2} \lambda^2 m_t^2 \cot^2\beta s_{2\theta_t}^2 F_3 - \lambda^2 \cot\beta \frac{m_t^2 A_t}{\mu(m_{\tilde{t}_1}^2 - m_{\tilde{t}_2}^2)} F \quad (4.17)$$

$$(\Delta\mathcal{M}_P^2)_{11} = -h_t^2 \tan\beta \frac{\mu A_t}{m_{\tilde{t}_1}^2 - m_{\tilde{t}_2}^2} F_A, \quad (4.18)$$

$$(\Delta\mathcal{M}_P^2)_{12} = -h_t^2 \frac{\mu A_t}{m_{\tilde{t}_1}^2 - m_{\tilde{t}_2}^2} F_A, \quad (4.19)$$

$$(\Delta\mathcal{M}_P^2)_{22} = -h_t^2 \cot\beta \frac{\mu A_t}{m_{\tilde{t}_1}^2 - m_{\tilde{t}_2}^2} F_A, \quad (4.20)$$

$$(\Delta\mathcal{M}_P^2)_{13} = -h_t \lambda \frac{m_t A_t}{m_{\tilde{t}_1}^2 - m_{\tilde{t}_2}^2} F_A, \quad (4.21)$$

$$(\Delta\mathcal{M}_P^2)_{23} = -h_t \lambda \cot\beta \frac{m_t A_t}{m_{\tilde{t}_1}^2 - m_{\tilde{t}_2}^2} F_A, \quad (4.22)$$

$$(\Delta\mathcal{M}_P^2)_{33} = -\lambda^2 \cot\beta \frac{m_t^2 A_t}{\mu(m_{\tilde{t}_1}^2 - m_{\tilde{t}_2}^2)} F_A, \quad (4.23)$$

where the functions F_i , F and F_A are combinations of the derivatives of ΔV evaluated at the minimum of the effective potential:

$$F_1 = \frac{\partial^2 \Delta V}{(\partial m_t^2)^2} + \frac{\partial^2 \Delta V}{(\partial m_{\tilde{t}_1}^2)^2} + \frac{\partial^2 \Delta V}{(\partial m_{\tilde{t}_2}^2)^2} + 2 \frac{\partial^2 \Delta V}{\partial m_t^2 \partial m_{\tilde{t}_1}^2} + 2 \frac{\partial^2 \Delta V}{\partial m_t^2 \partial m_{\tilde{t}_2}^2} + 2 \frac{\partial^2 \Delta V}{\partial m_{\tilde{t}_1}^2 \partial m_{\tilde{t}_2}^2}, \quad (4.24)$$

$$F_2 = \frac{\partial^2 \Delta V}{(\partial m_{\tilde{t}_1}^2)^2} - \frac{\partial^2 \Delta V}{(\partial m_{\tilde{t}_2}^2)^2} + \frac{\partial^2 \Delta V}{\partial m_t^2 \partial m_{\tilde{t}_1}^2} - \frac{\partial^2 \Delta V}{\partial m_t^2 \partial m_{\tilde{t}_2}^2}$$

³The differences with respect to eqs. (23)–(34) and (39) of ref. [8] are due to the fact that this dissertation adopts the opposite convention for the sign of λ and μ

$$-\frac{4c_{2\theta_t}^2}{m_{\tilde{t}_1}^2 - m_{\tilde{t}_2}^2} \left(\frac{\partial^2 \Delta V}{\partial c_{2\theta_t}^2 \partial m_{\tilde{t}_1}^2} + \frac{\partial^2 \Delta V}{\partial c_{2\theta_t}^2 \partial m_{\tilde{t}_2}^2} + \frac{\partial^2 \Delta V}{\partial c_{2\theta_t}^2 \partial m_{\tilde{t}_1}^2} \right), \quad (4.25)$$

$$F_3 = \frac{\partial^2 \Delta V}{(\partial m_{\tilde{t}_1}^2)^2} + \frac{\partial^2 \Delta V}{(\partial m_{\tilde{t}_2}^2)^2} - 2 \frac{\partial^2 \Delta V}{\partial m_{\tilde{t}_1}^2 \partial m_{\tilde{t}_2}^2} - \frac{2}{m_{\tilde{t}_1}^2 - m_{\tilde{t}_2}^2} \left(\frac{\partial \Delta V}{\partial m_{\tilde{t}_1}^2} - \frac{\partial \Delta V}{\partial m_{\tilde{t}_2}^2} \right) \\ + \frac{16c_{2\theta_t}^2}{(m_{\tilde{t}_1}^2 - m_{\tilde{t}_2}^2)^2} \left(c_{2\theta_t}^2 \frac{\partial^2 \Delta V}{(\partial c_{2\theta_t}^2)^2} + 2 \frac{\partial \Delta V}{\partial c_{2\theta_t}^2} \right) - \frac{8c_{2\theta_t}^2}{m_{\tilde{t}_1}^2 - m_{\tilde{t}_2}^2} \left(\frac{\partial^2 \Delta V}{\partial c_{2\theta_t}^2 \partial m_{\tilde{t}_1}^2} - \frac{\partial^2 \Delta V}{\partial c_{2\theta_t}^2 \partial m_{\tilde{t}_2}^2} \right) \quad (4.26)$$

$$F = \frac{\partial \Delta V}{\partial m_{\tilde{t}_1}^2} - \frac{\partial \Delta V}{\partial m_{\tilde{t}_2}^2} - \frac{4c_{2\theta_t}^2}{m_{\tilde{t}_1}^2 - m_{\tilde{t}_2}^2} \frac{\partial \Delta V}{\partial c_{2\theta_t}^2}, \quad (4.27)$$

$$F_A = \frac{\partial \Delta V}{\partial m_{\tilde{t}_1}^2} - \frac{\partial \Delta V}{\partial m_{\tilde{t}_2}^2} - \frac{4c_{2\theta_t}^2}{m_{\tilde{t}_1}^2 - m_{\tilde{t}_2}^2} \frac{\partial \Delta V}{\partial c_{2\theta_t}^2} + \frac{2z_t \mu \cot \beta}{A_t s_{2\theta_t}^2 (m_{\tilde{t}_1}^2 - m_{\tilde{t}_2}^2)} \frac{\partial \Delta V}{\partial c_{\varphi_t - \bar{\varphi}_t}}. \quad (4.28)$$

In eqs. (4.12)–(4.28) above we adopted the shortcuts $c_\phi \equiv \cos \phi$ and $s_\phi \equiv \sin \phi$ for a generic angle ϕ . The parameters μ and $\tan \beta$ are defined in eq. (2.28), and $z_t \equiv \text{sign}(A_t + \mu \cot \beta)$.

At one loop the top and stop contributions to ΔV depend only on the corresponding masses. In units of $N_c/(16\pi^2)$, where $N_c = 3$ is a color factor, the one-loop expressions for the functions appearing in eqs. (4.12)–(4.23) are

$$F_1^{1\ell} = \ln \frac{m_{\tilde{t}_1}^2 m_{\tilde{t}_2}^2}{m_t^4}, \quad F_2^{1\ell} = \ln \frac{m_{\tilde{t}_1}^2}{m_{\tilde{t}_2}^2}, \quad F_3^{1\ell} = 2 - \frac{m_{\tilde{t}_1}^2 + m_{\tilde{t}_2}^2}{m_{\tilde{t}_1}^2 - m_{\tilde{t}_2}^2} \ln \frac{m_{\tilde{t}_1}^2}{m_{\tilde{t}_2}^2}, \quad (4.29)$$

$$F^{1\ell} = F_A^{1\ell} = m_{\tilde{t}_1}^2 \left(\log \frac{m_{\tilde{t}_1}^2}{Q^2} - 1 \right) - m_{\tilde{t}_2}^2 \left(\log \frac{m_{\tilde{t}_2}^2}{Q^2} - 1 \right). \quad (4.30)$$

Inserting eqs. (4.29) and (4.30) in eqs. (4.12)–(4.23) we recover the well-known results [91] for the one-loop top/stop corrections to the NMSSM Higgs boson masses in the effective-potential approach.

Explicit expressions for the derivatives of the contribution to ΔV from two-loop diagrams with top, stop, gluino and gluon are provided in appendix C of ref. [8]. Rearranging the various terms, it can be shown that the 2×2 upper-left submatrices of $\Delta \mathcal{M}_S^2$ and $\Delta \mathcal{M}_P^2$ correspond to the $\mathcal{O}(\alpha_t \alpha_s)$ corrections derived in ref. [23] for the MSSM in the $\overline{\text{DR}}$ renormalization scheme. On the other hand, the corrections to the third row and third column of the mass matrices, which are specific to the NMSSM, were not previously available. If the one-loop part of the corrections is expressed in terms of OS parameters, the two-loop corrections must be supplemented with counterterm contributions that account for the shift from $\overline{\text{DR}}$ to OS, as described in section 2.4. The required $\mathcal{O}(\alpha_s)$ shifts in the parameters m_t , $m_{\tilde{t}_1}^2$, $m_{\tilde{t}_2}^2$, $s_{2\theta_t}$ and A_t can be found in appendix B of ref. [23].

The computation described above allows us to obtain also the two-loop $\mathcal{O}(\alpha_b \alpha_s)$ corrections induced by the bottom/sbottom sector, which can be relevant for large values of $\tan \beta$. To this purpose, the substitutions $t \rightarrow b$, $\tan \beta \leftrightarrow \cot \beta$, $(\Delta \mathcal{M}_{S,P}^2)_{11} \leftrightarrow (\Delta \mathcal{M}_{S,P}^2)_{22}$ and $(\Delta \mathcal{M}_{S,P}^2)_{13} \leftrightarrow (\Delta \mathcal{M}_{S,P}^2)_{23}$ must be performed in eqs. (4.12)–(4.28). In the case of the bottom/sbottom corrections, however, passing from the $\overline{\text{DR}}$ to the OS scheme involves additional complications, as explained in ref. [25].

In the case of the MSSM, the computation of the two-loop $\mathcal{O}(\alpha_t^2 + \alpha_t\alpha_b + \alpha_b^2)$ corrections induced by the Yukawa interactions of quarks, squarks, Higgs bosons and higgsinos is also available [27]. In contrast to the case of the $\mathcal{O}(\alpha_t\alpha_s + \alpha_b\alpha_s)$ corrections, however, this computation cannot be straightforwardly extended to the NMSSM, because the Higgs and higgsino sectors are extended by the presence of the singlet superfield.

Finally, since V_{eff} generates one-particle-irreducible Green's functions at vanishing external momentum, it is clear that the effective-potential approach neglects the momentum-dependent effects in the Higgs self-energies. The complete computation of the physical masses of the CP-even and CP-odd Higgs bosons requires the full, momentum-dependent two-point functions (a detailed discussion of the correspondence between the effective-potential approach and the full computation has been given in ref. [24]). However, in the last paper of ref. [89] it has been shown by direct calculation that, in the MSSM, the numerical effects of the two-loop momentum-dependent contributions to the Higgs boson masses are very small. There is no reason to expect that such effects would be much larger in the NMSSM.

4.3 Numerical examples

This section contains a brief discussion of the numerical effect of the one- and two-loop corrections to the NMSSM Higgs masses presented in sections 4.1 and 4.2, respectively.

Among the Lagrangian parameters that enter the computation of the NMSSM Higgs masses, the gauge and third-family Yukawa couplings, as well as the EWSB parameter v , can be extracted from the known values of various SM observables by taking into account the appropriate radiative corrections. We use the following input values for our analysis: the gauge boson masses $M_Z = 91.1876$ GeV and $M_W = 80.40$ GeV; the muon decay constant $G_\mu = 1.16637 \times 10^{-5}$ GeV⁻²; the strong coupling constant $\alpha_s(M_Z) = 0.1189$; the pole top mass $M_t = 173.1$ GeV; the running bottom mass $m_b(m_b) = 4.23$ GeV; the tau mass $m_\tau = 1.777$ GeV. Consistency with our computation of the one-loop radiative corrections requires that all the parameters entering the tree-level mass matrices be expressed in the $\overline{\text{DR}}$ renormalization scheme at a common scale Q_0 , which we take of the order of the soft SUSY-breaking masses. For consistency with the computation of the two-loop $\mathcal{O}(\alpha_t\alpha_s + \alpha_b\alpha_s)$ corrections, the top and bottom masses and Yukawa couplings entering the one-loop part of the corrections must also be expressed in the $\overline{\text{DR}}$ scheme. We determine the running electroweak gauge couplings and v directly at the scale Q_0 by means of eqs. (4.3) and (4.4). This procedure neglects the resummation of potentially large logarithms of the ratio of the weak scale to the scale Q_0 (incidentally, we also neglect the small SUSY contributions to δ_{VB}), but it is accurate enough for the purposes of our study. The top pole mass is converted into the corresponding running mass, then both the top and bottom masses are evolved up to the scale Q_0 by means of the SM renormalization group (RG) equations. At that scale the SM running masses are converted into NMSSM running masses by the inclusion of gluino-induced threshold corrections (which are the same as in the MSSM). The tau mass enters only the one-loop

part of the calculation and is not subject to QCD corrections, thus we use directly the pole mass. Finally, the strong gauge coupling α_s enters only the two-loop part of the calculation, therefore its precise definition amounts to a higher-order effect. We evolve α_s from M_Z to Q_0 by means of the SM RG equations.

To exemplify the effect of the one- and two-loop corrections to the neutral Higgs masses in the NMSSM, we choose the SUSY input parameters in such a way that the scalar component of the singlet is relatively light and has a sizable mixing with the lightest MSSM-like scalar. For what concerns the Higgs sector, we keep $-\lambda$ as a free parameter⁴ and fix the remaining parameters as

$$\kappa = -\lambda/5, \quad \tan\beta = 2, \quad A_\lambda = 500 \text{ GeV}, \quad A_\kappa = -10 \text{ GeV}, \quad \mu = -250 \text{ GeV}, \quad (4.31)$$

where we take μ as a proxy for the singlet vev $v_s = \mu/\lambda$. We adopt a common soft SUSY-breaking mass M_S for all of the squarks and sleptons, and fix the remaining soft SUSY-breaking parameters as

$$A_t = A_b = A_\tau = -1.5 M_S, \quad M_3 = 2 M_S, \quad M_2 = 2/3 M_S, \quad M_1 = M_S/3. \quad (4.32)$$

All of the parameters in eqs. (4.31) and (4.32) are meant as $\overline{\text{DR}}$ running parameters at the scale $Q_0 = M_S$.

Figures 4.1 and 4.2 exemplify the effect of the one-loop corrections to the NMSSM scalar masses. In figure 4.1 we plot the squared rotation matrix elements $(R_{13}^s)^2$ and $(R_{23}^s)^2$, which measure the strength of the singlet component in the two lightest scalars h_1 and h_2 , as a function of $-\lambda$ for $M_S = 300 \text{ GeV}$. In figure 4.2 we plot the masses of the two lightest scalars for the same choices of inputs. In both plots, the dotted lines correspond to the tree-level results; the dashed lines include the one-loop $\mathcal{O}(\alpha_t)$ and $\mathcal{O}(\alpha_b)$ corrections computed in the effective-potential approach; finally, the solid lines correspond to the results of the full one-loop calculation. For the full one-loop calculation of the rotation matrix the external momentum in the scalar self-energies is set to zero. It can be seen in figure 4.1 that, at small $|\lambda|$, the lightest scalar h_1 is dominantly MSSM-like while h_2 is dominantly singlet. When $|\lambda|$ increases the mixing between singlet and lightest MSSM-like Higgs increases as well. Meanwhile, the heaviest scalar h_3 has a mass of the order of 600 GeV and its singlet component is always small. It is interesting to note that – at least in this point of the parameter space – the value of $|\lambda|$ for which the two lightest mass eigenstates cross over (i.e., h_1 becomes dominantly singlet) depends quite strongly on the accuracy of the calculation. In particular, when only the quark/squark contributions to the radiative corrections are included the crossover occurs for much lower values of $|\lambda|$ than in the full one-loop calculation. Figure 4.2 shows the effect of the radiative corrections to the two lightest scalar masses. The rise with $|\lambda|$ in the tree-level masses is due to the well-known NMSSM contribution to the Higgs quartic coupling proportional to $\lambda^2 \sin^2 2\beta$. The comparison between the dotted and dashed lines shows that the $\mathcal{O}(\alpha_t)$ corrections induced by top and stop loops have a particularly large effect

⁴For consistency with the convention adopted for the MSSM parameter μ in the gluon-fusion calculation, this dissertation adopts for the sign of λ and μ the opposite convention w.r.t. ref. [8]. Consequently, the plots in figures 4.1, 4.2 and 4.5, which are taken from ref. [8], must be interpreted as showing results as a function of $-\lambda$.

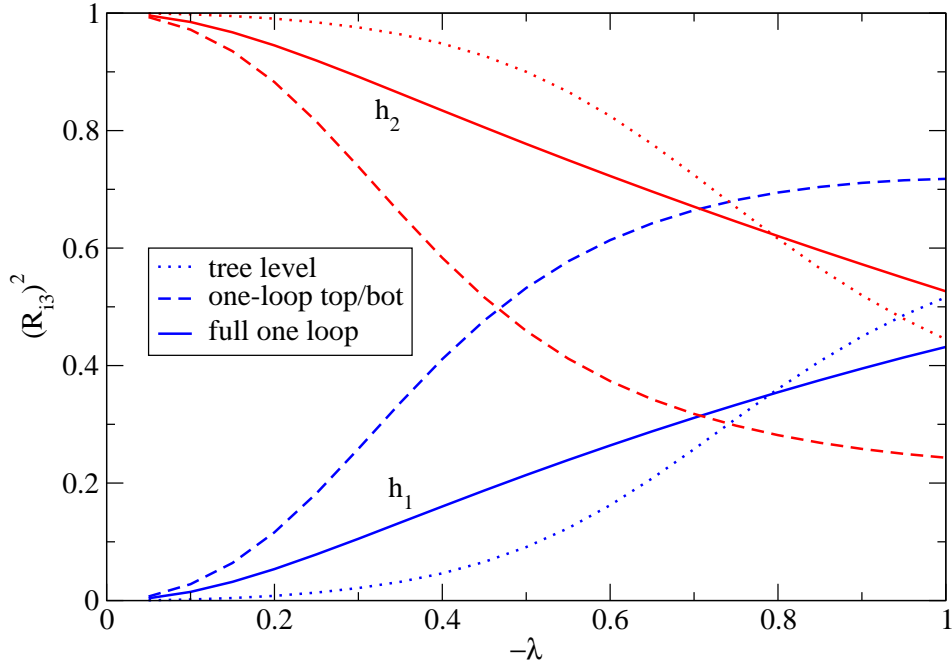


Figure 4.1: The squared rotation matrix element $(R_{i3}^s)^2$, measuring the singlet component in the scalars h_1 and h_2 , as a function of $-\lambda$, for $M_S = 300$ GeV. The values of the other input parameters and the meaning of the different curves are described in the text.

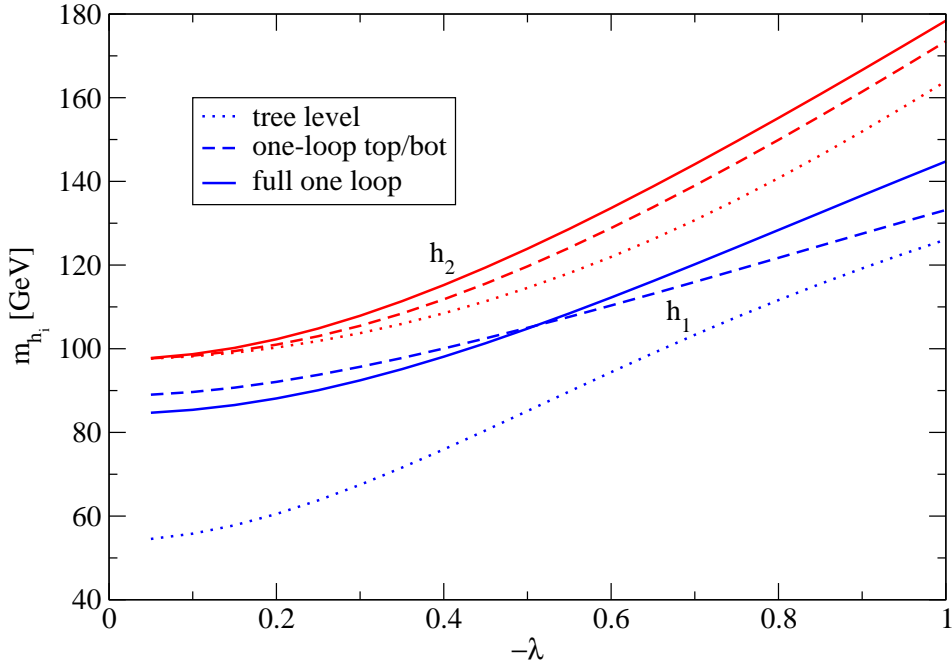


Figure 4.2: The masses of the two lightest scalars h_1 and h_2 as a function of $-\lambda$, for $M_S = 300$ GeV. The values of the other input parameters and the meaning of the curves are described in the text.

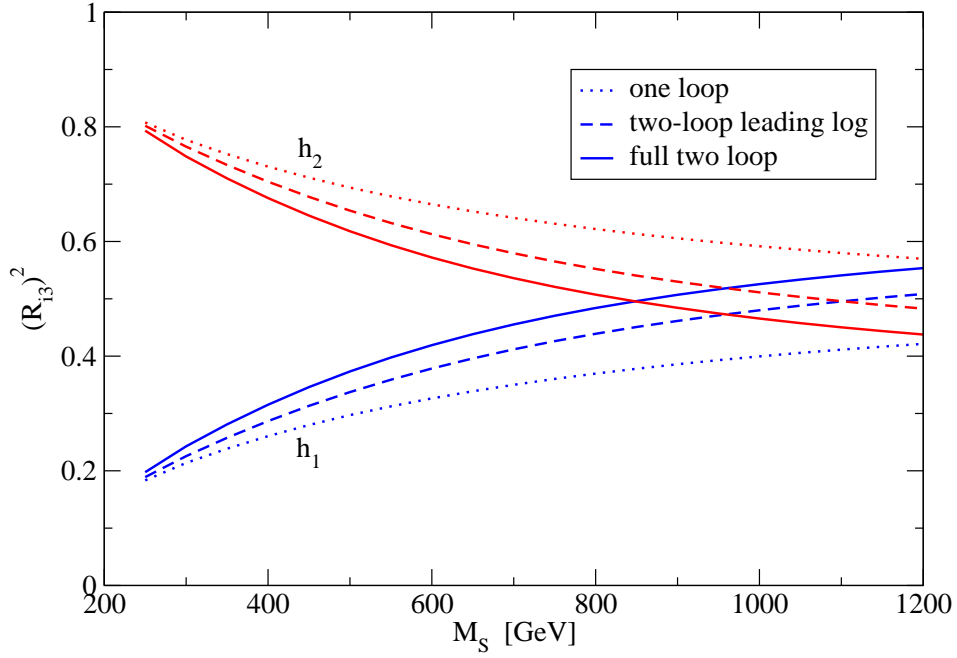


Figure 4.3: The squared rotation matrix element $(R_{i3}^S)^2$, measuring the singlet component in the scalars h_1 and h_2 , as a function of M_S , for $\lambda = -0.5$. The values of the other input parameters and the meaning of the different curves are described in the text.

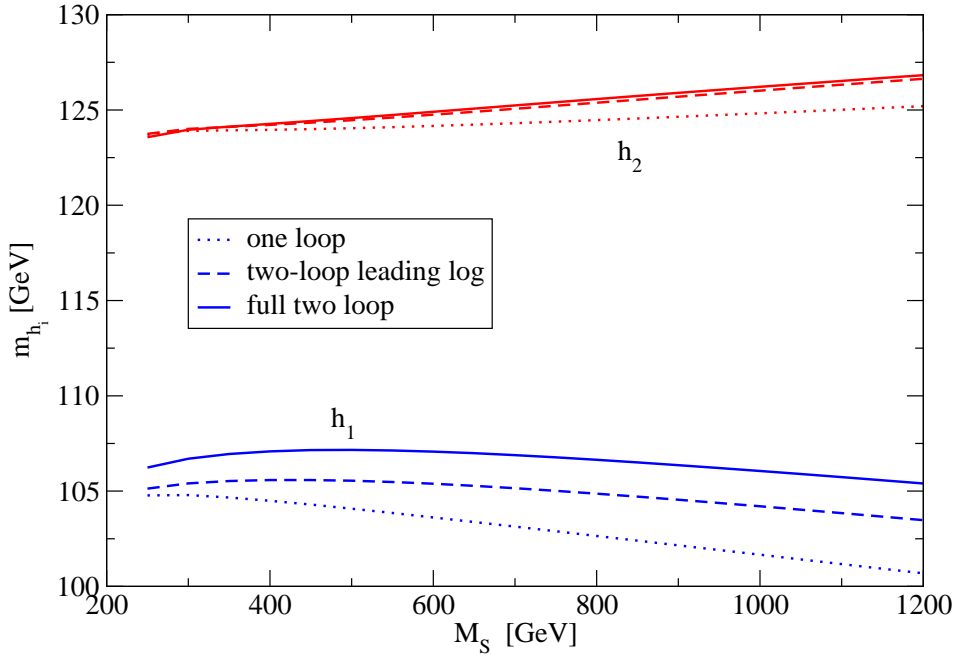


Figure 4.4: The masses of the two lightest scalars h_1 and h_2 as a function of M_S , for $\lambda = -0.5$. The values of the other input parameters and the meaning of the different curves are described in the text.

on m_{h_1} for small values of $|\lambda|$, when h_1 is light and mostly MSSM-like. The $\mathcal{O}(\alpha_b)$ corrections induced by bottom and sbottom loops are also included in the dashed lines, but they are negligible due to the small value of $\tan\beta$. When $|\lambda|$ increases the $\mathcal{O}(\alpha_t)$ corrections are shared between m_{h_1} and m_{h_2} , and become less relevant due to the increase in the tree-level masses. However, even for the heavier scalar h_2 these corrections can still amount to several GeV at large $|\lambda|$. Finally, the comparison between the solid and dashed lines in figure 4.2 shows that the remaining one-loop corrections – which constitute one of the original contributions of ref. [8] – are also relevant, and can account for shifts of 5–10 GeV in both masses.

Figures 4.3 and 4.4 exemplify the effect of the two-loop corrections to the NMSSM scalar masses. In figure 4.3 we plot $(R_{13}^S)^2$ and $(R_{23}^S)^2$ as a function of M_S for $\lambda = -0.5$. In figure 4.4 we plot the masses of the two lightest scalars for the same choices of inputs. In both plots, the dotted lines correspond to the full one-loop results (again, the rotation matrix is computed at zero external momentum); the dashed lines include the two-loop leading-logarithmic $\mathcal{O}(\alpha_t\alpha_s)$ contribution to the (2,2) entry of the scalar mass matrix as was implemented in `NMHDECAY` [42], i.e.

$$(\Delta\mathcal{M}_S^2)_{22}^{\text{LL}} = 6 \frac{\alpha_t\alpha_s}{\pi^2} m_t^2 \log^2 \frac{M_S^2}{m_t^2}. \quad (4.33)$$

Finally, the solid lines correspond to the results of our two-loop $\mathcal{O}(\alpha_t\alpha_s + \alpha_b\alpha_s)$ calculation. It can be seen in figure 4.3 that for small M_S the lightest scalar h_1 is mostly MSSM-like while h_2 is mostly singlet. When M_S increases, the radiative corrections increase the mixing between singlet and MSSM-like Higgs. Figure 4.4 shows that the two-loop corrections to the lightest scalar mass are positive and relatively small. This is a typical feature of the $\overline{\text{DR}}$ computation, in contrast to the OS computation in which the two-loop corrections are negative and much larger (for a discussion of this issue in the MSSM see ref. [29]). It is interesting to note that, in this scenario, the leading-logarithmic term accounts only for a fraction (30% to 60%, increasing with M_S) of the total $\mathcal{O}(\alpha_t\alpha_s)$ contribution to the (2,2) entry of the scalar mass matrix. Indeed, the leading-logarithmic approximation of eq. (4.33) neglects potentially large contributions controlled by powers of the ratio A_t/M_S , as well as the possibility of mass splittings among stops and gluino. The effect of the $\mathcal{O}(\alpha_t\alpha_s)$ corrections to the entries of the scalar mass matrix other than (2,2) is also non-negligible. The comparison between the dashed and solid curves for h_1 in figures 4.3 and 4.4 shows that, in this point of the parameter space, the non-leading-logarithmic contributions contained in our two-loop calculation induce a shift of 1–2 GeV in m_{h_1} , and have a sizable effect on the mixing matrix as well (on the other hand, the near overlap of the dashed and solid curves for h_2 in figure 4.4 is the result of an accidental cancellation). One of the attractive features of the NMSSM is the viability of scenarios in which M_S is not much above the weak scale. It is clear from figures 4.3 and 4.4 that, in those scenarios, the leading-logarithmic approximation is not satisfactory, and a reliable evaluation of the two-loop corrections requires at least the complete $\mathcal{O}(\alpha_t\alpha_s + \alpha_b\alpha_s)$ calculation.

To conclude this section, we show in figure 4.5 the effect of the radiative corrections to the mass of the lightest physical pseudoscalar A_1 . For the choice of parameters considered in this example A_1

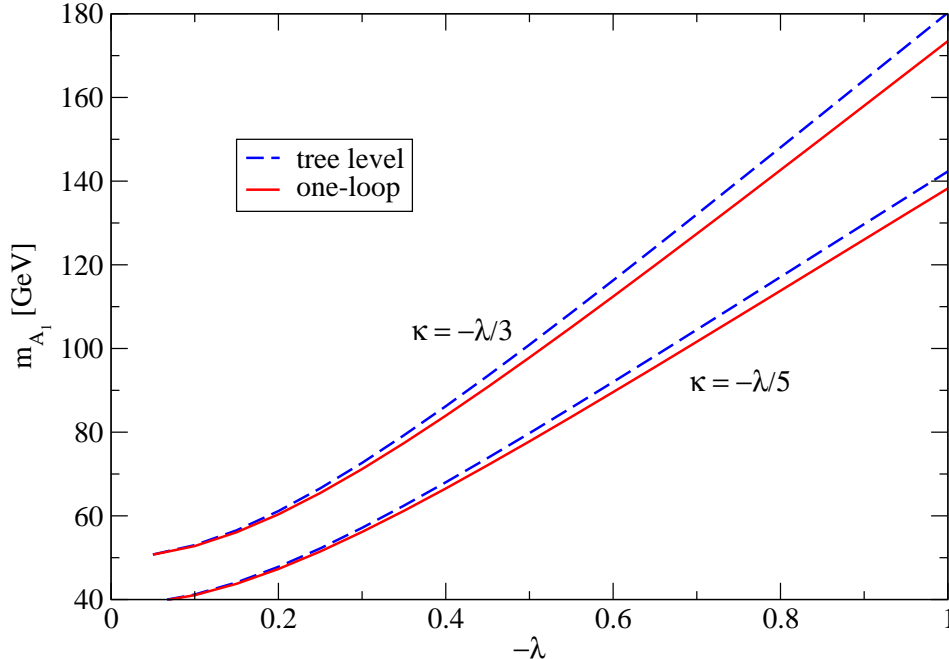


Figure 4.5: The masses of the lightest physical pseudoscalar A_1 as a function of $-\lambda$, for $M_S = 300$ GeV and κ set equal to either $-\lambda/5$ or $-\lambda/3$. The values of the other input parameters and the meaning of the different curves are described in the text.

is almost entirely singlet, therefore its mass is hardly affected by the one- and two-loop corrections involving quark/squark loops. The pseudoscalar A_2 , on the other hand, is almost entirely MSSM-like, but its tree-level mass is of the order of 600 GeV, thus it is also not much affected by the radiative corrections. However, the Higgs self-interactions and the Higgs-higgsino interactions controlled by the superpotential couplings λ and κ do induce non-negligible corrections to the lightest pseudoscalar mass. The dashed and solid lines in figure 4.5 correspond to the tree-level and one-loop determinations of m_{A_1} , respectively, as a function of $-\lambda$. The input parameters are chosen as in eqs. (4.31) and (4.32), but we show two sets of curves corresponding to $\kappa = -\lambda/5$ and $\kappa = -\lambda/3$. From the comparison between the dashed and solid curves it can be seen that the one-loop corrections to m_{A_1} can amount to several GeV when $|\lambda|$ and κ take on relatively large values. The two-loop corrections computed in section 4.2 include only the quark/squark contributions, therefore the corresponding curves would essentially overlap with the one-loop curves.

4.4 Further developments

In the years following the publication of ref. [8] the interest in the NMSSM as a plausible SUSY extension of the SM has risen, because the relatively large mass of the scalar found at the LHC makes the prediction of an additional contribution to the Higgs quartic coupling particularly appealing.

The results of ref. [8] for the one-loop corrections to the masses of the neutral Higgs bosons of the NMSSM were subsequently confirmed by two independent calculations. In ref. [43], the full one-loop tadpoles and self-energies were computed automatically with the Mathematica package SARAH [95], and found to be in perfect agreement with ref. [8] (taking into account that the Yukawa couplings of the first two generations were neglected in the latter paper). In ref. [96] the same one-loop computation was performed with FeynArts [60], again yielding perfect agreement with ref. [8].

The authors of ref. [96] also considered the effect of expressing the parameters in the tree-level mass matrices in eqs. (4.1) and (4.2), i.e.,

$$g, g', v, v_s, \tan\beta, \lambda, \kappa, A_\lambda, A_\kappa, \quad (4.34)$$

in renormalization schemes different from $\overline{\text{DR}}$. They found that trading g, g', v and A_λ in the tree-level mass matrices for α_{em} and the pole masses M_Z, M_W and M_{H^\pm} , and shifting the one-loop corrections by appropriate counterterm contributions, has a negligible impact on the results for the masses and mixing of the CP-even Higgs bosons. On the other hand, an OS scheme in which also the parameters λ, κ, v_s and A_κ are traded for physical observables (namely, combinations of the pole masses of pseudoscalars, charginos and neutralinos) was found to induce unphysically large corrections for $\lambda \rightarrow 0$, because some of the counterterms involved in the $\overline{\text{DR}}$ -OS conversion diverge in that limit. In a follow-up paper, ref. [97], the authors also studied the effect of allowing for CP-violating phases in the parameters that enter the tree-level mass matrices of the Higgs bosons, as well as in the stop-mixing term A_t entering the one-loop corrections.

The results for the one- and two-loop corrections to the Higgs boson masses presented in this chapter have been implemented in public codes for the computation of the NMSSM mass spectrum, and, as a result, they have become a standard ingredient of many phenomenological analyses of the NMSSM. In particular, I collaborated with the authors of NMHDECAY [42] in upgrading the partial one-loop calculation implemented in that code, which was based on the effective-potential results of ref. [91] and the leading-logarithmic results of ref. [92], to the full one-loop calculation described in section 4.1. In collaboration with K.H. Phan, I also computed the full one-loop corrections to the charged Higgs mass, which were not included in ref. [8]. These corrections were found to be in agreement with ref. [43], and they were also implemented in NMHDECAY. Finally, the two-loop corrections described in section 4.2 were implemented both in NMHDECAY – replacing the crude leading-logarithmic result of eq. (4.33) – and in the NMSSM version of SPheno [43].

Chapter 5

BR[$B \rightarrow X_s \gamma$] in the MSSM with MFV

The radiative B decays play a key role in the program of precision tests of the Standard Model and its extensions. The inclusive decay $B \rightarrow X_s \gamma$ is particularly well suited to this precision program, thanks to its low sensitivity to non-perturbative effects. The present experimental world average for the branching ratio of this decay, with a 1.6 GeV lower cut on the energy of the photon, is $\text{BR}[B \rightarrow X_s \gamma]_{\text{ex}} = (3.43 \pm 0.21 \pm 0.07) \times 10^{-4}$ [98]. The SM prediction for the branching ratio with the same cut on the photon energy is $\text{BR}[B \rightarrow X_s \gamma]_{\text{th}} = (3.15 \pm 0.23) \times 10^{-4}$ [99, 100] and includes most of the NNLO perturbative QCD contributions as well as the leading non-perturbative and electroweak effects. Both experiment and SM prediction have an uncertainty of about 7%.

New Physics (NP) can in principle induce sizable contributions to the decay $B \rightarrow X_s \gamma$, hence the good agreement between the SM prediction and the experimental result puts severe constraints on the flavor structure of NP models. However, the theoretical accuracy of the predictions for $\text{BR}[B \rightarrow X_s \gamma]$ in extensions of the SM is not at the same level as in the SM. Complete NLO-QCD calculations are available for minimal extensions such as the Two-Higgs-Doublet Model (THDM) [101, 102, 103, 9] and the Left-Right symmetric model [103]. In the case of the MSSM, the NLO-QCD contributions were first computed under the simplifying assumption of Minimal Flavor Violation (MFV), according to which the quark and squark mass matrices can be simultaneously diagonalized and the only source of flavor violation is the CKM matrix. In this scenario, the contributions of two-loop diagrams that include gluons and charginos were computed in refs. [103, 104], while the contributions involving gluinos were first considered in the heavy gluino limit in ref. [104], and in an effective-Lagrangian approach in refs. [105, 106, 107]. After a partial two-loop calculation [108], the full computation of the two-loop gluino contributions to $B \rightarrow X_s \gamma$ in the MSSM with MFV was finally presented in ref. [1].

In scenarios with a generic (i.e., non-MFV) flavor structure of the squark mass matrices, on the other hand, the dominant contributions to $B \rightarrow X_s \gamma$ arise from diagrams that involve flavor-violating quark-squark-gluino vertices (rather than electroweak charged-current vertices controlled by the CKM matrix). The NLO-QCD contributions in these scenarios were recently computed in ref. [109], and can be seen as complementary to the ones computed in ref. [1] for the MFV case.

Once again, the usefulness of complicated two-loop calculations risks being rather limited, unless the results are made available to the physics community in the form of computer codes. Several codes for the determination of the MSSM mass spectrum and other SUSY observables (e.g. `FeynHiggs` [30], `SuSpect` [32], `SPheno` [33], `NMHDECAY` [42], `micrOMEGAs` [110], `CPsuperH` [111] and `SuperIso` [112]) contain calculations of $\text{BR}[B \rightarrow X_s \gamma]$ in various approximations. However, in all of these codes the two-loop gluino contributions to $B \rightarrow X_s \gamma$ are included, if at all, only in the effective Lagrangian approximation of refs. [105, 106, 107], which is valid in the limit of heavy superpartners and large $\tan \beta$. In ref. [4] we presented a new fortran code, `SusyBSG`, dedicated to the full NLO-QCD calculation of $\text{BR}[B \rightarrow X_s \gamma]$ in the MSSM with MFV. The code includes the full results of ref. [1] for the two-loop gluino contributions to the Wilson coefficients of the magnetic and chromo-magnetic operators relevant to the $B \rightarrow X_s \gamma$ decay, and the results of refs. [103, 104] for the two-loop gluon contributions. For the sake of comparison, `SusyBSG` can also provide evaluations of $\text{BR}[B \rightarrow X_s \gamma]$ in the SM and in various versions of the THDM, as well as in the MSSM with two-loop gluino contributions computed in the effective-Lagrangian approximation.

In this chapter I describe the NLO-QCD calculation of $\text{BR}[B \rightarrow X_s \gamma]$ implemented in `SusyBSG`, focusing in particular on the two-loop gluino contributions presented in ref. [1].

5.1 NLO determination of $\text{BR}[B \rightarrow X_s \gamma]$

This section summarizes the weak-scale matching conditions for the $\Delta B = 1$ effective Hamiltonian in the MSSM with Minimal Flavor Violation, as well as the NLO relation between the Wilson coefficients computed at the weak scale and the branching ratio for the decay $B \rightarrow X_s \gamma$.

The $\Delta B = 1$ effective Hamiltonian at the matching scale μ_0 where the heavy particles are integrated out of the theory is given by

$$\mathcal{H} = -\frac{4G_F}{\sqrt{2}} V_{ts}^{\text{CKM}*} V_{tb}^{\text{CKM}} \sum_i C_i(\mu_0) Q_i(\mu_0), \quad (5.1)$$

where G_F is the Fermi constant and $V_{ts}^{\text{CKM}}, V_{tb}^{\text{CKM}}$ are elements of the CKM matrix. The operators relevant to our calculation are

$$Q_1 = (\bar{s}_L \gamma_\mu T^a c_L)(\bar{c}_L \gamma^\mu T^a b_L), \quad (5.2)$$

$$Q_2 = (\bar{s}_L \gamma_\mu c_L)(\bar{c}_L \gamma^\mu b_L), \quad (5.3)$$

$$Q_3 = (\bar{s}_L \gamma_\mu b_L) \sum_q (\bar{q} \gamma_\mu q), \quad (5.4)$$

$$Q_4 = (\bar{s}_L \gamma_\mu T^a b_L) \sum_q (\bar{q} \gamma_\mu T^a q), \quad (5.5)$$

$$Q_5 = (\bar{s}_L \gamma_\mu \gamma_\nu \gamma_\rho b_L) \sum_q (\bar{q} \gamma^\mu \gamma^\nu \gamma^\rho q), \quad (5.6)$$

$$Q_6 = (\bar{s}_L \gamma_\mu \gamma_\nu \gamma_\rho T^a b_L) \sum_q (\bar{q} \gamma^\mu \gamma^\nu \gamma^\rho T^a q), \quad (5.7)$$

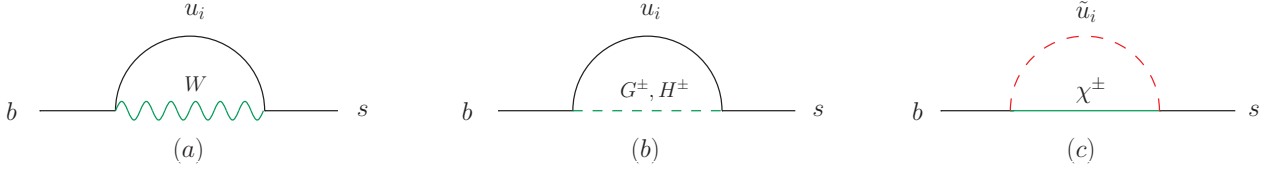


Figure 5.1: Diagrams contributing at LO to the Wilson coefficients of the magnetic and chromo-magnetic operators. A photon or gluon is attached in all possible ways to the particles in the loops.

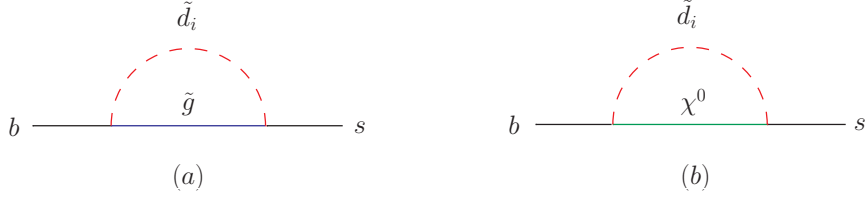


Figure 5.2: Same as figure 5.1 for the diagrams involving flavor-changing quark-squark-gaugino or quark-squark-neutralino interactions, relevant only in presence of flavor mixing in the sdown sector.

$$Q_7 = \frac{e}{16\pi^2} m_b \bar{s}_L \sigma^{\mu\nu} b_R F_{\mu\nu}, \quad (5.8)$$

$$Q_8 = \frac{g_s}{16\pi^2} m_b \bar{s}_L \sigma^{\mu\nu} T^a b_R G_{\mu\nu}^a. \quad (5.9)$$

Additional operators Q'_i can be obtained via the exchange $L \leftrightarrow R$ in eqs. (5.2)–(5.9). However, in MFV scenarios the contributions of those operators to the $b \rightarrow s\gamma$ transition are suppressed by the ratio m_s/m_b , and can be neglected under our approximations.

When the QCD corrections are considered, the Wilson coefficients of the operators Q_i can be organized in the following way

$$C_i(\mu_0) = C_i^{(0)\text{SM}}(\mu_0) + C_i^{(0)H^\pm}(\mu_0) + C_i^{(0)\text{SUSY}}(\mu_0) + \frac{\alpha_s(\mu_0)}{4\pi} \left[C_i^{(1)\text{SM}}(\mu_0) + C_i^{(1)H^\pm}(\mu_0) + C_i^{(1)\text{SUSY}}(\mu_0) \right], \quad (5.10)$$

where the various LO contributions are classified according to whether the corresponding diagrams contain only SM fields, a physical charged Higgs boson and an up-type quark, or two superparticles. The expressions for $C_i^{(0)\text{SM}}$ and $C_i^{(0)H^\pm}$ can be found, e.g., in ref. [101], while those for $C_i^{(0)\text{SUSY}}$ can be found, e.g., in eq. (4) of ref. [104]. Note that at LO only the coefficients of the magnetic and chromo-magnetic operators Q_7 and Q_8 receive contributions from diagrams involving non-SM fields, depicted in figure 5.1. The one-loop gluino- and neutralino-exchange diagrams depicted in figure 5.2 do not contribute to $C_{7,8}^{(0)\text{SUSY}}$ under the MFV assumption, but can contribute to both $C_{7,8}^{(0)\text{SUSY}}$ and $C'_{7,8}{}^{(0)\text{SUSY}}$ in the presence of flavor mixing in the sdown sector.

The NLO coefficients $C_i^{(1)\text{SM}}$ and $C_i^{(1)H^\pm}$ contain the gluonic corrections to the SM and charged-Higgs contributions, and can be found for instance in ref. [101]. Formulae for $C_i^{(1)H^\pm}$ in the so-called Manohar-Wise model [44], which features an additional color-octet scalar with the same electroweak quantum numbers as the SM Higgs, can be found in ref. [9]. Concerning the NLO supersymmetric contributions $C_i^{(1)\text{SUSY}}$, the chargino-gluon contributions can be found in refs. [103, 104]. The full computation of $C_i^{(1)\text{SUSY}}$ in the MSSM with MFV includes also the contributions from diagrams involving both a gluino exchange and electroweak charged-current interactions. The two-loop gluino contributions to $C_{7,8}^{(1)\text{SUSY}}$ were computed in ref. [1], and will be discussed in section 5.2. In addition, there are one-loop gluino contributions to $C_{1,2}^{(1)\text{SUSY}}$ that can be found in appendix A of ref. [4].

The Wilson coefficients must be evolved from a matching scale of the order of the heavy-particle masses down to a low scale μ_b , where the matrix elements for the $b \rightarrow s\gamma$ decay are computed. In `SusyBSG` we follow the approach of ref. [113], in which the branching ratio for $B \rightarrow X_s \gamma$ with a cutoff E_0 on the photon energy in the rest frame of B is related to the measured rate $\text{BR}[B \rightarrow X_c e \bar{\nu}]_{\text{exp}}$ by

$$\frac{\text{BR}[B \rightarrow X_s \gamma]_{E_\gamma > E_0}}{\text{BR}[B \rightarrow X_c e \bar{\nu}]_{\text{exp}}} = \left| \frac{V_{ts}^{\text{CKM}*} V_{tb}^{\text{CKM}}}{V_{cb}^{\text{CKM}}} \right|^2 \frac{6 \alpha_{\text{em}}}{\pi C} \left[|K|^2 + |K'|^2 + B(E_0) + N(E_0) \right], \quad (5.11)$$

where C is the “non-perturbative semileptonic phase-space factor” defined in appendix C of ref. [113]. The quantities $B(E_0)$ and $N(E_0)$ represent the gluon-bremsstrahlung and non-perturbative contributions, respectively, and are also described in ref. [113]. The factor K contains the contributions to the $b \rightarrow s\gamma$ amplitude from the operators Q_i in eqs. (5.2)–(5.9), and is dominated by the effective Wilson coefficient for the magnetic operator at the low scale. The factor K' , which we include here at LO only, contains instead the contribution of the “primed” operators with inverted quark chirality, relevant only when the MFV assumption is relaxed.

The factor K can be written as

$$K = K_c + r(\mu_t) [K_t + K_{\text{NP}}] + \varepsilon_{\text{ew}}. \quad (5.12)$$

Following ref. [113] we separate K into the light-quark contribution K_c , the top-quark contribution K_t , the new-physics contribution K_{NP} and the electroweak correction ε_{ew} . For the latter we adopt the results of ref. [114], including the available NP contributions where appropriate. We compute the top and NP contributions to the matching conditions for the Wilson coefficients at a scale μ_t of the order of the top mass, and in K_t and K_{NP} we keep the bottom Yukawa coupling renormalized at μ_t by introducing the quantity

$$r(\mu_t) \equiv \frac{m_b^{\overline{\text{MS}}}(\mu_t)}{m_b^{1S}} = \frac{m_b^{\overline{\text{MS}}}(\mu_t)}{m_b^{\overline{\text{MS}}}(\mu_b)} \times \left[1 - \frac{\alpha_s(m_b^{1S})}{4\pi} \left(\frac{16}{3} + 8 \ln \frac{m_b^{1S}}{\mu_b} \right) + \frac{2}{9} \alpha_s(m_b^{1S})^2 \right], \quad (5.13)$$

where the “1S mass” m_b^{1S} is defined as half of the perturbative contribution to the Υ -mass. The ratio of masses on the r.h.s. of eq. (5.13) accounts for the evolution of the running bottom mass from μ_t to μ_b , while the term in the square brackets accounts for the shift between $m_b^{\overline{\text{MS}}}(\mu_b)$ and m_b^{1S} .

Explicit formulas for the light-quark and top contributions to K as implemented in **SusyBSG** can be found in appendix D of ref. [4]. After factoring out $r(\mu_t)$, the NP contribution reads

$$\begin{aligned}
K_{\text{NP}} = & \left[1 - \frac{2}{9} \alpha_s(m_b^{1S})^2 \right] \left[\eta_t^{\frac{4}{23}} C_7^{(0)\text{NP}}(\mu_t) + \frac{8}{3} \left(\eta_t^{\frac{2}{23}} - \eta_t^{\frac{4}{23}} \right) C_8^{(0)\text{NP}}(\mu_t) \right] \\
& + \frac{\alpha_s(\mu_b)}{4\pi} \left\{ \sum_{k=1}^8 \eta_t^{(a_k + \frac{11}{23})} \left[f_k C_1^{(1)\text{NP}}(\mu_t) + h_k C_2^{(1)\text{NP}}(\mu_t) + e_k C_4^{(1)\text{NP}}(\mu_t) \right] \right. \\
& + \eta_t^{\frac{4}{23}} \left[\eta_t C_7^{(1)\text{NP}}(\mu_t) - 2 \left(\frac{12523}{3174} - \frac{7411}{4761} \eta_t - \frac{2}{9} \pi^2 - \frac{4}{3} \ln \frac{m_b^{1S}}{\mu_b} \right) C_7^{(0)\text{NP}}(\mu_t) \right. \\
& \quad \left. \left. - \frac{8}{3} \eta_t C_8^{(1)\text{NP}}(\mu_t) - 2 \left(-\frac{50092}{4761} + \frac{1110842}{357075} \eta_t + \frac{16}{27} \pi^2 + \frac{32}{9} \ln \frac{m_b^{1S}}{\mu_b} \right) C_8^{(0)\text{NP}}(\mu_t) \right] \right. \\
& \left. + \eta_t^{\frac{2}{23}} \left[\frac{8}{3} \eta_t C_8^{(1)\text{NP}}(\mu_t) - 2 \left(\frac{2745458}{357075} - \frac{38890}{14283} \eta_t - \frac{4}{9} \pi^2 - \frac{16}{9} \ln \frac{m_b^{1S}}{\mu_b} \right) C_8^{(0)\text{NP}}(\mu_t) \right] \right\} , \tag{5.14}
\end{aligned}$$

where $\eta_t = \alpha_s(\mu_t)/\alpha_s(\mu_b)$, the ‘‘magic numbers’’ f_k, h_k , and e_k can be found in appendix D of ref. [4] and references therein, and, following the classification in eq. (5.10), we define $C_i^{\text{NP}} \equiv C_i^{H^\pm} + C_i^{\text{SUSY}}$.

In addition to μ_t and μ_b , the NLO result for $\text{BR}[B \rightarrow X_s \gamma]$ described above depends on two renormalization scales entering the light-quark contribution K_c : a weak scale μ_W at which we compute the contributions to the matching conditions for the Wilson coefficients coming from loops with light quarks, and the scale μ_c at which we express the running charm mass entering the matrix elements. The dependence on these four scales is part of the theoretical uncertainty of the NLO calculation, and could be partially compensated for by implementing in **SusyBSG** the lengthy NNLO contributions, which have been computed only for the SM [99, 100]. However, it is safe to expect that the users of **SusyBSG** will be mainly interested in the deviation from the SM prediction induced by the NP contribution of eq. (5.14), which is known at NLO only. In this situation, a pragmatic approach consists in adjusting the four renormalization scales in such a way that **SusyBSG** reproduces the known NNLO result of the SM when $K_{\text{NP}} = 0$. To this effect, we adopt the default values

$$\mu_t = \mu_W = 2 m_W, \quad \mu_b = 2.5 \text{ GeV}, \quad \mu_c = 1 \text{ GeV}. \tag{5.15}$$

Using these values for the scales, and setting the SM input parameters to the partially outdated values used in ref. [99], we obtain a SM prediction for $\text{BR}[B \rightarrow X_s \gamma]$ of 3.15×10^{-4} , in agreement with the NNLO result of ref. [99]. If we use instead the same input values as in ref. [115], we obtain a SM prediction for $\text{BR}[B \rightarrow X_s \gamma]$ of 3.27×10^{-4} , in agreement with the NNLO result of ref. [115]. Very good agreement, within at most 2%, is also found at various values of $\tan \beta$ and m_{H^\pm} with the partial NNLO implementation of the type-II THDM from ref. [99].

It should be noted, however, that μ_c in eq. (5.15) is adjusted to a very low value in order to mimic the NNLO contributions that are not present in our calculation. Therefore, in this case, the

variation of the renormalization scales should not be used to estimate the intrinsic uncertainty of our calculation. Indeed, the result of the NLO calculation depends quite sharply on μ_c around the value that reproduces the NNLO result. For example, using $\mu_c = 1.224$ GeV, with the other scales fixed as in eq. (5.15) and the remaining input parameters set as in ref. [99], we find $\text{BR}[B \rightarrow X_s \gamma] = 3.29 \times 10^{-4}$, a 4% variation from the result of ref. [99].

Concerning the theoretical uncertainty of our prediction, we recall that in the SM analysis of refs. [99, 100] the error is dominated by a 5% uncertainty due to unknown $\mathcal{O}(\alpha_s \Lambda_{\text{QCD}}/m_b)$ non-perturbative contributions to the matrix elements. An additional $\sim 4\%$ intrinsic uncertainty stems from the perturbative part of the calculation and from the estimate of missing NNLO contributions. The parametric uncertainty in the SM is only about 3%. All of these sources of uncertainty are present in the MSSM calculation as well. Therefore, we recommend using *at least* a 7% intrinsic uncertainty, throughout the parameter space, to be added in quadrature with the parametric uncertainty.

5.2 Two-loop gluino contributions to the Wilson coefficients

This section describes the calculation of the two-loop gluino contributions to the Wilson coefficients of the magnetic and chromo-magnetic operators presented in ref. [1]. At NLO, the supersymmetric contribution $C_{7,8}^{(1)\text{SUSY}}$ can be decomposed as

$$C_{7,8}^{(1)\text{SUSY}} = C_{7,8}^{(1)\tilde{g}} + C_{7,8}^{(1)\chi^\pm}, \quad (5.16)$$

where $C_{7,8}^{(1)\tilde{g}}$ contains two-loop diagrams with a gluino together with a Higgs or W boson, while $C_{7,8}^{(1)\chi^\pm}$ corresponds to two-loop diagrams with a chargino together with a gluon or a gluino or a quartic squark coupling. It should be recalled that, unlike $C_{7,8}^{(1)\text{SM}}$ and $C_{7,8}^{(1)H^\pm}$, the two-loop gluonic corrections to the chargino loops are not UV finite: as shown in [104], in order to obtain a finite result one has to combine them with the chargino-gluino diagrams. The chargino-gluon two-loop contributions have been fully computed in refs. [103, 104]. On the other hand, two-loop contributions involving gluinos (in both $C_{7,8}^{(1)\tilde{g}}$ and $C_{7,8}^{(1)\chi^\pm}$) have been considered in ref. [104] only in the heavy-gluino limit. We are now going to relax this approximation and to compute $C_{7,8}^{(1)\text{SUSY}}$ for arbitrary gluino mass. We restrict our calculation to the MFV scenario, i.e. we assume that the mass matrices for quarks and squarks can be simultaneously diagonalized, so that the tree-level quark-squark-gluino interaction does not violate flavor, and diagrams such as the one in figure 5.2a vanish.

The two-loop diagrams containing a gluino or a quartic squark coupling that contribute to $C_{7,8}^{(1)\tilde{g}}$ and $C_{7,8}^{(1)\chi^\pm}$ are shown in figures 5.3 and 5.4, respectively. Together with the diagrams with gluons, they complete the QCD contribution to the Wilson coefficients of $Q_{7,8}$ in the MSSM under the MFV assumption. The effective theory is trivial, and the Wilson coefficients are directly given by the result of the Feynman diagrams. We followed the same methods employed in [101], in particular we performed our calculation in the background-field gauge [59], neglected terms suppressed by powers of m_b/M_W or m_b/M_{SUSY} (after factoring out a bottom mass in the definition of the operators Q_7 and Q_8), and

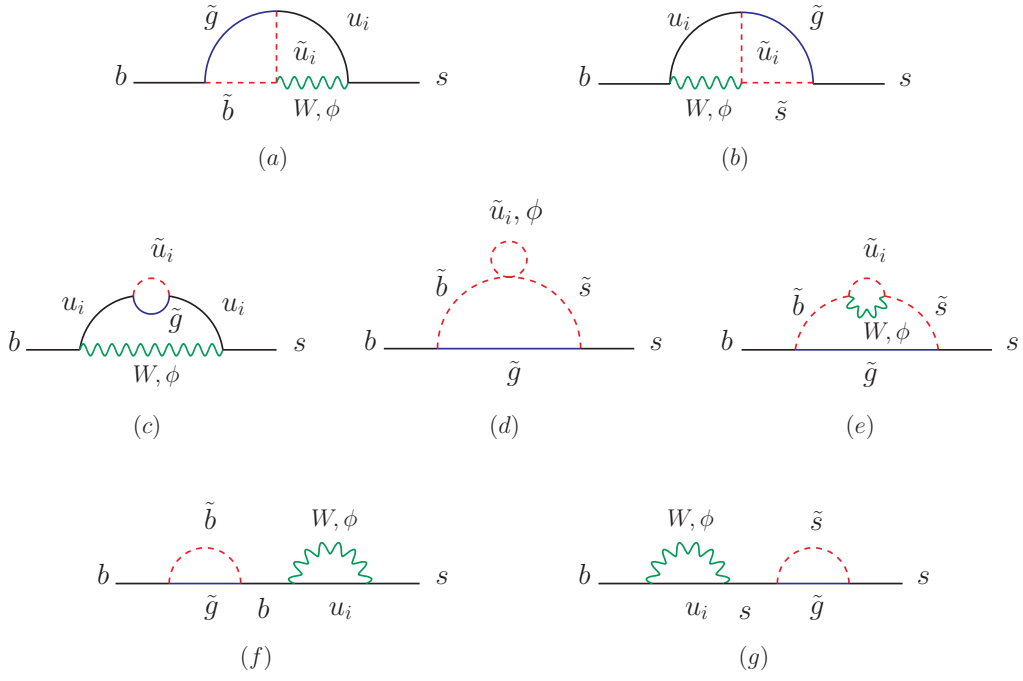


Figure 5.3: Feynman diagrams containing a gluino and a W or a Higgs boson ($\phi = H^\pm, G^\pm$). A photon or gluon is attached in all possible ways to the particles in the loops.

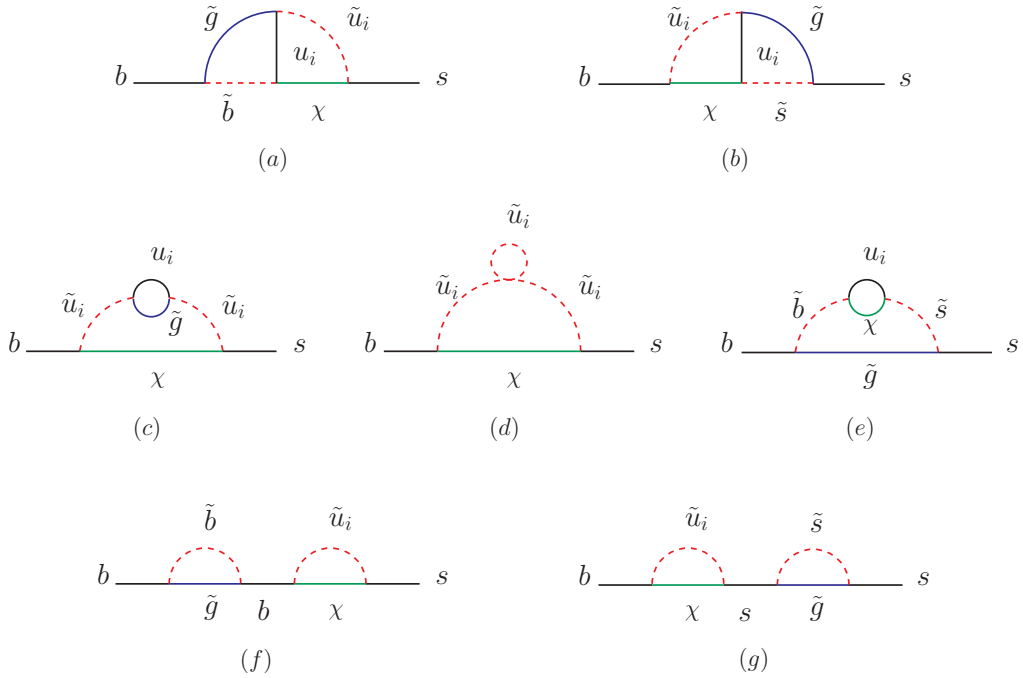


Figure 5.4: Same as figure 5.3 for diagrams containing a chargino and a gluino or a quartic squark coupling. The index i labels the three generations of up-type quarks and squarks.

regularized the ultraviolet divergences using dimensional regularization (DREG). In principle, suitable shifts must be introduced in the $\chi^\pm d\tilde{u}$ couplings to restore supersymmetric Ward identities that are not respected by DREG [61]. However, the resulting contributions to $C_{7,8}^{(1)\chi^\pm}$ were already included in the gluon-chargino contributions computed in ref. [104]. The result for each of the diagrams in figures 5.3 and 5.4 depends on a number of mass and coupling parameters; it can be simplified assuming the up-type squarks of the first two generations to be degenerate in mass, and neglecting the masses of all quarks of the first two generations. These assumptions allow us to exploit the unitarity of the CKM matrix and factor out the combination $V_{ts}^* V_{tb}$ in the effective Hamiltonian of eq. (5.1).

The complete calculation of the two-loop gluino contribution presents a novel feature with respect to the heavy-gluino analysis of ref. [104], namely the need for flavor-changing counterterms. Indeed, there are two-loop gluino diagrams that contain the effective flavor-changing interactions $\tilde{b}s\tilde{g}$ or $b\tilde{s}\tilde{g}$ (see, e.g., diagrams (a) and (b) in figures 5.3 and 5.4, respectively). These one-loop electroweak vertices are divergent and need to be renormalized. The corresponding contributions were irrelevant in ref. [104] because they are suppressed by inverse powers of the gluino mass. We therefore distinguish between flavor-conserving counterterms, already considered in ref. [104], and flavor-changing counterterms of electroweak origin.

Flavor-conserving counterterms are of $\mathcal{O}(\alpha_s)$ and originate from the masses of the bottom and top quarks, from the masses and left-right mixing of the up-type squarks that enter the one-loop diagrams with charginos, and from the flavor-diagonal part of the on-shell wave-function renormalization (WFR) of the external quarks. The finite parts of these counterterms depend on our choice of renormalization scheme for the masses and mixing angles that enter the one-loop results. In order to facilitate the inclusion and resummation of some large higher-order effects, one can also distinguish between the top and bottom masses that originate from the loops or from the use of equations of motion, and those arising from Yukawa couplings or their supersymmetric equivalent.

In the MFV framework, the remaining *flavor-changing* counterterms are of electroweak origin and arise from the renormalization of the flavor mixing of quarks and squarks and from the flavor-changing part of the external-leg WFR. To discuss them, we start from the gluino-quark-squark interaction Lagrangian in the super-CKM basis, where the matrices of Yukawa couplings are diagonal and the squarks are rotated parallel to their fermionic superpartners:

$$\mathcal{L} \supset -g_s \sqrt{2} \left(\bar{g}^a b_L T^a \tilde{b}_L^* - \bar{g}^a b_R T^a \tilde{b}_R^* + \bar{g}^a s_L T^a \tilde{s}_L^* - \bar{g}^a s_R T^a \tilde{s}_R^* \right) + \text{h.c.} \quad (5.17)$$

where g_s is the strong coupling constant and T^a are SU(3) generators. We can restrict to the mixing between second and third generations, and since we are neglecting m_s , we need not consider the terms involving s_R or \tilde{s}_R . Upon renormalization of the mixing matrices, the *bare* quark and squark fields are rotated as follows:

$$\begin{pmatrix} \tilde{d}_1 \\ \tilde{d}_2 \\ \tilde{d}_3 \end{pmatrix} = (U^r + \delta U) \begin{pmatrix} \tilde{b}_L \\ \tilde{b}_R \\ \tilde{s}_L \end{pmatrix}, \quad \begin{pmatrix} d_{1L} \\ d_{2L} \end{pmatrix} = (u^{Lr} + \delta u^L) \begin{pmatrix} b_L \\ s_L \end{pmatrix}. \quad (5.18)$$

The MFV assumption translates into the requirement that the renormalized mixing matrices be flavor diagonal:

$$U^r = \begin{pmatrix} B & 0 \\ 0 & 1 \end{pmatrix} = \begin{pmatrix} \cos \theta_b & \sin \theta_b & 0 \\ -\sin \theta_b & \cos \theta_b & 0 \\ 0 & 0 & 1 \end{pmatrix}, \quad u^{Lr} = \begin{pmatrix} 1 & 0 \\ 0 & 1 \end{pmatrix}, \quad (5.19)$$

where B is a 2×2 mixing matrix in the sbottom sector and θ_b is the sbottom mixing angle. Under this requirement, the mass eigenstates for the down-type squarks relevant to our calculation can be identified with the usual sbottoms \tilde{b}_1 and \tilde{b}_2 and the left super-strange \tilde{s}_L . However, even if we assume that the renormalized mixing matrices for quarks and squarks are flavor-diagonal, this is not the case for the corresponding counterterms δu^L and δU . They generate the flavor-changing interactions:

$$\mathcal{L} \supset -g_s \sqrt{2} \left[(\delta U_{3i}^\dagger + B_{1i}^\dagger \delta u_{21}^L) \bar{s}_L g^a T^a \tilde{b}_i + (\delta U_{31} - \delta u_{21}^L) \bar{g}^a b_L T^a \tilde{s}_L^* - \delta U_{32} \bar{g}^a b_R T^a \tilde{s}_L^* \right] + \text{h.c.} \quad (5.20)$$

As already mentioned, additional flavor-changing renormalization effects are due to the on-shell WFR of the external quarks (see diagrams *(f)* and *(g)* in figures 5.3 and 5.4). The divergent parts of the mixing counterterms δu^L and δU are determined in a gauge-invariant way by the requirement that they cancel the divergence of the anti-hermitian part of the corresponding WFR matrix [116]. Using $m_s \rightarrow 0$ and neglecting terms suppressed by m_b/M_W , we obtain:

$$\delta u_{21}^L = -\frac{1}{2} \left[\Sigma_{sb}^L(0) + 2 \Sigma_{sb}^S(0) \right], \quad (5.21)$$

where we have decomposed the generic quark self-energy as

$$\Sigma_{ij}(p) \equiv \Sigma_{ij}^L(p^2) \not{p} P_L + \Sigma_{ij}^R(p^2) \not{p} P_R + \Sigma_{ij}^S(p^2) (m_i P_L + m_j P_R), \quad (5.22)$$

P_L and P_R being chiral projectors. The counterterm for the squark mixing matrix is instead

$$\delta U_{ik} = \frac{1}{2} \Sigma_{j \neq i} \frac{\Pi_{ij}(m_j^2) + \Pi_{ji}^*(m_i^2)}{m_i^2 - m_j^2} U_{jk}, \quad (5.23)$$

which, for the terms that appear in eq. (5.20), specializes to:

$$\delta U_{3i}^\dagger = \frac{1}{2} \frac{\Pi_{\tilde{s}_L \tilde{b}_i}(m_{\tilde{s}_L}^2) + \Pi_{\tilde{s}_L \tilde{b}_i}(m_{\tilde{b}_i}^2)}{m_{\tilde{b}_i}^2 - m_{\tilde{s}_L}^2}, \quad \delta U_{3j} = -\frac{1}{2} \Sigma_i \frac{\Pi_{\tilde{s}_L \tilde{b}_i}(m_{\tilde{s}_L}^2) + \Pi_{\tilde{s}_L \tilde{b}_i}(m_{\tilde{b}_i}^2)}{m_{\tilde{b}_i}^2 - m_{\tilde{s}_L}^2} B_{ij}. \quad (5.24)$$

Once the flavor-changing vertices of eq. (5.20) are inserted into one-loop diagrams with a gluino and a down-type squark, the resulting counterterm contributions cancel the UV poles arising from: *i)* the diagrams *(d)* and *(e)* in figure 5.3 and *(e)* in figure 5.4; *ii)* the diagrams *(a)* and *(b)* in figure 5.4 with the photon or gluon attached to the down-type squark or to the gluino; *iii)* the flavor-changing WFR diagrams *(f)* and *(g)* in figures 5.3 and 5.4. The remaining UV poles of the diagrams in figures 5.3 and 5.4 are canceled by the flavor-conserving counterterms, but for a residual pole in the diagrams with gluino and chargino of figure 5.4. This is the pole that was found in ref. [104] in the limit of heavy gluino; it is compensated for by a corresponding pole in the diagrams with gluon and chargino.

The finite parts of the counterterms in eqs. (5.21) and (5.24) are related to the way we interpret the MFV requirement in eq. (5.19). In particular, if we perform a minimal subtraction we are imposing the MFV condition on the $\overline{\text{MS}}$ -renormalized parameters of the Lagrangian evaluated at some scale μ_{MFV} . In this scheme $C_{7,8}^{(1)\text{SUSY}}$ contains logarithms of the ratio $M_{\text{SUSY}}/\mu_{\text{MFV}}$, where M_{SUSY} represents the mass of the superparticles entering the loops. An alternative option consists in subtracting also the finite part of the anti-hermitian WFR: this results in a conventional (and gauge-dependent) on-shell renormalization scheme [116], in which $C_{7,8}^{(1)\text{SUSY}}$ is independent of μ_{MFV} . In practice, the use of on-shell mixing counterterms is equivalent to assuming that MFV is valid at the scale of the supersymmetric masses entering the loops.

It is thus clear that, in models where the MFV condition is imposed at a scale much larger than the superparticle masses (such as, e.g., gravity-mediation models where one identifies μ_{MFV} with the GUT scale), the Wilson coefficients computed in the minimal subtraction scheme contain very large logarithms of $M_{\text{SUSY}}/\mu_{\text{MFV}}$. In this case, no matter which renormalization scheme is chosen, the fixed-order calculation does not provide a good approximation to the correct result. Indeed, in such models the soft SUSY-breaking mass parameters – which are flavor-diagonal at the scale μ_{MFV} – must be evolved down to M_{SUSY} with the appropriate RGE, thus generating some flavor violation in the squark mass matrices. When the squark mass matrices are diagonalized, the resummed logarithms of the ratio $M_{\text{SUSY}}/\mu_{\text{MFV}}$ are absorbed in the couplings of the resulting squark mass eigenstates with the gluinos (and the charginos and neutralinos). Typically, the effects of the RG-induced flavor mixing are relatively small, and in `SusyBSG` we include them only at LO, in the one-loop diagrams with gluinos and down-type squarks of figure 5.2a – which would vanish if the MFV condition was valid at the low scale M_{SUSY} – and in the one-loop diagrams with charginos and up-type squarks of figure 5.1c. Once the logarithmic effects have been taken into account in this way, the genuine two-loop MFV contributions in $C_{7,8}^{(1)\text{SUSY}}$ can be computed by setting artificially $\mu_{\text{MFV}} \sim M_{\text{SUSY}}$. In this case, using either the on-shell scheme or the minimal subtraction scheme to renormalize the flavor mixing will give basically the same result.

To conclude this section, I list several studies and comparisons that we performed to check the correctness of our calculation:

- We verified that the flavor-changing counterterms in eqs. (5.21) and (5.24) renormalize correctly the $\tilde{d}d'\tilde{g}$ vertex, and that their divergent parts can be reproduced starting from the known one-loop RG equations of the MSSM [117].
- Ref. [108] presented a calculation of the $\tan\beta$ -enhanced part of the contribution to the Wilson coefficients coming from the diagrams (b) in figure 5.3 that involve a charged Higgs boson. We verified that, if we restrict our calculation to the same subset of diagrams and adopt the same input parameters as in ref. [108], we can reproduce exactly figure 8 of that paper.
- A calculation of the QCD contributions to the Wilson coefficients from the diagrams (d) in figure 5.4, involving a chargino and a quartic squark coupling, was presented in ref. [103]. We checked

that, if we assume MFV in the up squark sector and perform a $\overline{\text{MS}}$ renormalization, we find complete agreement with the analytic formulae of ref. [103]. On the other hand, the contribution of the diagrams (*d*) in figure 5.4 is removed by the corresponding counterterm contribution if the squark masses and mixing are defined on shell.

- As already mentioned, the results for $C_{7,8}$ depend on the renormalization scheme for a number of parameters. In the case all parameters are renormalized in the on-shell scheme, the QCD corrections to the Wilson coefficients still depend on the matching scale μ_0 at which the effective operators $Q_{7,8}$ are renormalized, see eq. (5.1). This dependence can be expressed in terms of the LO anomalous dimension matrix [104] and we reproduce it correctly.

5.3 Treatment of the $\tan\beta$ -enhanced contributions

As discussed in sections 2.4 and 3.4, in the MSSM the relation between the bottom quark mass m_b and the bottom Yukawa coupling h_b is subject to $\tan\beta$ -enhanced threshold corrections [45]. If the bottom Yukawa coupling entering the one-loop part of the Wilson coefficients is expressed in terms of the SM value of the running bottom mass, the SUSY threshold corrections induce counterterm contributions that, although being formally of higher order in the loop expansion, are enhanced by powers of $\tan\beta$ and may therefore be sizable when $\tan\beta$ is large. However, such potentially large corrections can be absorbed in the one-loop results by a suitable redefinition of the bottom Yukawa coupling [46]. In `SusyBSG` we multiply the contributions of the one-loop diagrams that involve a bottom Yukawa coupling by a factor κ , defined as

$$\kappa = \frac{1 + \delta_b}{1 + \epsilon_b \tan\beta}, \quad (5.25)$$

where δ_b and ϵ_b are SUSY contributions to the bottom self-energy, see eq. (2.47), and the $\mathcal{O}(\alpha_s)$ part of ϵ_b , denoted below as $\epsilon_b^{(s)}$, is given in eq. (2.48). This manipulation amounts to defining h_b in terms of the MSSM running bottom mass in the one-loop contributions to the Wilson coefficients, with the result that the counterterm contributions at higher orders do not contain terms enhanced by powers of $\tan\beta$. For consistency we multiply by κ also the contributions of the two-loop diagrams that involve a bottom Yukawa coupling, but we neglect there the small effect of δ_b .

In addition to the $\tan\beta$ -enhanced contributions that arise from the threshold corrections to the bottom mass, there are $\tan\beta$ -enhanced contributions arising from corrections to the Higgs-quark-quark vertices [105, 106, 107]. All the contributions of this kind controlled by the strong gauge coupling are fully accounted for by the explicit two-loop calculation described in section 5.2.

The $\tan\beta$ -enhanced contributions to the Wilson coefficients controlled by the top and bottom Yukawa couplings are implemented in `SusyBSG` using the effective-Lagrangian approach of refs. [105, 106, 107]. They include a contribution of $\mathcal{O}(\alpha_t)$ to the bottom-quark self-energy,

$$\epsilon_b^{(t)} = \frac{\alpha_t}{4\pi} \frac{A_t \mu}{m_Q^2 - m_U^2} \left(\frac{m_Q^2}{\mu^2 - m_Q^2} \ln \frac{m_Q^2}{\mu^2} - \frac{m_U^2}{\mu^2 - m_U^2} \ln \frac{m_U^2}{\mu^2} \right), \quad (5.26)$$

such that we must use $\epsilon_b = \epsilon_b^{(s)} + \epsilon_b^{(t)}$ when computing the factor κ in eq. (5.25). In addition, there is a contribution to the Wilson coefficients arising from a correction of $\mathcal{O}(\alpha_t)$ to the effective $G^+ - t - b$ vertex:

$$\delta C_{7,8} = -\frac{\epsilon_b^{(t)} \tan \beta}{1 + \epsilon_b \tan \beta} F_{7,8}^{(2)}(m_t^2/m_W^2), \quad (5.27)$$

where the loop functions $F_{7,8}^{(2)}(x)$ are defined, e.g., in eq. (2.4) of ref. [105]. In the limit of heavy superparticles the contribution in eq. (5.27) cancels an analogous term originating from the redefinition of the bottom Yukawa coupling, thus ensuring the decoupling of new-physics effects from the SM contribution.

There are also contributions to the Wilson coefficients involving the bottom Yukawa coupling and higher powers of $\tan \beta$ [107, 118]:

$$\begin{aligned} \delta C_{7,8} = & -\frac{\epsilon_b^{(t)} \epsilon_t^{(b)} \tan^2 \beta}{(1 + \epsilon_b \tan \beta)(1 + \epsilon_b^{(s)} \tan \beta)} F_{7,8}^{(2)}(m_t^2/m_{H^\pm}^2) \\ & -\frac{a_{7,8} \epsilon_b^{(t)} \tan^3 \beta}{(1 + \epsilon_b \tan \beta)^2 (1 + \epsilon_b^{(s)} \tan \beta)} \frac{m_b^2}{36 m_{H^\pm}^2}, \end{aligned} \quad (5.28)$$

where $a_7 = 1$, $a_8 = -3$ and the $\mathcal{O}(\alpha_b)$ vertex correction $\epsilon_t^{(b)}$ is defined as

$$\epsilon_t^{(b)} = -\frac{\alpha_b}{4\pi} \frac{A_b \mu}{m_Q^2 - m_D^2} \left(\frac{m_Q^2}{\mu^2 - m_Q^2} \ln \frac{m_Q^2}{\mu^2} - \frac{m_D^2}{\mu^2 - m_D^2} \ln \frac{m_D^2}{\mu^2} \right). \quad (5.29)$$

Being suppressed by an additional loop factor and by $m_b^2/m_{H^\pm}^2$, respectively, the two terms in eq. (5.28) tend to be numerically small, but, as stressed in ref. [107], they can become relevant in special cases where the leading $\mathcal{O}(\alpha_s)$ and $\mathcal{O}(\alpha_t)$ effects cancel each other.

When implementing in `SusyBSG` the $\tan \beta$ -enhanced contributions controlled by the top and bottom Yukawa couplings, eqs. (5.26)–(5.29), we have neglected the mixing between superpartners, approximating the squark masses with the corresponding soft SUSY-breaking terms and the masses of the higgsino components of charginos and neutralinos with the superpotential parameter μ . Indeed, the effective-Lagrangian approach used to derive these results relies on the assumption that the superpartners are much heavier than the weak scale and can be integrated out of the theory, leaving behind only non-decoupling corrections to the Higgs-quark-quark vertices. In this case the effect of the mixing, which is due to the breaking of electroweak symmetry, can reasonably be expected to be small, and anyway is of the same order of magnitude as other effects that are neglected under the effective Lagrangian approximation. Formulae for the $\tan \beta$ -enhanced contributions to the Wilson coefficients that take into account the effect of superpartner mixing have been presented in refs. [105, 110, 119, 120].

Finally, it is important to remark that in scenarios with a generic (i.e., non-MFV) flavor structure of the soft SUSY-breaking terms there are additional $\tan \beta$ -enhanced NLO contributions [121] which are not accounted for by `SusyBSG`.

5.4 Further developments

Conceptual issues: The issue of the renormalization of quark and squark mixing matrices in the MFV scenario, summarized here in section 5.2, was further elaborated on by different groups. The authors of ref. [118] pointed out that the chargino-stop contributions to the flavor-changing WFR of the external quarks – see diagrams (*f*) and (*g*) in figure 5.4 – contain potentially large terms enhanced by $\tan\beta$, which are not absorbed in the bottom Yukawa coupling by the manipulation in eq. (5.25). They discussed how to resum those terms to all orders in the perturbative expansion through an effective-Lagrangian approach. It is interesting to note that the presence of these $\tan\beta$ -enhanced terms depends on the choice of a minimal renormalization condition for the quark mixing matrix entering the quark-squark-gluino vertex. If, instead, the MFV condition in eq. (5.19) is imposed on the mixing matrix renormalized on shell, the $\tan\beta$ -enhanced terms in the flavor-changing WFR of the external quarks are canceled by the finite part of the counterterms for the quark-mixing matrix, eqs. (5.20) and (5.21).

The authors of ref. [122] applied the renormalization procedure outlined in section 5.2 to the full one-loop computation of the flavor-changing decay $\tilde{t}_1 \rightarrow c\chi_1^0$, for which an approximated leading-logarithmic result had been presented long ago in ref. [123]. They imposed minimal renormalization conditions on the quark and squark matrices, and investigated the occurrence of potentially large logarithms of μ_{MFV} when the MFV condition is imposed at a high scale. Finally, they showed how the large logarithms can be resummed with a RGE procedure analogous to the one described in section 5.2 and implemented in `SusyBSG`.

The code `SusyBSG`: After its publication in ref. [4], our code has undergone several improvements and extensions. For example, the THDM calculation has been extended to include the results of ref. [9] for the Manohar-Wise model, in which there is an additional color-octet scalar with the same EW quantum numbers as the SM Higgs. Also, we have included in the calculation of the branching ratio the effect of the chirally-swapped operators $Q'_{7,8}$, retaining in particular the contributions of one-loop diagrams with gluino and sdown squarks. In MFV scenarios, where the departure from flavor diagonality in the sdown sector is induced by RG evolution, the effect of these new contributions is suppressed by m_s/m_b and can be neglected. However, with this extension the code can be used – albeit with only LO-QCD accuracy – to determine $\text{BR}[B \rightarrow X_s \gamma]$ in non-MFV scenarios in which the soft SUSY-breaking masses induce a sizable $\tilde{b}_L - \tilde{s}_R$ mixing.

At the time of writing, `SusyBSG` has been employed by different groups in about thirty phenomenological analyses of the MSSM and of the THDM. In particular, in a paper of which I am co-author [7] we used `SusyBSG` to investigate the flavor structure of the MSSM with anomaly-mediated SUSY breaking, and found that $B \rightarrow X_s \gamma$ provided the strongest constraints on the parameter space of the model. We also investigated the constraints arising from the decay $B_s \rightarrow \mu^+ \mu^-$, for which only a 95% exclusion bound existed back in 2009. The AMSB predictions for the branching ratios of those two rare decays, as a function of $\tan\beta$ in a scenario with a gravitino mass $m_{3/2} = 40$ TeV, are shown for

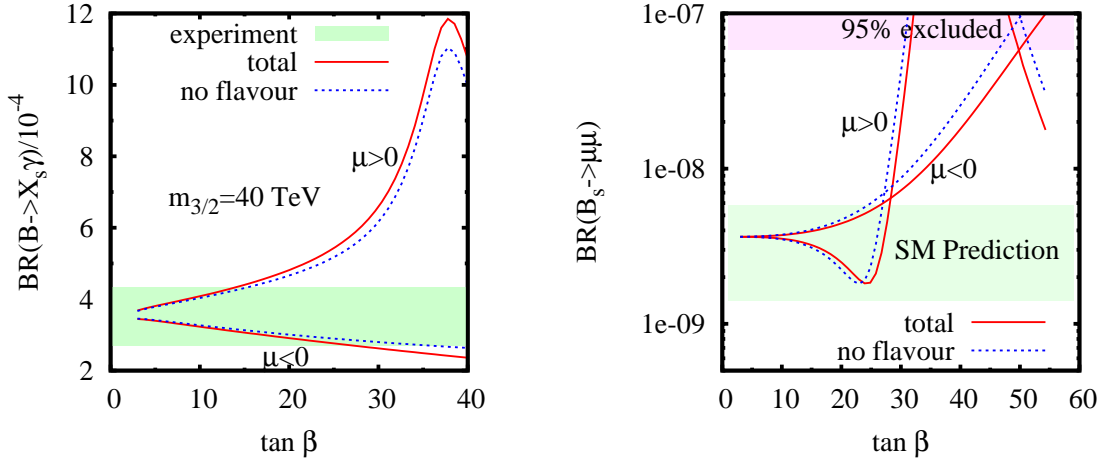


Figure 5.5: Constraints on the AMSB parameter space from the rare decays $B \rightarrow X_s \gamma$ (left) and $B_s \rightarrow \mu^+ \mu^-$ (right), for $m_{3/2} = 40$ TeV. The plots are from ref. [7], which adopted for the sign of μ the opposite convention with respect to this dissertation.

illustration in figure 5.5. In the two plots, the solid (dotted) lines include (do not include) the effect of the one-loop diagrams with flavor-changing gluino-quark-squark interactions. A detailed analysis would certainly be warranted, but it is likely that the recent observation of $B_s \rightarrow \mu^+ \mu^-$ by the LHCb experiment [124], with a rate compatible with the SM prediction, induces on this and on many other MSSM scenarios bounds comparable to or even stronger than those arising from $B \rightarrow X_s \gamma$.

Chapter 6

Outlook

The discovery at the LHC of a Higgs boson with mass around 125 GeV puts the phenomenological studies of the Higgs sector in SUSY extensions of the SM in an entirely new perspective. In order to remain viable, a point in the parameter space of a given SUSY model must not only pass all the (ever stricter) experimental bounds on superparticle masses, but also lead to the prediction of a scalar with mass, production cross section and decay rates compatible with those measured at the LHC. This, in turn, puts new emphasis on the need for accurate theoretical predictions of those quantities.

In the case of the MSSM, the two-loop characterization of the Higgs sector – with information on masses, production and decays – is quite advanced, at least for what concerns the dominant corrections controlled by the strong gauge coupling and the top and bottom Yukawa couplings. Nevertheless, the theoretical accuracy of the prediction for the lightest-scalar mass implemented in many public codes for the calculation of the MSSM mass spectrum was estimated to be about 3 GeV [28, 29], i.e., already comparable to the accuracy of the mass measurement at the LHC. Leaving aside the fact that the current estimate of the accuracy should itself be reassessed in the light of the new information on the Higgs boson, it is clear that an improvement in the prediction for the MSSM Higgs masses, with the inclusion of the remaining two-loop effects and at least the dominant three-loop effects, will at some point become unavoidable.

Indeed, a substantial effort is still needed to combine the existing predictions for the properties of the MSSM Higgs bosons in a consistent way, and make them available to the experimentalists in the form of computer programs that can be efficiently used to analyze the LHC data. In this context, my plans for the short/medium term include: *i*) the development of a new code for the calculation of the MSSM mass spectrum in split-SUSY scenarios where some of the superparticles are much heavier than the weak scale; *ii*) detailed studies of the theoretical uncertainty of the NLO predictions for the Higgs-production cross section in the MSSM, in collaboration with the authors of `SusHi`; *iii*) the inclusion of the bottom-quark annihilation process – which for some choices of the MSSM parameters can prevail over gluon fusion – in our `POWHEG` implementation of Higgs production; *iv*) the inclusion of the two-loop SUSY-QCD contributions to the Higgs decays into photons or gluons in the existing codes

for the computation of the Higgs decay width. Each of these steps will also involve phenomenological studies of the MSSM parameter space to assess the relevance of the various contributions.

The situation in other SUSY extensions of the SM is much less advanced than in the MSSM. Even in the simplest non-minimal extension, the NMSSM, only a partial two-loop calculation of the Higgs masses is available, and radiative corrections to Higgs production and decay processes have been studied only at one-loop accuracy (if at all). In order to bring the accuracy of the predictions for the NMSSM Higgs sector to the level already achieved in the MSSM, and to allow for a meaningful comparison between the two models, at least two steps will be necessary. The first is the adaptation to the NMSSM of the results for the two-loop SUSY-QCD contributions to Higgs production and decays that were computed for the MSSM in the past few years. The second step is the computation of the two-loop corrections to the NMSSM Higgs masses controlled only by the top and bottom Yukawa couplings. As in the case of the MSSM, the results of these calculations should then be implemented in public computer codes. Another subject that I could explore in the medium term is the precise characterization of the Higgs sector in SUSY models with Dirac gauginos.

The second main line of my research in the coming years – somewhat complementary to the precision computation of the properties of the Higgs bosons – will consist in working out the implications for different BSM scenarios of any new information that should come from the LHC and from other sources, such as, e.g., direct and indirect searches for Dark Matter. Obviously, the timing and the direction of this kind of research will depend on the experimental developments, and cannot be foreseen in much detail. At the time of writing, it seems likely that – barring last-minute surprises at the Summer 2013 conferences – neither superparticles nor an extended Higgs sector were discovered in the first two years of ATLAS and CMS operations, nor did LHCb measure sizable deviations from the SM predictions in the flavor sector. However, the Higgs-boson mass turned out to be sitting in a particularly fortunate range where various search channels, sensitive to different Higgs couplings, contribute to its discovery. This provides different ways to test whether the properties of the Higgs boson follow the SM predictions or they are affected by new physics, even if the new physics fails to manifest itself directly in the data collected so far. For example, an excess in the rate of Higgs-boson decays into photons – for which the evidence is still inconclusive – would constitute a striking manifestation of physics beyond the SM. The interpretation of such an excess in the context of different SUSY (and non-SUSY) models, based on state-of-the-art computations of the relevant observables, would certainly become a priority of my research activity. In any case, the data collected at the LHC after the 2013–2014 shutdown, during which the collider will be upgraded to its design energy and luminosity, should clarify whether it is indeed SUSY that stabilizes the weak scale, thus determining the direction of my research in the longer term.

Bibliography

- [1] G. Degrandi, P. Gambino and P. Slavich, “*QCD corrections to radiative B decays in the MSSM with minimal flavor violation*”, Phys. Lett. B **635** (2006) 335 [hep-ph/0601135].
- [2] N. Bernal, A. Djouadi and P. Slavich, “*The MSSM with heavy scalars*”, JHEP **0707** (2007) 016 [arXiv:0705.1496 [hep-ph]].
- [3] A. Delgado, G. F. Giudice and P. Slavich, “*Dynamical mu term in gauge mediation*”, Phys. Lett. B **653** (2007) 424 [arXiv:0706.3873 [hep-ph]].
- [4] G. Degrandi, P. Gambino and P. Slavich, “*SusyBSG: A Fortran code for BR[B → X(s) gamma] in the MSSM with Minimal Flavor Violation*”, Comput. Phys. Commun. **179** (2008) 759 [arXiv:0712.3265 [hep-ph]].
- [5] B. C. Allanach *et al.*, “*SUSY Les Houches Accord 2*”, Comput. Phys. Commun. **180** (2009) 8 [arXiv:0801.0045 [hep-ph]].
- [6] G. Degrandi and P. Slavich, “*On the NLO QCD corrections to Higgs production and decay in the MSSM*”, Nucl. Phys. B **805** (2008) 267 [arXiv:0806.1495 [hep-ph]].
- [7] B. C. Allanach, G. Hiller, D. R. T. Jones and P. Slavich, “*Flavour Violation in Anomaly Mediated Supersymmetry Breaking*”, JHEP **0904** (2009) 088 [arXiv:0902.4880 [hep-ph]].
- [8] G. Degrandi and P. Slavich, “*On the radiative corrections to the neutral Higgs boson masses in the NMSSM*”, Nucl. Phys. B **825** (2010) 119 [arXiv:0907.4682 [hep-ph]].
- [9] G. Degrandi and P. Slavich, “*QCD Corrections in two-Higgs-doublet extensions of the Standard Model with Minimal Flavor Violation*”, Phys. Rev. D **81** (2010) 075001 [arXiv:1002.1071 [hep-ph]].
- [10] G. Degrandi and P. Slavich, “*NLO QCD bottom corrections to Higgs boson production in the MSSM*”, JHEP **1011** (2010) 044 [arXiv:1007.3465 [hep-ph]].
- [11] F. Mahmoudi *et al.*, “*Flavour Les Houches Accord: Interfacing Flavour related Codes*”, Comput. Phys. Commun. **183** (2012) 285 [arXiv:1008.0762 [hep-ph]].

- [12] G. Degrandi, S. Di Vita and P. Slavich, “*NLO QCD corrections to pseudoscalar Higgs production in the MSSM*”, JHEP **1108** (2011) 128 [arXiv:1107.0914 [hep-ph]].
- [13] E. Bagnaschi, G. Degrandi, P. Slavich and A. Vicini, “*Higgs production via gluon fusion in the POWHEG approach in the SM and in the MSSM*”, JHEP **1202** (2012) 088 [arXiv:1111.2854 [hep-ph]].
- [14] G. Degrandi, S. Di Vita and P. Slavich, “*On the NLO QCD corrections to the production of the heaviest neutral Higgs scalar in the MSSM*”, Eur. Phys. J. C **72** (2012) 2032 [arXiv:1204.1016 [hep-ph]].
- [15] P. Gambino, G. F. Giudice and P. Slavich, “*Gluino decays in split supersymmetry*”, Nucl. Phys. B **726** (2005) 35 [hep-ph/0506214].
- [16] P. Z. Skands *et al.*, “*SUSY Les Houches accord: Interfacing SUSY spectrum calculators, decay packages, and event generators*”, JHEP **0407** (2004) 036 [hep-ph/0311123].
- [17] S. P. Martin, “*A Supersymmetry primer*”, In *Kane, G.L. (ed.): Perspectives on supersymmetry II* 1-153 [hep-ph/9709356].
- [18] A. Djouadi, “*The Anatomy of electro-weak symmetry breaking. I: The Higgs boson in the standard model*”, Phys. Rept. **457** (2008) 1 [hep-ph/0503172].
- [19] A. Djouadi, “*The Anatomy of electro-weak symmetry breaking. II. The Higgs bosons in the minimal supersymmetric model*”, Phys. Rept. **459** (2008) 1 [hep-ph/0503173].
- [20] U. Ellwanger, C. Hugonie and A. M. Teixeira, “*The Next-to-Minimal Supersymmetric Standard Model*”, Phys. Rept. **496** (2010) 1 [arXiv:0910.1785 [hep-ph]].
- [21] G. Aad *et al.* [ATLAS Collaboration], “*Observation of a new particle in the search for the Standard Model Higgs boson with the ATLAS detector at the LHC*”, Phys. Lett. B **716** (2012) 1 [arXiv:1207.7214 [hep-ex]].
- [22] S. Chatrchyan *et al.* [CMS Collaboration], “*Observation of a new boson at a mass of 125 GeV with the CMS experiment at the LHC*”, Phys. Lett. B **716** (2012) 30 [arXiv:1207.7235 [hep-ex]].
- [23] G. Degrandi, P. Slavich and F. Zwirner, “*On the neutral Higgs boson masses in the MSSM for arbitrary stop mixing*”, Nucl. Phys. B **611** (2001) 403 [hep-ph/0105096].
- [24] A. Brignole, G. Degrandi, P. Slavich and F. Zwirner, “*On the $O(\alpha(t)^{**2})$ two loop corrections to the neutral Higgs boson masses in the MSSM*”, Nucl. Phys. B **631** (2002) 195 [hep-ph/0112177].
- [25] A. Brignole, G. Degrandi, P. Slavich and F. Zwirner, “*On the two loop sbottom corrections to the neutral Higgs boson masses in the MSSM*”, Nucl. Phys. B **643** (2002) 79 [hep-ph/0206101].

- [26] A. Dedes and P. Slavich, “*Two loop corrections to radiative electroweak symmetry breaking in the MSSM*”, Nucl. Phys. B **657** (2003) 333 [hep-ph/0212132].
- [27] A. Dedes, G. Degrandi and P. Slavich, “*On the two loop Yukawa corrections to the MSSM Higgs boson masses at large $\tan\beta$* ”, Nucl. Phys. B **672** (2003) 144 [hep-ph/0305127].
- [28] G. Degrandi, S. Heinemeyer, W. Hollik, P. Slavich and G. Weiglein, “*Towards high precision predictions for the MSSM Higgs sector*”, Eur. Phys. J. C **28** (2003) 133 [hep-ph/0212020].
- [29] B. C. Allanach, A. Djouadi, J. L. Kneur, W. Porod and P. Slavich, “*Precise determination of the neutral Higgs boson masses in the MSSM*”, JHEP **0409** (2004) 044 [hep-ph/0406166].
- [30] S. Heinemeyer, W. Hollik and G. Weiglein, “*FeynHiggs: A Program for the calculation of the masses of the neutral CP even Higgs bosons in the MSSM*”, Comput. Phys. Commun. **124** (2000) 76 [hep-ph/9812320]; M. Frank, T. Hahn, S. Heinemeyer, W. Hollik, H. Rzehak and G. Weiglein, “*The Higgs Boson Masses and Mixings of the Complex MSSM in the Feynman-Diagrammatic Approach*”, JHEP **0702** (2007) 047 [hep-ph/0611326].
- [31] B. C. Allanach, “*SOFTSUSY: a program for calculating supersymmetric spectra*”, Comput. Phys. Commun. **143** (2002) 305 [hep-ph/0104145].
- [32] A. Djouadi, J. -L. Kneur and G. Moultaka, “*SuSpect: A Fortran code for the supersymmetric and Higgs particle spectrum in the MSSM*”, Comput. Phys. Commun. **176** (2007) 426 [hep-ph/0211331].
- [33] W. Porod, “*SPheno, a program for calculating supersymmetric spectra, SUSY particle decays and SUSY particle production at e^+e^- colliders*”, Comput. Phys. Commun. **153** (2003) 275 [hep-ph/0301101].
- [34] S. Dittmaier *et al.* [LHC Higgs Cross Section Working Group Collaboration], “*Handbook of LHC Higgs Cross Sections: 1. Inclusive Observables*”, arXiv:1101.0593 [hep-ph].
- [35] S. Dittmaier *et al.*, “*Handbook of LHC Higgs Cross Sections: 2. Differential Distributions*”, arXiv:1201.3084 [hep-ph].
- [36] S. Heinemeyer *et al.*, “*Handbook of LHC Higgs Cross Sections: 3. Higgs properties*”, in preparation.
- [37] C. Anastasiou, S. Beerli and A. Daleo, “*The Two-loop QCD amplitude $gg \rightarrow h, H$ in the Minimal Supersymmetric Standard Model*”, Phys. Rev. Lett. **100** (2008) 241806 [arXiv:0803.3065 [hep-ph]].
- [38] M. Muhlleitner, H. Rzehak and M. Spira, “*SUSY-QCD Corrections to MSSM Higgs Boson Production via Gluon fusion*”, PoS RADCOR **2009** (2010) 043 [arXiv:1001.3214 [hep-ph]].

- [39] R. V. Harlander and M. Steinhauser, “*Supersymmetric Higgs production in gluon fusion at next-to-leading order*”, JHEP **0409** (2004) 066 [hep-ph/0409010].
- [40] R. V. Harlander and F. Hofmann, “*Pseudo-scalar Higgs production at next-to-leading order SUSY-QCD*”, JHEP **0603** (2006) 050 [hep-ph/0507041].
- [41] R. V. Harlander, S. Liebler and H. Mantler, “*SusHi: A program for the calculation of Higgs production in gluon fusion and bottom-quark annihilation in the Standard Model and the MSSM*” Computer Physics Communications **184** (2013) pp. 1605 [arXiv:1212.3249 [hep-ph]].
- [42] U. Ellwanger, J. F. Gunion and C. Hugonie, “*NMHDECAY: A Fortran code for the Higgs masses, couplings and decay widths in the NMSSM*”, JHEP **0502** (2005) 066 [hep-ph/0406215]; U. Ellwanger and C. Hugonie, “*NMHDECAY 2.0: An Updated program for sparticle masses, Higgs masses, couplings and decay widths in the NMSSM*”, Comput. Phys. Commun. **175** (2006) 290 [hep-ph/0508022].
- [43] F. Staub, W. Porod and B. Herrmann, “*The Electroweak sector of the NMSSM at the one-loop level*”, JHEP **1010** (2010) 040 [arXiv:1007.4049 [hep-ph]].
- [44] A. V. Manohar and M. B. Wise, “*Flavor changing neutral currents, an extended scalar sector, and the Higgs production rate at the CERN LHC*”, Phys. Rev. D **74** (2006) 035009 [hep-ph/0606172].
- [45] L. J. Hall, R. Rattazzi and U. Sarid, “*The Top quark mass in supersymmetric SO(10) unification*”, Phys. Rev. D **50** (1994) 7048 [arXiv:hep-ph/9306309].
- [46] M. S. Carena, D. Garcia, U. Nierste and C. E. M. Wagner, “*Effective Lagrangian for the $\bar{t}bH^+$ interaction in the MSSM and charged Higgs phenomenology*”, Nucl. Phys. B **577** (2000) 88 [arXiv:hep-ph/9912516]; J. Guasch, P. Hafliger and M. Spira, “*MSSM Higgs decays to bottom quark pairs revisited*” Phys. Rev. D **68** (2003) 115001 [arXiv:hep-ph/0305101].
- [47] S. Heinemeyer, W. Hollik, H. Rzehak and G. Weiglein, “*High-precision predictions for the MSSM Higgs sector at $O(\alpha(b)\alpha(s))$* ”, Eur. Phys. J. C **39** (2005) 465 [hep-ph/0411114].
- [48] S. Heinemeyer, H. Rzehak and C. Schappacher, “*Proposals for Bottom Quark/Squark Renormalization in the Complex MSSM*”, Phys. Rev. D **82** (2010) 075010 [arXiv:1007.0689 [hep-ph]].
- [49] M. Spira, A. Djouadi, D. Graudenz and P. M. Zerwas, “*Higgs boson production at the LHC*”, Nucl. Phys. B **453** (1995) 17 [hep-ph/9504378].
- [50] R. Harlander and P. Kant, “*Higgs production and decay: Analytic results at next-to-leading order QCD*”, JHEP **0512** (2005) 015 [hep-ph/0509189].
- [51] S. Dawson, A. Djouadi and M. Spira, “*QCD Corrections to SUSY Higgs Production: The Role of Squark Loops*”, Phys. Rev. Lett. **77** (1996) 16 [arXiv:hep-ph/9603423].

- [52] C. Anastasiou, S. Beerli, S. Bucherer, A. Daleo and Z. Kunszt, “*Two-loop amplitudes and master integrals for the production of a Higgs boson via a massive quark and a scalar-quark loop*”, JHEP **0701** (2007) 082 [hep-ph/0611236].
- [53] U. Aglietti, R. Bonciani, G. Degrossi and A. Vicini, “*Analytic Results for Virtual QCD Corrections to Higgs Production and Decay*”, JHEP **0701** (2007) 021 [hep-ph/0611266].
- [54] R. Bonciani, G. Degrossi and A. Vicini, “*Scalar particle contribution to Higgs production via gluon fusion at NLO*”, JHEP **0711** (2007) 095 [arXiv:0709.4227 [hep-ph]].
- [55] M. Muhlleitner and M. Spira, “*Higgs Boson Production via Gluon Fusion: Squark Loops at NLO QCD*”, Nucl. Phys. B **790** (2008) 1 [hep-ph/0612254].
- [56] A. I. Davydychev and J. B. Tausk, “*Two loop selfenergy diagrams with different masses and the momentum expansion*”, Nucl. Phys. B **397** (1993) 123.
- [57] M. A. Shifman, A. I. Vainshtein, M. B. Voloshin and V. I. Zakharov, “*Low-Energy Theorems For Higgs Boson Couplings To Photons*”, Sov. J. Nucl. Phys. **30** (1979) 711 [Yad. Fiz. **30** (1979) 1368];
- [58] B. A. Kniehl and M. Spira, “*Low-energy theorems in Higgs physics*”, Z. Phys. C **69** (1995) 77 [hep-ph/9505225].
- [59] H. Kluberg-Stern and J. B. Zuber, “*Renormalization Of Nonabelian Gauge Theories In A Background Field Gauge: 1. Green Functions*”, Phys. Rev. D **12** (1975) 482; L. F. Abbott, “*The Background Field Method Beyond One Loop*”, Nucl. Phys. B **185** (1981) 189; A. Denner, G. Weiglein and S. Dittmaier, “*Application of the background field method to the electroweak standard model*”, Nucl. Phys. B **440** (1995) 95 [hep-ph/9410338].
- [60] T. Hahn, “*Generating Feynman diagrams and amplitudes with FeynArts 3*”, Comput. Phys. Commun. **140** (2001) 418 [arXiv:hep-ph/0012260]; T. Hahn and C. Schappacher, “*The implementation of the minimal supersymmetric standard model in FeynArts and FormCalc*”, Comput. Phys. Commun. **143** (2002) 54 [arXiv:hep-ph/0105349].
- [61] S. P. Martin and M. T. Vaughn, “*Regularization dependence of running couplings in softly broken supersymmetry*”, Phys. Lett. B **318** (1993) 331 [arXiv:hep-ph/9308222].
- [62] G. Passarino and M. J. G. Veltman, “*One Loop Corrections For $E^+ E^-$ Annihilation Into $Mu^+ Mu^-$ In The Weinberg Model*”, Nucl. Phys. B **160** (1979) 151.
- [63] G. 't Hooft and M. J. G. Veltman, “*Regularization and Renormalization of Gauge Fields*”, Nucl. Phys. B **44** (1972) 189.

- [64] S. A. Larin, “*The Renormalization of the axial anomaly in dimensional regularization*”, Phys. Lett. **B303** (1993) 113-118. [hep-ph/9302240].
- [65] S. L. Adler and W. A. Bardeen, “*Absence of higher order corrections in the anomalous axial vector divergence equation*”, Phys. Rev. **182** (1969) 1517.
- [66] R. V. Harlander, F. Hofmann and H. Mantler, “*Supersymmetric Higgs production in gluon fusion*”, JHEP **1102** (2011) 055 [arXiv:1012.3361 [hep-ph]].
- [67] L. Mihaila and C. Reisser, “ *$O(\alpha_s^2)$ corrections to fermionic Higgs decays in the MSSM*”, JHEP **1008** (2010) 021 [arXiv:1007.0693 [hep-ph]].
- [68] A. Kurz, M. Steinhauser and N. Zerf, “*Decoupling Constant for α_s and the Effective Gluon-Higgs Coupling to Three Loops in Supersymmetric QCD*”, JHEP **1207** (2012) 138 [arXiv:1206.6675 [hep-ph]].
- [69] K. Nakamura *et al.* [Particle Data Group], “*Review of particle physics*”, J. Phys. G **37** (2010) 075021.
- [70] [Tevatron Electroweak Working Group and for the CDF and D0 Collaborations], “*Combination of CDF and DO results on the mass of the top quark using up to 5.8 fb⁻¹ of data*”, arXiv:1107.5255 [hep-ex].
- [71] J. H. Kuhn, “*Precise Charm- and Bottom-Quark Masses: Recent Updates*”, arXiv:1001.5173 [hep-ph].
- [72] S. Frixione, P. Nason and C. Oleari, “*Matching NLO QCD computations with Parton Shower simulations: the POWHEG method*”, JHEP **0711** (2007) 070 [arXiv:0709.2092 [hep-ph]]; S. Alioli, P. Nason, C. Oleari and E. Re, “*A general framework for implementing NLO calculations in shower Monte Carlo programs: the POWHEG BOX*”, JHEP **1006** (2010) 043 [arXiv:1002.2581 [hep-ph]].
- [73] S. Alioli, P. Nason, C. Oleari and E. Re, “*NLO Higgs boson production via gluon fusion matched with shower in POWHEG*” JHEP **0904** (2009) 002 [arXiv:0812.0578 [hep-ph]].
- [74] R. V. Harlander and W. B. Kilgore, “*Next-to-next-to-leading order Higgs production at hadron colliders*”, Phys. Rev. Lett. **88** (2002) 201801 [hep-ph/0201206]; C. Anastasiou and K. Melnikov, “*Higgs boson production at hadron colliders in NNLO QCD*”, Nucl. Phys. B **646** (2002) 220 [hep-ph/0207004]; V. Ravindran, J. Smith and W. L. van Neerven, “*NNLO corrections to the total cross-section for Higgs boson production in hadron hadron collisions*”, Nucl. Phys. B **665** (2003) 325 [hep-ph/0302135].
- [75] R. V. Harlander and W. B. Kilgore, “*Production of a pseudoscalar Higgs boson at hadron colliders at next-to-next-to leading order*”, JHEP **0210** (2002) 017 [hep-ph/0208096]; C. Anastasiou and

- K. Melnikov, “Pseudoscalar Higgs boson production at hadron colliders in NNLO QCD”, Phys. Rev. D **67** (2003) 037501 [hep-ph/0208115].
- [76] S. Actis, G. Passarino, C. Sturm and S. Uccirati, “NLO Electroweak Corrections to Higgs Boson Production at Hadron Colliders”, Phys. Lett. B **670** (2008) 12 [arXiv:0809.1301 [hep-ph]], “NNLO Computational Techniques: The Cases $H \rightarrow \gamma\gamma$ and $H \rightarrow gg$ ”, Nucl. Phys. B **811** (2009) 182 [arXiv:0809.3667 [hep-ph]].
- [77] U. Aglietti, R. Bonciani, G. Degrossi and A. Vicini, “Two loop light fermion contribution to Higgs production and decays”, Phys. Lett. B **595** (2004) 432 [hep-ph/0404071]; R. Bonciani, G. Degrossi and A. Vicini, “On the Generalized Harmonic Polylogarithms of One Complex Variable”, Comput. Phys. Commun. **182** (2011) 1253 [arXiv:1007.1891 [hep-ph]].
- [78] M. Carena, S. Heinemeyer, O. Stl, C. E. M. Wagner and G. Weiglein, “MSSM Higgs Boson Searches at the LHC: Benchmark Scenarios after the Discovery of a Higgs-like Particle”, arXiv:1302.7033 [hep-ph].
- [79] M. Spira, “HIGLU: A program for the calculation of the total Higgs production cross-section at hadron colliders via gluon fusion including QCD corrections”, hep-ph/9510347.
- [80] T. Sjostrand, S. Mrenna and P. Z. Skands, “PYTHIA 6.4 Physics and Manual”, JHEP **0605** (2006) 026 [hep-ph/0603175].
- [81] Y. Okada, M. Yamaguchi and T. Yanagida, “Upper bound of the lightest Higgs boson mass in the minimal supersymmetric standard model”, Prog. Theor. Phys. **85** (1991) 1, “Renormalization Group Analysis On The Higgs Mass In The Softly Broken Supersymmetric Standard Model”, Phys. Lett. B **262** (1991) 54; J. R. Ellis, G. Ridolfi and F. Zwirner, “Radiative corrections to the masses of supersymmetric Higgs bosons”, Phys. Lett. B **257** (1991) 83, “On radiative corrections to supersymmetric Higgs boson masses and their implications for LEP searches”, Phys. Lett. B **262** (1991) 477; H. E. Haber and R. Hempfling, “Can the mass of the lightest Higgs boson of the minimal supersymmetric model be larger than $m(Z)$?”, Phys. Rev. Lett. **66** (1991) 1815.
- [82] P. H. Chankowski, S. Pokorski and J. Rosiek, “Charged and neutral supersymmetric Higgs boson masses: Complete one loop analysis”, Phys. Lett. B **274**, 191 (1992); A. Brignole, “Radiative corrections to the supersymmetric neutral Higgs boson masses”, Phys. Lett. B **281**, 284 (1992); A. Dabelstein, “The One loop renormalization of the MSSM Higgs sector and its application to the neutral scalar Higgs masses”, Z. Phys. C **67**, 495 (1995) [arXiv:hep-ph/9409375].
- [83] D. M. Pierce, J. A. Bagger, K. T. Matchev and R. J. Zhang, “Precision corrections in the minimal supersymmetric standard model”, Nucl. Phys. B **491**, 3 (1997) [arXiv:hep-ph/9606211].
- [84] M. S. Carena, J. R. Espinosa, M. Quiros and C. E. M. Wagner, “Analytical expressions for radiatively corrected Higgs masses and couplings in the MSSM”, Phys. Lett. B **355**, 209 (1995)

- [arXiv:hep-ph/9504316]; M. S. Carena, M. Quiros and C. E. M. Wagner, “*Effective potential methods and the Higgs mass spectrum in the MSSM*”, Nucl. Phys. B **461**, 407 (1996) [arXiv:hep-ph/9508343]; H. E. Haber, R. Hempfling and A. H. Hoang, “*Approximating the radiatively corrected Higgs mass in the minimal supersymmetric model*”, Z. Phys. C **75**, 539 (1997) [arXiv:hep-ph/9609331]; J. R. Espinosa and I. Navarro, “*Radiative corrections to the Higgs boson mass for a hierarchical stop spectrum*”, Nucl. Phys. B **615**, 82 (2001) [arXiv:hep-ph/0104047].
- [85] R. Hempfling and A. H. Hoang, “*Two loop radiative corrections to the upper limit of the lightest Higgs boson mass in the minimal supersymmetric model*”, Phys. Lett. B **331**, 99 (1994) [arXiv:hep-ph/9401219].
- [86] S. Heinemeyer, W. Hollik and G. Weiglein, “*QCD corrections to the masses of the neutral CP-even Higgs bosons in the MSSM*”, Phys. Rev. D **58**, 091701 (1998) [arXiv:hep-ph/9803277], “*Precise prediction for the mass of the lightest Higgs boson in the MSSM*”, Phys. Lett. B **440**, 296 (1998) [arXiv:hep-ph/9807423], “*The Masses of the neutral CP - even Higgs bosons in the MSSM: Accurate analysis at the two loop level*”, Eur. Phys. J. C **9**, 343 (1999) [arXiv:hep-ph/9812472].
- [87] R. J. Zhang, “*Two-loop effective potential calculation of the lightest CP-even Higgs-boson mass in the MSSM*”, Phys. Lett. B **447**, 89 (1999) [arXiv:hep-ph/9808299]; J. R. Espinosa and R. J. Zhang, “*MSSM lightest CP-even Higgs boson mass to $O(\alpha(s)\alpha(t))$: The effective potential approach*”, JHEP **0003**, 026 (2000) [arXiv:hep-ph/9912236].
- [88] J. R. Espinosa and R. J. Zhang, “*Complete two-loop dominant corrections to the mass of the lightest CP-even Higgs boson in the minimal supersymmetric standard model*”, Nucl. Phys. B **586**, 3 (2000) [arXiv:hep-ph/0003246].
- [89] S. P. Martin, “*Two loop effective potential for the minimal supersymmetric standard model*”, Phys. Rev. D **66** (2002) 096001 [hep-ph/0206136], “*Complete two loop effective potential approximation to the lightest Higgs scalar boson mass in supersymmetry*”, Phys. Rev. D **67** (2003) 095012 [hep-ph/0211366], “*Strong and Yukawa two-loop contributions to Higgs scalar boson self-energies and pole masses in supersymmetry*”, Phys. Rev. D **71** (2005) 016012 [hep-ph/0405022].
- [90] S. P. Martin, “*Three-loop corrections to the lightest Higgs scalar boson mass in supersymmetry*”, Phys. Rev. D **75** (2007) 055005 [hep-ph/0701051]; R. V. Harlander, P. Kant, L. Mihaila and M. Steinhauser, “*Higgs boson mass in supersymmetry to three loops*”, Phys. Rev. Lett. **100** (2008) 191602 [Erratum: Phys. Rev. Lett. **101** (2008) 039901] [arXiv:0803.0672 [hep-ph]], “*Light MSSM Higgs boson mass to three-loop accuracy*”, JHEP **1008** (2010) 104 [arXiv:1005.5709 [hep-ph]].
- [91] U. Ellwanger, “*Radiative corrections to the neutral Higgs spectrum in supersymmetry with a gauge singlet*”, Phys. Lett. B **303** (1993) 271 [hep-ph/9302224]; T. Elliott, S. F. King and P. L. White, “*Squark contributions to Higgs boson masses in the next-to-minimal supersymmetric standard*

- model*”, Phys. Lett. B **314** (1993) 56 [hep-ph/9305282]; P. N. Pandita, “*One loop radiative corrections to the lightest Higgs scalar mass in nonminimal supersymmetric Standard Model*”, Phys. Lett. B **318** (1993) 338.
- [92] U. Ellwanger and C. Hugonie, “*Yukawa induced radiative corrections to the lightest Higgs boson mass in the NMSSM*”, Phys. Lett. B **623** (2005) 93 [arXiv:hep-ph/0504269].
- [93] S. Chang, R. Dermisek, J. F. Gunion and N. Weiner, “*Nonstandard Higgs Boson Decays*”, Ann. Rev. Nucl. Part. Sci. **58** (2008) 75 [arXiv:0801.4554 [hep-ph]].
- [94] A. Sirlin, “*Radiative Corrections In The SU(2)-L X U(1) Theory: A Simple Renormalization Framework*”, Phys. Rev. D **22** (1980) 971; G. Degrassi, S. Fanchiotti and A. Sirlin, “*RELATIONS BETWEEN THE ON-SHELL AND MS FRAMEWORKS AND THE $m(W) - m(Z)$ INTERDEPENDENCE*”, Nucl. Phys. B **351** (1991) 49.
- [95] F. Staub, “*Automatic Calculation of supersymmetric Renormalization Group Equations and Self Energies*”, Comput. Phys. Commun. **182** (2011) 808 [arXiv:1002.0840 [hep-ph]].
- [96] K. Ender, T. Graf, M. Muhlleitner and H. Rzehak, “*Analysis of the NMSSM Higgs Boson Masses at One-Loop Level*”, Phys. Rev. D **85** (2012) 075024 [arXiv:1111.4952 [hep-ph]].
- [97] T. Graf, R. Grober, M. Muhlleitner, H. Rzehak and K. Walz, “*Higgs Boson Masses in the Complex NMSSM at One-Loop Level*”, JHEP **1210** (2012) 122 [arXiv:1206.6806 [hep-ph]].
- [98] Heavy Flavor Averaging Group, <http://www.slac.stanford.edu/xorg/hfag/>.
- [99] M. Misiak *et al.*, “*The first estimate of $B(\text{anti-}B \rightarrow X/s \text{ gamma})$ at $O(\alpha(s)^{**2})$* ”, Phys. Rev. Lett. **98** (2007) 022002 [arXiv:hep-ph/0609232].
- [100] M. Misiak and M. Steinhauser, “*NNLO QCD corrections to the anti- $B \rightarrow X/s \text{ gamma}$ matrix elements using interpolation in $m(c)$* ”, Nucl. Phys. B **764** (2007) 62 [arXiv:hep-ph/0609241].
- [101] M. Ciuchini, G. Degrassi, P. Gambino and G. F. Giudice, “*Next-to-leading QCD corrections to $B \rightarrow X/s \text{ gamma}$: Standard model and two-Higgs doublet model*”, Nucl. Phys. B **527** (1998) 21 [hep-ph/9710335].
- [102] P. Ciafaloni, A. Romanino and A. Strumia, “*Two-loop QCD corrections to charged-Higgs-mediated $b \rightarrow s \text{ gamma}$ decay*”, Nucl. Phys. B **524** (1998) 361 [hep-ph/9710312]; F. M. Borzumati and C. Greub, “*2HDMs predictions for anti- $B \rightarrow X/s \text{ gamma}$ in NLO QCD*”, Phys. Rev. D **58** (1998) 074004 [hep-ph/9802391].
- [103] C. Bobeth, M. Misiak and J. Urban, “*Matching conditions for $b \rightarrow s \text{ gamma}$ and $b \rightarrow s \text{ gluon}$ in extensions of the standard model*”, Nucl. Phys. B **567** (2000) 153 [hep-ph/9904413].

- [104] M. Ciuchini, G. Degrassi, P. Gambino and G. F. Giudice, “*Next-to-leading QCD corrections to $B \rightarrow X/s$ gamma in supersymmetry*”, Nucl. Phys. B **534** (1998) 3 [hep-ph/9806308].
- [105] G. Degrassi, P. Gambino and G. F. Giudice, “ *$B \rightarrow X/s$ gamma in supersymmetry: Large contributions beyond the leading order*”, JHEP **0012** (2000) 009 [hep-ph/0009337].
- [106] M. Carena, D. Garcia, U. Nierste and C. E. M. Wagner, “ *$b \rightarrow s$ gamma and supersymmetry with large $\tan(\beta)$* ”, Phys. Lett. B **499** (2001) 141 [hep-ph/0010003].
- [107] G. D’Ambrosio, G. F. Giudice, G. Isidori and A. Strumia, “*Minimal flavour violation: An effective field theory approach*”, Nucl. Phys. B **645** (2002) 155 [hep-ph/0207036].
- [108] F. Borzumati, C. Greub and Y. Yamada, “*Beyond leading-order corrections to anti- $B \rightarrow X/s$ gamma at large $\tan(\beta)$: The charged-Higgs contribution*”, Phys. Rev. D **69** (2004) 055005 [hep-ph/0311151].
- [109] C. Greub, T. Hurth, V. Pilipp, C. Schupbach, M. Steinhauser and , “*Complete next-to-leading order gluino contributions to $b \rightarrow s$ gamma and $b \rightarrow s g$* ”, Nucl. Phys. B **853** (2011) 240 [arXiv:1105.1330 [hep-ph]].
- [110] G. Belanger, F. Boudjema, A. Pukhov and A. Semenov, “*MicrOMEGAs: Version 1.3*”, Comput. Phys. Commun. **174** (2006) 577 [arXiv:hep-ph/0405253], “*MicrOMEGAs 2.0: A Program to calculate the relic density of dark matter in a generic model*”, Comput. Phys. Commun. **176** (2007) 367 [hep-ph/0607059].
- [111] J. S. Lee, A. Pilaftsis, M. S. Carena, S. Y. Choi, M. Drees, J. R. Ellis and C. E. M. Wagner, “*CPsuperH: A computational tool for Higgs phenomenology in the minimal supersymmetric standard model with explicit CP violation*” Comput. Phys. Commun. **156** (2004) 283 [arXiv:hep-ph/0307377]; J. S. Lee, M. Carena, J. Ellis, A. Pilaftsis and C. E. M. Wagner, “*CPsuperH2.0: an Improved Computational Tool for Higgs Phenomenology in the MSSM with Explicit CP Violation*” Comput. Phys. Commun. **180** (2009) 312 [arXiv:0712.2360 [hep-ph]].
- [112] F. Mahmoudi, “*SuperIso: A program for calculating the isospin asymmetry of $B \rightarrow K^*$ gamma in the MSSM*” Comput. Phys. Commun. **178** (2008) 745 [arXiv:0710.2067 [hep-ph]], “*SuperIso v2.3: A Program for calculating flavor physics observables in Supersymmetry*”, Comput. Phys. Commun. **180** (2009) 1579 [arXiv:0808.3144 [hep-ph]].
- [113] P. Gambino and M. Misiak, “*Quark mass effects in anti- $B \rightarrow X/s$ gamma*”, Nucl. Phys. B **611** (2001) 338 [hep-ph/0104034].
- [114] P. Gambino and U. Haisch, “*Complete electroweak matching for radiative B decays*”, JHEP **0110** (2001) 020 [arXiv:hep-ph/0109058].

- [115] P. Gambino and P. Giordano, “*Normalizing inclusive rare B decays*”, Phys. Lett. B **669** (2008) 69 [arXiv:0805.0271 [hep-ph]].
- [116] A. Denner and T. Sack, “*Renormalization Of The Quark Mixing Matrix*”, Nucl. Phys. B **347** (1990) 203; B. A. Kniehl and A. Pilaftsis, “*Mixing Renormalization in Majorana Neutrino Theories*”, Nucl. Phys. B **474** (1996) 286 [hep-ph/9601390]; P. Gambino, P. A. Grassi and F. Madricardo, “*Fermion mixing renormalization and gauge invariance*”, Phys. Lett. B **454** (1999) 98 [hep-ph/9811470]; Y. Yamada, “*Gauge dependence of the on-shell renormalized mixing matrices*”, Phys. Rev. D **64** (2001) 036008 [hep-ph/0103046].
- [117] S. P. Martin and M. T. Vaughn, “*Two loop renormalization group equations for soft supersymmetry breaking couplings*”, Phys. Rev. D **50** (1994) 2282 [hep-ph/9311340] and references therein.
- [118] L. Hofer, U. Nierste and D. Scherer, “*Resummation of tan-beta-enhanced supersymmetric loop corrections beyond the decoupling limit*”, JHEP **0910** (2009) 081 [arXiv:0907.5408 [hep-ph]].
- [119] A. J. Buras, P. H. Chankowski, J. Rosiek and L. Slawianowska, “*Delta(M(d,s)), B/(d,s)0 → mu+ mu- and B → X/s gamma in supersymmetry at large tan(beta)*” Nucl. Phys. B **659** (2003) 3 [arXiv:hep-ph/0210145].
- [120] M. E. Gomez, T. Ibrahim, P. Nath and S. Skadhauge, “*An improved analysis of b → s gamma in supersymmetry*”, Phys. Rev. D **74** (2006) 015015 [arXiv:hep-ph/0601163].
- [121] K. i. Okumura and L. Roszkowski, “*Large beyond-leading-order effects in b → s gamma in supersymmetry with general flavor mixing*”, JHEP **0310** (2003) 024 [arXiv:hep-ph/0308102].
- [122] M. Muhlleitner and E. Popeno, “*Light Stop Decay in the MSSM with Minimal Flavour Violation*”, JHEP **1104** (2011) 095 [arXiv:1102.5712 [hep-ph]].
- [123] K. i. Hikasa and M. Kobayashi, “*Light Scalar Top At E+ E- Colliders*”, Phys. Rev. D **36** (1987) 724.
- [124] RAaij *et al.* [LHCb Collaboration], “*First evidence for the decay Bs → mu+ mu-*”, Phys. Rev. Lett. **110** (2013) 021801 [arXiv:1211.2674 [Unknown]].